A. Ion

Impact of "Lost C2 Link" on Key ATM Performance Indicators in a Mixed RPAS - Manned Aircraft Operational Environment

TU Delft

EUROCONTROL

Impact of "Lost C2 Link" on Key ATM Performance Indicators in a Mixed RPAS - Manned Aircraft Operational Environment

By

Andrei Ion

In fulfilment of the requirements for the degree of

Master of Science
in Aerospace Engineering

at Delft University of Technology,
to be defended publicly on the 12th of December, 2017 at 15:00

Student Number:	4201124	
Project Duration:	March – November 2017	
Thesis Committee:	Dr. ir. H.G. Visser,	TU Delft, supervisor
	Dr. M. A. Mitici,	TU Delft, supervisor
	M. Lissone,	EUROCONTROL, supervisor
	D. Zarouchas,	TU Delft

This thesis is confidential and cannot be made public until December 12, 2017.

TU Delft

EUROCONTROL

Acknowledgements

I remember as it was yesterday the moment when I arrived at Schiphol airport and a group of TU Delft students was waiting for me and others like me, who embarked hours ago on a journey to a new country and to a new life - the university life! They took all of us to the *Survival Cafe*, where a welcome package was waiting for us with information about the university, the city of Delft and other practical matters. Since then, time has flown by so fast: lectures, projects, exams, DSE, internships... I cannot believe that I am now writing the final words of my master thesis. It has been an incredible time and I am very happy to have had the opportunity to study at TU Delft and to have called Delft my home for the past five years. I would like to take this opportunity to thank the following people for their invaluable support during the duration of my thesis project.

I would like to express my gratitude to my thesis supervisors Dries Visser and Mihaela Mitici from TU Delft and Mike Lissone and Dominique Colin from EUROCONTROL for their guidance and advice over the past nine months. I am very grateful for the enlightening explanations and support material that you have provided me with from both sides, for the impromptu meetings and our regular progress calls. The advice given by Iliyana Simeonova has been instrumental in setting up the AirTOp environment, conducting the simulations and analyzing the results. Thank you very much for supporting me from the EEC side and for all your tips and tricks! I extend my grateful thanks to Dan Ivanescu for his help with getting me a hold of AirTOp.

Additional thanks go to Julia Sanchez and Anastasiia Sobchenko for their entire support during my time with EUROCONTORL, for making me feel part of the RPAS team and for motivating me all the time, even in the most stressful moments.

I would also like to thank the ECTL-trainees for being part of my "Brussels" family, for making my experience in Belgium a memorable one and for managing to take my mind off work outside the office.

Last but not least I would like to thank my parents and my brother for their constant support (not only during the thesis, but also for the entire period since I moved to the Netherlands). Even though you have been far away, you were always my rocks. Thank you all for your unconditional love!

Andrei

Delft, November 2017

Abstract

Remotely Piloted Aircraft Systems (RPAS) are becoming more and more popular with an increasing number of companies using them in the fields of precision agriculture, emergency delivery of medical aid and preventive maintenance. Trials are being made to extend their use to public safety, monitoring traffic, providing internet and even air taxi services. These RPAS operations are currently handled on a case-by-case basis and operated in segregated airspace by creating temporary restricted areas for other traffic. With the SESAR Joint Undertaking (SJU) estimating that in the next 30 years 20% of the traffic will be remotely piloted, the option of airspace segregation will no longer be feasible. Therefore, integrating RPAS with current manned operations will be required. In doing so, however, the current levels of safety and efficiency should not be compromised.

The command and control link (C2), which connects the remotely piloted aircraft and the remote pilot station, plays a pivotal role in the controllability of the aircraft, ATC communication and conflict detection and avoidance systems (CDA). This project, which is conducted between Delft University of Technology and EUROCONTROL, aims at establishing a methodology of determining how different percentages of flights that are remotely piloted and different C2 link failure rates influence the number of separation losses (blind encounters). For this, fast time simulations of a 24-hour period of the Dutch airspace are performed in AirTOp. This study will contribute to the integration of RPAS in non-segregated airspace and will serve as an input for the regulatory bodies which are yet to set performance standards on RPAS, particularly the C2 link.

Replacing between 10 - 50% of the flights in the Dutch airspace by RPAS with failure rates of the C2 link of 0.01 - 0.001 resulted in 1 - 15 flights being replaced by an RPAS with C2 link failure. This generated an additional number of blind encounters between 1.8 - 23.6, or an increase of 0.09 - 1.18% compared to the baseline situation (same traffic, no RPAS). Also, a linear relationship was found between the number of RPAS experiencing a failure of the C2 link and the number of blind encounters.

The project also investigates how an RPAS that experiences a failure of the C2 link right at the moment when it enters an ATC sector in Langen FIR (EDGGPHHM) penalizes key ATM performance indicators. The considered KPIs are: number of potential conflicts, air traffic controller task load, sector occupancy, distance flown, flight time, fuel consumption and altitude deviation. The scope is limited to en-route operations above 500 ft and the contingency strategy followed by the RPAS once it loses the C2 link is to proceed to its destination along its originally submitted flight plan. At the same time, air traffic controllers would enforce a separation bubble around the RPAS, such that a buffer is created for the situations in which the remotely piloted aircraft might deviate from it route or behave erratically. Two RPAS performance models are considered: MQ-9 Reaper, a turboprop with a lower cruise speed and climb/descent performance than current civil aircraft and RQ-4A Global Hawk, a turbofan with a cruise speed close to that of civil aircraft and a rate of climb slightly higher.

The results of the Monte Carlo tests are analyzed using ANOVA and MANOVA tests. Increasing the size of the separation bubble around the RPAS with C2 link failure by 20%, 40% and 60% resulted in an increase in the number of potential conflicts of 8.3%, 9.2% and 12.0% when a MQ-9 was used. The impact on controller task load was found to be small (increase of 0.4%) and not affected by the size of the separation bubble. Similarly the other KPIs were not affected by a separation increases of up to 60%. Switching 10-30% of the flights to RPAS and using even larger sizes of the separation bubble (twice or three times as large as the minimum ICAO standards) increased the number of potential conflicts by up to 72.9%, sector occupancy by 11.2% and the additional time spent in the sector by 1.4%. Based on the separation requirements which will be enforced around RPAS, the methodology used in the report can be used to assess the impact of experiencing a C2 link loss on the ATM environment.

Contents

List of Figures

List of Tables

List of Abbreviations

ACC - Area Control Center
ADS-B - Automatic Dependent Surveillance-Broadcast
AIRAC - Aeronautical Information Regulation and Control
AIRC - Aeronautical Information Regulation and Control
ALL_FT+ - Traffic File from EUROCONTROL DDR
ALO - Light Observation Aircraft
ANOVA - Analysis of Variance
ANSP - Air Navigation Service Provider
APA - American Psychological Association
ASCII - American Standard Code for Information Interchange
ATC - Air Traffic Control
ATCo - Air Traffic Controller
ATFM - Air Traffic Flow Management
ATM - Air Traffic Management
ATS - Air Traffic Services
BADA - Base of Aircraft Data
BRLOS - Beyond Radio Line of Sight
BVLOS - Beyond Visual Line of Sight
C2 - Command and Control Link
CDA - Conflict Detection and Avoidance
CIP - Conflict Intrusion Parameter
CONOPS - Concept of Operations
CPA - Closest Point of Approach
CRRB - Conflict Resolution Rule Base
CRRBT - Conflict Resolution Rule Base Tree
CSP - Communication Service Provider
DAA - Detect And Avoidance
DDR - EUROCONTROL Demand Data Repository
DFS - Deutsche Flugsicherung GmbH
DLR - German Aerospace Centre
EASA - European Aviation Safety Agency
eDEP - Early Demonstration and Simulation Platform
EUROCAE - European Organisation for Civil Aviation Equipment
EUROCONTROL - European Organisation for the Safety of Air Navigation
FACET - Future Air Traffic Management Concepts Evaluation Tool
FIR - Flight Information Region
FRMS - Flight and Radio Management system
FRONTEX - European Agency for the Management of Operational Cooperation at the External Borders of the Member States of the EU
GASEL - Environment File from EUROCONTROL DDR
GNSS - Global Navigation Satellite System
HALE - High Altitude Long Endurance
IAF - Initial Approach Fix
ICAO - International Civil Aviation Organization
IFR - Instrument Flight Rules
INTA - Spanish National Institute for Aerospace Technology
ISIS - Icarus Simulation Integrated Scenario
JARUS - Joint Authorities for Rulemaking on Unmanned Systems
KPA - Key Performance Area
KPI - Key Performance Indicator

LALE - Low Altitude Long Endurance
LASE - Low Altitude Short-Endurance
LOS - Loss of Separation
MALE - Medium Altitude Long Endurance
MANOVA - Multivariate Analysis of Variance
MAV - Micro Air Vehicle
MOE - Margin of Error
MSE - Mean Squared Error
MTBF - Mean Time Between Failure
MTOW - Maximum Take-Off Weight
NASA - US National Aeronautics Space Administration
NATS - National Air Traffic Services (UK)
NAV - Nano Air Vehicle
NEST - Network Strategic Tool
NLR - National aerospace laboratory (Netherlands)
ORP - Oceanic, Remote and Polar
PIC - Pilot in Command
RAMS - Reorganised ATC Mathematical (Model) Simulator (EEC)
RCP - Required Communications Performance
RLOS - Radio Line of Sight
RLP - Required (C2) Link Performance
RLTP - Required C2 Link Technical Performance
RMSE - Root Mean Square Error
RP/RPIL - Remote Pilot
RPA - Remotely Piloted Aircraft
RPAS - Remotely Piloted Aircraft Systems
RPORT - Remote Pilot Operation Response Time
RPS - Remote Pilot Station
RS - Radio System
SESAR - Single European Sky ATM Research
SID - Standard Instrument Departure
SJU - SESAR Joint Undertaking
STAR - Standard Instrument Arrival
TBO - Trajectory Based Operations
TLX - Task Load Index
TMA - Terminal Control Area
TWR - Tower Control Unit
UAS - Unmanned Aircraft Systems
UAV - Unmanned Aerial Vehicle
UIR - Upper FIR
UTM - UAS Traffic Management
VFR - Visual Flight Rules
VHF - Very High Frequency
VHL - Very High Level Operations
VLL - Very Low Level Operations
VLOS - Visual Line Of Sight
VTOL - Vertical Take-Off and Landing
WC - Well Clearance

PART I

BACKGROUND

1 Introduction

Unmanned aerial vehicles date back long before the first official manned flight performed by the Wright brothers. In 1804 Sir George Cayley tested an unmanned glider which was 1.5 meters long and consisted of a kite attached at an angle of 6° to the rod fuselage and a cruciform tail (Figure 1.1). [1] Almost half a century later, when revolutions swept through Europe, unmanned balloons were used in 1849 by the Austrians in their attack on Venice. [2] Their purpose was to transport explosives across the lagoon and attack the city. However, as the balloons were truly unmanned and autonomous, once the wind changed direction, their trajectories were unpredictable and the operation was not successful [1].

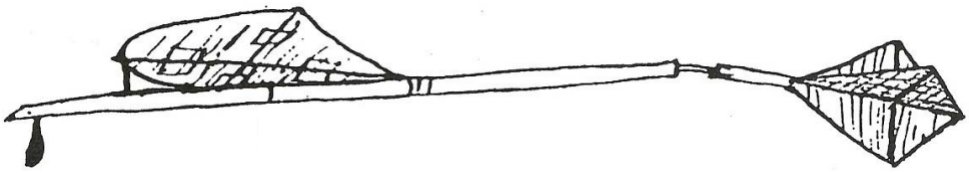

Figure 1.1: Glider Design of Sir George Cayley [1]

Nowadays, with a large number of companies around the world using drones as part of their daily business, the use of remotely piloted aircraft systems (RPAS) has flourished within the past years[2]. UPS introduced its first residential delivery drone, with a lifespan of 30 minutes. Launched from its electric van, this RPA will help increase the number of deliveries. DHL completed 130 successful delivery missions with its automated drone delivery system Parcelcopter. In the UK, police trials were conducted with HD camera equipped drones that helped searching for missing people and monitoring traffic accidents. Internet company BT is experimenting with drones that would provide temporary internet service in hard-to-reach zones and disaster areas. On the other spectrum, Dubai's Roads and Transportation Agency revealed plans to begin regular services with people-carrying drones in the summer of 2017. The vehicle will be able to transport a passenger weighting up to 100 kg for a time of around 30 minutes.

Through these new business models, it has become clear that the introduction of RPAS in controlled airspace will generate economic benefits and job opportunities. [3] Not only will these vehicles be used for commercial purposes such as cargo delivery, entertainment and transportation, but also for civilian purposes such as surveillance, weather monitoring, precision agriculture, mapping, disaster relief and traffic monitoring. [4] The high benefit-to-cost ratio will be the main reason for integrating RPAS in the airspace system. [5] However, since technological developments come at a higher pace than for manned aviation, the challenge is to safely and efficiently integrate the two worlds, as both types of aircraft will be sharing the same airspace. [6]

[1] Remote Piloted Aerial Vehicles: An Anthology, `http://www.ctie.monash.edu.au/hargrave/rpav_home.html` [accessed on 30/10/2017]

[2] Techworld, `http://www.techworld.com/picture-gallery/personal-tech/best-uses-of-drones-in-business-3605145-3605145/` [accessed on 24/03/2017]

It is paramount that the safety of existing traffic will not be affected with the introduction of RPAS flights. New technologies such as detect and avoid systems and a harmonized regulatory framework should be developed. [7] This is because current requirements regarding operational performance and integration were not designed to accommodate for large numbers of RPAS operations. For instance, at any given moment there are 5,000 flights in the US, while at the same time more than 469,000 registered Remotely Piloted Aircraft (RPA) users[3]. [4] SESAR, the Single European Sky ATM Research Programme estimates that unmanned aerial vehicles will represent a quarter of the traffic by 2050. [8] This means that the density of operations in the airspace will be higher than in the current environment, which requires an analysis on how it will impact the safety and efficiency of current manned flights. Therefore, the focus of this study will be on the impact of RPAS flights on the efficiency of surrounding manned aircraft flights.

This project is a joint collaboration between Delft University of Technology and EUROCONTROL, the leader of ATM integration and key contributor to the European RPAS road-map. [9]

This document is divided in five main parts. The first one offers a theoretical background on remotely piloted aircraft systems and the research questions and objectives of the study. The second and third parts focus on the two different experiments that were conducted, the results obtained and recommendations for future studies. The fourth part analyzes the results of the second experiment from a statistical point of view. Conclusions and recommendations are the focus of the last part.

The outline of this document is the following: Chapter 2 contains the background information on RPAS, C2 link, types of operations and traffic classes. This chapter also presents the current state-of-the-art on remotely piloted aircraft systems. The research objectives and questions are defined in Chapter 3 and the selected simulation tool (AirTOp) is introduced in Chapter 4. The experimental set-up for the first experiment which looks at the impact of RPAS on a country level is also explained in Chapter 4. The two experiments make use of the Monte Carlo method which is introduced in Chapter 5. The results of this experiment are given in Chapter 6 and conclusions and limitations of this approach are drawn in Chapter 6.2. The experimental set-up for the second experiment which looks at the impact of RPAS on a sector level is explained in Chapter 7. The results of this experiment are given in Chapter 9 which are then analyzed using ANOVA and MANOVA tests (Chapters 10 and 11). The conflict detection and resolution module used for this experiment is detailed in Chapter 8 and then conclusion and recommendations are drawn in Chapter 12.

[3] This figure excludes the large Beyond Radio Line of Sight (BRLOS) unmanned aircraft [4]

2

Theoretical Background

The focus of this chapter is to define and explore RPAS concepts. First an RPAS forecast is presented in Section 2.1 which highlights the importance of this study. Section 2.2 deals with the technical aspects of remotely piloted aircraft systems. Their integration into the current ATM is addressed in Section 2.3, while Section 2.4 presents the requirements that would have to be met by the command and control link. The current state of the art is discussed in Section 2.5. AirTOp, the simulation platform used for this project is introduced in Section 2.6.

2.1. RPAS Forecast

SESAR Joint Undertaking (SJU), which is the European public-private partnership that manages the development phase of the Single European Sky ATM Research (SESAR) Programme, investigated the capabilities of the drone market (all types of UAS, including RPAS) both in Europe and globally and established a forecast for the period up to 2050.

In its European Drones Outlook Study [10], SJU states that there is not a question of *if* the drone market will significantly bring greater benefits, but *when* and *whether* Europe will take on the chance to be a significant player in this rapidly changing market. In the period up to 2050 the European drone fleet will account for 400,000 commercial and government drones (relaying on BVLOS capabilities) and approximately 7 million leisure ones. The sectors which are envisioned to see the largest number of drones are [10]:

- Agriculture: more than 100,000 drones to be used in precision farming
- Energy: approximately 10,000 drones to be used in preventive maintenance inspections
- Delivery: 100,000 drones used for transporting emergency medical supplies and "premium" deliveries
- Public safety and security: approximately 50,000 drones used for police, fire fighting and humanitarian missions

In the controlled airspace approximately 20% of the flights are expected to be remotely piloted by 2050. The first larger unmanned commercial vehicles are expected to begin operations after 2030, initially for the transportation of cargo and later on for passenger services. [10]

SJU forecasts that the market will be dominated by multi-national scale companies that will conduct cross border missions. These missions will generate an additional EUR 10 billion annually by 2035 and over EUR 15 billion per year by 2050. [10]

The forecast identifies four areas of research in which the European institutions shall invest over the next 5 - 10 years in order to be able to accommodate this new traffic [10]:

- Detect and avoid technology;
- Air traffic management;
- Security and cyber reliance;
- Authorized and safe testing environments.

2.2. Introduction on Remotely Piloted Aircraft Systems

Currently aviation professionals, regulatory bodies and users refer to remotely piloted aircraft by using four terms: RPAS, UAS, UAV and drone. However, a distinction should be made between these most common terms in order to understand the underlying differences. **RPAS** (or Remotely Piloted Aircraft System) is a concept introduced by ICAO in Doc. 10019 [11] which refers to an aircraft that is piloted from a remote location and all the systems which are associated to it (the remote pilot station, command and control links, etc.). A **UAS**, or Unmanned Aircraft System, is a term used by ICAO [11] for any aircraft that has no pilot on board and its associated elements. Document 10019 [11] further defines an **UAV** (Unmanned Aerial Vehicle) as an aircraft without a pilot on board that can be flown in three ways: by a remote pilot, programmed, or in a fully autonomous way. **Drone** is a generic term used to refer to any unmanned or remotely piloted aircraft, encompassing the concepts of RPAS and UAS.

A classification of remotely piloted aircraft systems in terms of size and performances is the focus of Section 2.2.1. Current RPAS operations and their societal benefits are addressed in Section 2.2.2. EUROCONTROL envisions the organization of RPAS traffic into seven classes. These will be detailed in Section 2.2.3. The technical details behind the command and control link, which is critical for safe RPAS operations, are covered in Section 2.2.4. The contingency procedures in case of a C2 link loss are discussed in Section 2.2.5.

2.2.1. Classification of RPAS and its Elements

Remotely piloted aircraft were included in the aircraft classification scheme of the International Civil Aviation Organization (ICAO) Amendment 6 of Annex 7 to the Convention on International Civil Aviation. This document defines an RPAS as an unmanned aircraft which is piloted from a remote pilot station. [12] Unmanned aircraft need to carry a registration plate similar to the case of manned airplanes. Furthermore, the cockpit of the RPA does not need to accommodate a person. According to Amendment 43 to the International Standards Rules of the Air, a remotely piloted aircraft shall be operated in a manner that minimizes hazards to persons, properties and other aircraft. [13] Circular 328 of ICAO [14] on unmanned aircraft systems defines a remotely piloted aircraft as an airborne vehicle with a structure similar to that of an airplane, which encompasses the following elements:

- **RPA**, the remotely piloted aircraft itself;
- **RPS**, the remote pilot station which is located outside the aircraft and is the place where the remote pilot (RP) is stationed. The RPS can be anything from a hand-help device to a multi-console station and could be located either outside or inside a building.;
- **C2**, the command and control link which connects the RPA and RPS and helps with managing the flight.
- Other elements such as: ATC communications and surveillance equipment, navigation equipment, launch and recovery equipment, flight control computer, flight management system, etc. [6]

RPAS can be classified in four categories based on their size. [15] Very small RPAS are shown in Figure 2.1 and are typically the size of a large insect (30-50 cm long). The Mosquito UAV developed by Israel Aerospace Industries is one example. Being very small in size and lightweight, this device is often used in surveillance missions. [16] Small RPAS have at least one dimension greater than 50 cm, but not larger than 2 meters. Examples of these can be seen in Figures 2.2 and 2.3[1]. Many of the models in this category have fixed wings and are hard launched, by throwing them in the air. Medium RPAS typically have a wingspan of 5-10 meters and are too heavy to be carried by on person. However, they are smaller than a light aircraft. Usually these types of aircraft carry payloads between 100 - 200 kg. Some examples of medium RPA are shown in Figure 2.4. The final category includes large RPAS such as the Predator (MQ9-Reaper) or Global Hawk (RQ4A), which are mainly used for combat operations by the army. These can be seen in Figures 2.5 and 2.6[2].

Based on the performance of the RPAS in terms of endurance, cruise speed and flight levels, remotely piloted aircraft can be divided in the following categories [18]:

- **MAV (Micro) or NAV (Nano) Air Vehicles**: miniature UAV, operating below 100 ft and with limited endurance.

[1] Source: `http://olive-drab.com/idphoto/id_photos_uav_rq7.php` [accessed on 24/03/2017]
[2] Source: `https://www.nasa.gov/multimedia/imagegallery/image_feature_2362.html` [accessed on 24/03/2017]

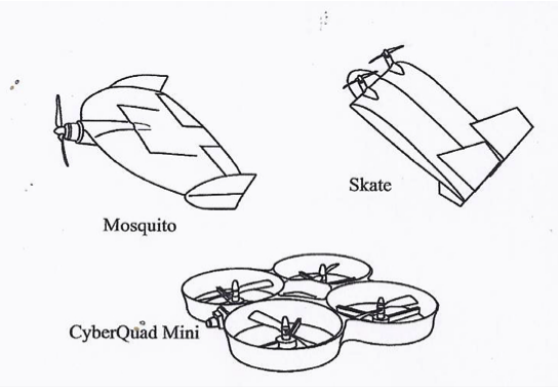

Figure 2.1: Examples of very small RPAS [17]

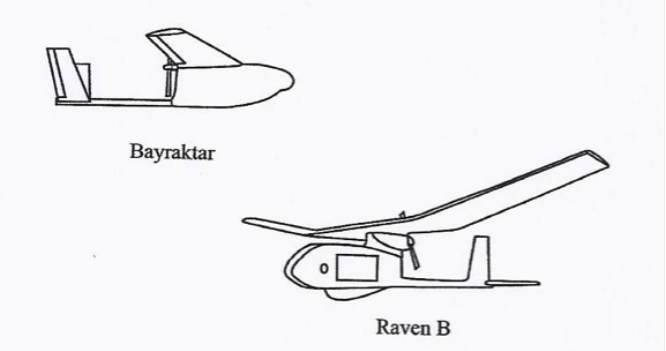

Figure 2.2: Examples of small RPAS [17]

Figure 2.3: A US army RQ-7 Shadow (small RPAS)

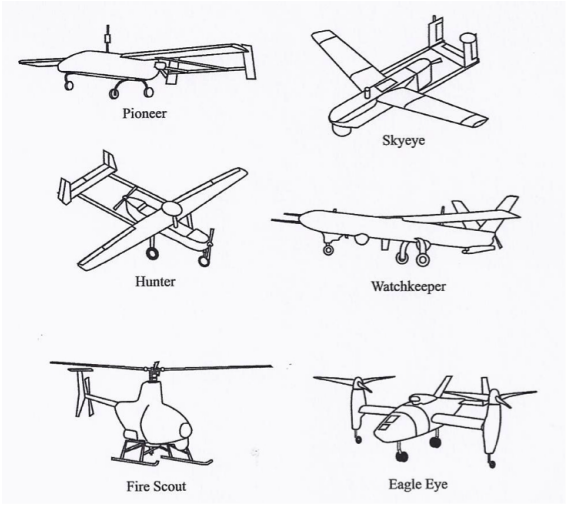

Figure 2.4: Examples on medium RPAS [17]

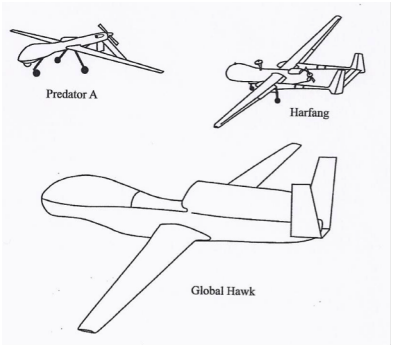

Figure 2.5: Examples on large RPAS [17]

Figure 2.6: NASA Global Hawk (large RPAS)

- **VTOL (Vertical Take-Off Landing)**: an alternative to large fix-winged unmanned aircraft, capable to hover with a wide spectrum of size and performance capabilities.
- **LASE (Low Altitude, Short-Endurance)**: VLOS flights up to 120 minutes below 1500 ft.
- **LALE (Low Altitude, Long Endurance)**: unmanned aircraft capable to fly up to one day at altitudes up to 16500 ft.
- **MALE (Medium Altitude, Long Endurance)**: advanced design enabling flights 20-40 hours long between FL165-FL300, with the possibility to fly up to FL400. Performance is linked to payload and mission type.
- **HALE (High Altitude, Long Endurance)**: unmanned vehicles capable of flying very long periods of time (days, weeks or months) at altitudes above 45000 ft.

2.2.2. Current RPAS Operations and their Benefits

Because RPAS are small in size and do not have a pilot on board, they are ideal for flying missions in area that are dangerous or inaccessible to manned aviation. For instance, companies such as AETOS[3], The Sniffers[4] and AIRACOM[5] use remotely piloted aircraft for the inspection of oil and gas pipes, power lines, bridges, wind turbines, train lines and solar installations. Furthermore, Atmosphere Aerial[6] uses drones for radiation measuring and monitoring. By using drones, these companies achieved an increase in safety and precision of their operations while reducing operational time and costs. NASA used in 2006 the Predator RPAS for a fire-fighting operations called Ikhana, in which the RPA provided information about the progress of the wildfires and their hot spots. [19]

The US Electric Power Research Institute established that the use of unmanned aircraft systems for the inspection of solar photovoltaics power-plants not only reduces costs, but also improves operations and maintenance strategies. [20] Through pattern recognition and data analytics capabilities, UAS are able to better predict the health of the power-plant and enable companies to plan maintenance tasks accordingly.

Following a successful three-month trial, DHL integrated its Parcelcopter, a quadcopter of around 1 meter in size, in its logistics chain[7]. The trials included 130 autonomous flights in Reit im Winkl, Germany which tested the quadcopter's ability to handle changing weather conditions and severe temperature fluctuation. Parcelcopter (shown in Figure 2.7) delivered urgently needed medicine from the valley to the plateau in 8 minutes, a journey that takes more than half an hour during winter months.

The Ambulance Drone (Figure 2.8) developed by Delft University of Technology[8] aims at increasing the chances of surviving a cardiac arrest, by delivering an Automated Defibrillator (AED). A fast response to a cardiac arrest is critical, as brain damage or even death could occur in 4-6 minutes, whereas emergency services typically respond in 10 minutes.

Figure 2.7: DHL Parcelcopter (Source: DHL)

Figure 2.8: TU Delft Ambulance Drone (Source: TU Delft)

[3]Source: `http://www.aetosgroup.com/#air` [accessed on 14/10/2017]
[4]Source: `https://www.the-sniffers.com` [accessed on 14/10/2017]
[5]Source: `http://www.airacom.com/industrial-iot/drone-based-inspections/` [accessed on 14/10/2017]
[6]Source: `https://atmosphereaerial.com/` [accessed on 14/10/2017]
[7]DHL Parcelcopter Press Release, source: `http://www.dhl.com/en/press/releases/releases_2016/` [accessed on 14/10/2017]
[8]Source: `https://www.tudelft.nl/en/ide/research/research-labs/applied-labs/ambulance-drone/` [accessed on 14/10/2017]

In precision agriculture, remotely piloted aircraft are used to analyze the soil, monitor the crops and perform health assessments. [21] This is useful for spraying the correct amount of liquid, which increases efficiency and reduces the amount of chemicals penetrating into groundwater. Scanning the crop with near-infrared light, enables the farmer to asses the health of the plants and apply any remedies, if necessary.

FRONTEX, the European Border and Coast Guard Agency, held two public tenders in 2016 for the acquisition of a fleet of UAVs that would monitor European borders and control irregular immigration[9]. In the United States, the Customs and Border Protection agency already used the MQ9-Reaper and RQ4A Global Hawk for securing the US-Mexico border and combating illegal cross-border activity. [22]

2.2.3. Traffic Classes

EUROCONTROL proposes in the RPAS ATM CONOPS [6] the organization of RPAS traffic into seven classes and defines four types of RPAS operations. These are summarized in Table 2.1.

Table 2.1: RPAS Types of Operations and Classes (Based on [6])

Altitude	Type of Operation	RPAS Classes
0 - 500ft	Very Low Level operations (VLL)	I, II, III, IV
500ft - FL600 (incl. airports)	IFR/VFR operation	V, VI
FL600 - 100 km	Very High Level operations (VHL)	VII
100 km and above	Space operations	VII

Excluding space operations, the three types of RPAS operations identified in [6] are summarized below:

- **Very Low Level operations (VLL)**, which deal with operations below 500ft. Currently this environment is used by numerous operators such as the police, armed forces, gliders, fire-fighters and ultra-light aircraft. This category can be subdivided into the following sub-categories, which will be detailed in Section 2.2.4:
  - **Visual line-of-sight (VLOS)**: RP and RPA are in direct unaided visual contact and no further than 500 meters away.
  - **Extended visual line-of-sight (E-VLOS)**: when additional observers are present, the VLOS range can be extended.
  - **Beyond visual line-of-sight (B-VLOS)**: when neither RP nor RPA can maintain direct visual contact
- Very High Level operations (VHL), which refer to suborbital unmanned flights, operating at altitudes above FL600. Currently this airspace is used by space rockets and the military.
- IFR/VFR Operations, which refer to airports, TMA and en-route airspaces that the RPAS will be sharing with normal transport aircraft. This will require the RPA to meet certain minimum performance requirements with respect to speed, climb/descend rates, turn performance and communication latency.

Because RPAS can have different shapes, sizes and performances, the classification proposed by EUROCONTROL in the ATM CONOPS [6] distinguishes between remotely piloted aircraft based on the flight rules, procedures and system capabilities of the RPAS and the operator during the flight. The seven classes are summarized below:

- **Class I**: the "buy-and-fly" drones that are operated in VLOS and flown in low risk environments, staying clear of airports and other no-drone zones.
- **Class II**: free flights (VLOS or BVLOS) either specific or certified category according to EASA [23]
- **Class III**: BVLOS medium/long-haul flights (free flight or structured commercial route). Either a specific RPAS, or one certified for longer routes.
- **Class IV**: special operations (VLOS or BVLOS) by either specific or certified RPAS. This category is to be assessed on a case by case basis.
- **Class V**: IFR/VFR operations outside the Network. The RPAS is not flying SID/STARs. Segregation will be enforced around airports for launch and recovery and manned aviation will not be impacted. No additional performance requirements to be imposed on the RPAS compared to manned aviation.

[9] Source: `http://www.investigate-europe.eu/en/76-million-to-survey-migration-routes-largest-eu-public-drone-tender-decided/` [accessed on 14/10/2017]

- **Class VI**: IFR operations (Network/ TMA/ Airport operations) capable of flying SID/STARs. Manned transport aircraft capable to fly without a pilot, or new types that are able to meet the performance requirements of the Network, TMA and airports.
- **Class VII**: IFR operations above FL600, involving the RPAS to transit through segregated / non-segregated airspace. Dedicated launch and recovery sites unless performance requirements of Class VI are met.

2.2.4. The Command and Control (C2) Link

According to ICAO Annex 2, the C2 link is defined as the data link responsible for managing the flight, connecting the remotely piloted aircraft and the remote pilot station. [24] The C2 link plays a pivotal role in the controllability of the aircraft, ATC communication and conflict detection and avoidance systems (CDA). In addition to flying the aircraft, the remote pilot is also responsible for managing and monitoring the C2 link. From a technical standpoint, the C2 link is used for exchanging information and safely integrating the RPAS into the global aviation, communication, navigation and surveillance operational environment. [25] The Annex D of the JARUS CONOPS defines the C2 link as an exchange of data necessary to aviate the RPAS, supporting also:

- communication with other airspace users and ATC;
- navigation of RPA according to navigation concepts, and
- integration of RPA into airspace along with the other users.

The physical limits of the C2 link are shown in Figure 2.9. As can be seen here, the C2 link encompasses everything in between the RPA and RPS transmitters (TX) and receivers (RX), thus including a physical part of the RPA/RPS. After broadcasting the signal, third party service providers could be involved in relaying, transforming or amplifying it. [25] If the RPS is connected via a ground line to a service provider then the antenna will not be part of the RPS side, but will be part of the third party communications service provider that supports the RPS.

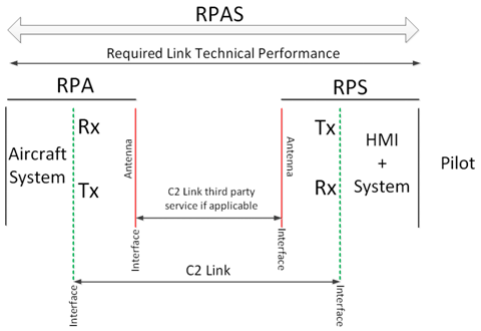

Figure 2.9: Physical limits of the C2 link [25]

The general architecture of the C2 link as defined in Annex D of the JARUS CONOPS [25] is shown in Figure 2.10. The acronyms used in this figure are explained below:

- CSP: Communication Service Provider
- FRMS: Flight and Radio Management system
- RLTP: Required C2 Link Technical Performance
- RPORT: Remote Pilot Operation Response Time
- RS: Radio System

As already mentioned in Section 2.2.3, the C2 can either operate in radio line-of-sight (RLOS) or beyond radio line-of-sight (BRLOS). RLOS means that transmitters and receivers are using a direct radio frequency line (mutual radio link coverage), while BRLOS refers to a configuration in which the transmitters and receivers are not in RLOS. [14] In cases like this, relays such as satellite systems or terrestrial networks are used for communication. Figures 2.11 - 2.12 illustrates the two communication options. As can be seen here, compared to manned aircraft, the RPA communication link is not always a direct one. Therefore, the main difference between RLOS and BRLOS is the variable delay in communications.

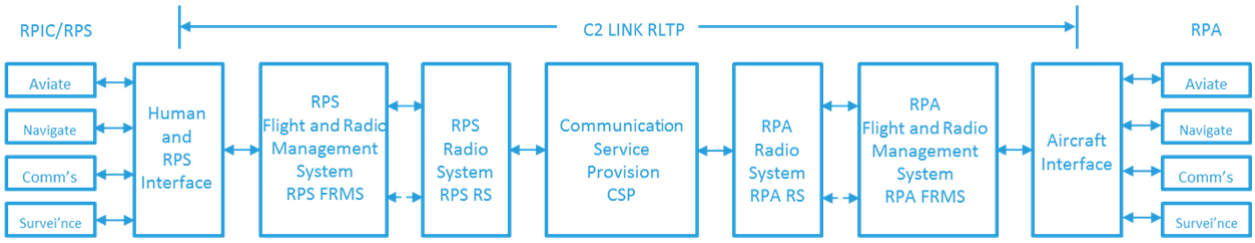

Figure 2.10: Generic Technical Architecture of the C2 Link [25]

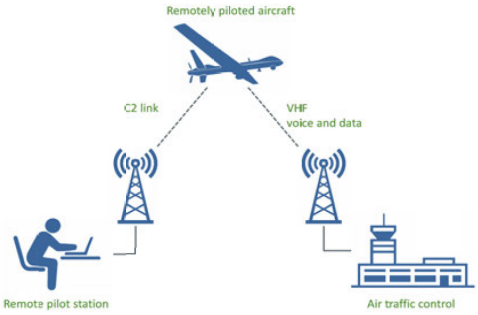

Figure 2.11: Radio Line of Sight [11]

Figure 2.12: Beyond Radio Line of Sight [11]

EUROCAE defines in [26] that the maximum one way voice ATC communication delay is 485 ms in oceanic, remote and polar areas (ORP) and 130 ms in the other areas. When communication is done via a satellite typical latency values are 500 - 700 ms. Considering the two RLOS and BRLOS situations (Figures 2.11 and 2.12) the following differences in communication latencies are found:

(a) **RLOS:** C2 + VHF = 700 + 130 = 830 ms (non-ORP areas), or: C2 + ORP = 700 + 485 = 1185 ms (ORP areas)
(b) **BRLOS:** C2 + C2 + VHF = 1530 ms (non-ORP areas), or: C2 + C2 + ORP = 1885 ms (ORP areas)

Two classifications are available for any C2 link: depending on the data flow supported by the RPAS the C2 link can be either cooperative or non-cooperative and depending on the communication architecture required the C2 link can be either dependent or non-dependent. [25] While a non-cooperative C2 link only supports the "aviate" function, a cooperative C2 link also supports the "communicate", "navigate" and "integrate" functions. A non-dependent C2 link is a link entirely internal to the RPAS, while the dependent one requires an external communication architecture. Based on this classification, the typical C2 link usage is shown in Figure 2.13.

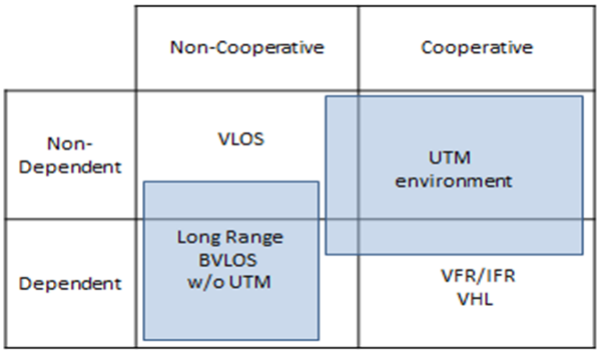

Figure 2.13: Typical C2 Link class usage [25]

2.2.5. Contingency Procedures in case of C2 Link failure

This section looks at the reasons why a C2 link could be delayed or lost, what the consequences would be and what contingency strategies could be enforced in such a situation.

The C2 link loss is defined as the period when the communication and control link is unavailable for a certain period of time. This period may vary depending on the stage of the flight, or the operational environment: for instance during final approach, even a brief interruption might trigger the lost link procedures, while over oceanic areas waiting for a longer period of time might be acceptable. [27] A loss of signal or delay is one of the biggest challenges, especially in BRLOS (beyond radio line of sight) operations. In this case the RPA and RPS are not directly linked and the signal latency is longer than in RLOS (radio line of sight) operations. Possible reasons for a delay or even a loss of the C2 link were identified by R. R. Cordon et al. [28] and H. Jung et al. [29] and are summarized below:

- meteorological conditions;
- terrestrial interferences which might contribute to a degradation of communication;
- the situation when the RPA crosses different sectors and the RP maintains contact with multiple ATC units and
- the situation when there is excessive signal delay between the RPA and the RPS (either due to distance to RPA or indirect communication between the RPA and RPS).

Apart from the loss of the C2 link itself, the C2 link might also be affected by the electro-magnetic environment in which the RPAS operates. Though not intending to harm it, the increase in white noise generated by human activities can alter the C2 link transmission. Also, lack of coordination with the spectrum used for the C2 link may create RPAS-RPAS interferences. Other sources of interference could be the payload transmissions, which are not part of the RPAS C2 link.

M. Perez-Batlle et al. [30] and R. Jay Shively et al. [27] identify four consequences of loosing communication and control of the RPA:

- reduction of overall situational awareness, by preventing the RP to take the right decision in time in case of an emergency;
- increase in uncertainty of the way separation manoeuvres are performed due to autonomous and unpredictable separation manoeuvres performed by the RPAS;
- loss of some of the Detect and Avoid system capabilities;
- increase in operational risk and a reduction in safety which may hinder the permission of future RPAS to operate in the network and
- limitation of system capacity.

Furthermore, when the RPA is manually controlled and there is a delay of the C2 link, pilot induced oscillations might occur. [27] This would require an on-board flight control automation tool for stability. When the RPAS is automatically controlled, a delay of the communication and control link will not affect the aircraft's stability, but would increased the workload of the ATCo. [15]

As previously discussed, a C2 link may be delayed or lost for a number of reasons. When this happens, the RPA can pose a serious hazard for nearby traffic. Furthermore, the ATCo should not be taken by surprise by the behaviour of the aircraft, when such a situation occurs. Therefore, pre-programmed safe and predictable procedures must enable the RPA to fly until the link is resumed. A number of contingency strategies are defined in [31] and [11] for such cases:

- The RPA will follow the original flight plan to the base. A number of holding points are established along the way, where it would wait for a predefined time to re-establish connection and allow fuel to be consumed. Afterwards, an emergency landing will be performed on the runway which was set up at take-off time;
- Direct return to departure airport;
- Landing at nearest airport, or
- Climbing/ Descending to a predefined altitude and attempting to regain the C2 link.

The contingency procedure used for this study is that of following the original flight plan.

2.3. ATM Integration

The main idea behind the integration of RPAS in the European Airspace, as presented in the RPAS CONOPS [6] is that the RPAS should emulate themselves to the current operational requirements and procedures and should not expect the existing actors to adapt to RPAS operations in order to ensure safety. Furthermore, there will be no differentiation between civil and military traffic, since RPAS integration challenges are identical in both cases. EUROCONTROL envisions the RPAS integration in two steps: the first one would cover the time-frame up to 2023, in which dedicated corridors or separation bubbles around the RPA will be created. This will enable the operation of RPAS flights before the technology and regulations are in place. In the second stage, from 2023 onwards, RPAS will be able to integrate as any other airspace user, with the help of supporting technology, regulations and standards. The remainder of this section will focus on the three operational conceptual options defined in [6]: current present situation, free-flight and route structure.

Due to the relatively low number of RPAS operations, the first option is to conduct operations below 500 ft preserving the status quo, without the necessity of performing an airspace assessment. Operations will be prohibited in no-drone zones (NDZ) such as: airports, nuclear power stations and hospitals.

Once RPAS traffic increases to a level that requires a more clear structure, Class I RPAS operations will be limited to 150 ft in areas with high traffic volumes. An airspace assessment will be required in this case to identify the regions in which Class I traffic should be restricted and determine the general traffic flows of RPAS. Free flights up to 500 ft will still be allowed for Class II and III. The Detect and Avoid system could be based on the "bubble concept" that will enforce a different separation requirement around the RPAS. In this case, because of the free flights, the requirements on the DAA system would be high.

The third option is an alternative to the second case when there is a high increase in traffic demand. Once there will be repetitive flights to and from an area, a route structure would be put into place. In order to minimize the impact on safety, privacy and noise, an airspace assessment shall determine the best areas for such routes. Possible options could be above rivers or rail roads. Compared to the case of free flights, this option would lower the requirements on the DAA system.

In the time frame between 2019 - 2023 it is expected that the required documentation will be in place to allow certified RPAS to operate IFR in all airspace classes based on the traffic classes described in Section 2.2.3. VLOS and E-VLOS operations would be a completely integrated with all other airspace users. B-VLOS operations will be further expanded and possibly cater for cargo flights, but it is not expected to encounter such operations in urban areas during this time frame. [6]

2.4. Requirements on RPAS C2 link

As was discussed in Section 2.2.4, the C2 link is critical for safe RPAS operations. Therefore, communication performance requirements need to be set for the C2 link. While in the context of ATM (when the pilot is located inside the aircraft) the Required Communications Performance concept (RCP) was developed [32], this cannot be directly transposed to the C2 link. JARUS proposed the creation of the Required (C2) Link Performance concept (RLP), a concept similar to the RCP, but adapted to the RPAS C2 link communications. [33] This concept is being revised by ICAO to be compatible with the RCP one (ICAO Doc. 9869 [34]). The ICAO RLP concept sets allocations on the performance required for communication capabilities without reference to any specific technology, making it open to new technologies. The C2 link performance parameters are:

- communication transaction time: *The maximum time for the completion of the operational communication transaction after which the initiator should revert to an alternative procedure*;
- continuity: *The probability that an operational communication transaction can be completed within the communication transaction time*;
- availability: *The probability that an operational communication transaction can be initiated when needed*; and
- integrity: *The probability of one or more undetected errors in a completed communication transaction.*

Table 2.2 shows C2 link RLP types envisaged for general application. When a state decides to prescribe a cer-

tain RLP several factors shall be taken into account such as the safety level required in the airspace and the type of operation that will be carried out. As can be seen in this table, envisioned failure rates of the C2 link are in the order of 10^{-4} - 10^{-5} failures per flight hour.

Table 2.2: Examples of C2 link RCP types (informative figures) [33]

C2 link RCP type	**Transaction time (sec.)**	**Continuity (Probability per flight hour)**	**Availability (Probability per flight hour)**	**Integrity (Acceptable rate per flight hour)**
C2 link RCP A	3	0.999	0.9999	10^{-5}
C2 link RCP B	5	0.999	0.999	10^{-4}
...	15	0.999	0.999	10^{-4}

The following section will present current and past studies in the field of RPAS operations and lost C2 link occurrences, setting the ground for the research questions and objectives of this study, which will be addressed in Chapter 3.

2.5. State of the Art

Previous studies on the integration of RPAS into non-segregated airspace and the ability of ATCo to handle contingency procedures were based on real-time human-in-the-loop simulations. A range of different simulators were used, such as: FACET (Future Air Traffic Management Concepts Evaluation Tool) developed by NASA Ames Research Center [35], DELPHINS ATC simulator [36], X-Plane Simulator (in combination with Matlab) [37], eDEP (Early Demonstration and Evaluation Platform) developed by EUROCONTROL [38] and ISIS [39], a human-in-the-loop simulator which requires two roles: one of the pilot (who will exchange information with ATC) and another of the air traffic controller.

The German WASLA-HALE project conducted 18 simulations of a high altitude long endurance unmanned aircraft that would fly alongside 36 other flights through zones of controlled airspace in order to reach its required flight level. The RPAS would loose its C2 link and the RPIL would request a new flight plan for an emergency landing. These real-time simulations determined that RPAS can be successfully integrated in controlled airspace. [40] Another study by Schmitt et al. determined that also two remotely piloted aircraft can successfully be integrated in a non-segregated airspace, provided that the RPAS fly according to the rules of manned aircraft. [41] Two single engine MALE UAVs were used for the experiments that involved performing emergency landings at Frankfurt Airport. A delay of 1.5 seconds was added to the C2 link both ways. The results showed that controller workload increased by 14% when measured by the NASA-TLX methodology.

A linear trend between the number of RPAS and the number of potential conflicts is suggested in [42]. This study performed 9 real-time human-in-the-loop simulations of an ATC sector in which 1 - 4 flights were replaced by an RPAS. Two RPAS options were available: a fast one and a slow one. There was no clear trend between the distance travelled and the number of RPAS present in the sector. With two RPAS present, more efficient traffic flows occurred at faster speeds. However, when four RPAS were present, slower speeds meant more efficient traffic. Furthermore, in this study the controller workload went down as the number of RPAS flights increases and total number of flights is kept constant. Also, increasing the speed of the RPAS increased controller workload.

Jung et al. focused in [29] on the impact of a lost C2 link on air traffic flow and ATCo workload, by analyzing two different ATM environments: conventional radar vectoring and Trajectory Based Operations (TBO). The flights at Incheon International Airport were considered during a 30 minute period (13 departures and 28 arrivals). Out of these flights 3 of them were replaced by an RPAS with the same performance as the manned aircraft that it replaced. A temporal C2 link loss was simulated by adding delays of 1, 2 and 10 seconds to the data link. The real-time human-in-the-loop experiments revealed an increase in flight time between 14 - 15% was recorded for the conventional radar vectoring approach and an increase between 2.5 - 3.5 % when TBO

was employed. In both approaches ATCos faced a higher workload, but in the TBO approach the NASA Task Load Index score was lower. The study concluded that while a C2 link delay or failure negatively impacts the air traffic flow and ATC workload, TBO is a possible solution to mitigate such an impact.

The introduction of UAS flights in US National Airspace was studied in [5]. Three scenarios were considered: 2018 (near-future), 2025 (mid-term future) and 2040 (far-future). For the last two scenarios traffic was assumed to increase by 10% and 40% compared to the 2018 case. For all three scenarios 20% of the flights were assumed to be UAS flights. The study concluded that the overall number of blind encounters (potential conflicts) would increase by 41% and 67% compared to the 2018 case. Furthermore, the introduction of UAS flights did not result in delays of manned flights, but it increased the overall agglomeration of the sectors (by approximately 0.3%).

The ERAINT project, a joint program of EUROCONTROL, SESAR Joint Undertaking and Ministerio de Economia y Competitividad of Spain, used eDEP and ISIS+ to analyze the impact of RPAS insertion in non-segregated airspace. [43] Two scenarios were considered, one with a HALE RQ-4A in southern Iceland, with the RPAS departing from Germany (overflying a high traffic density area in central Europe) and a second FRONTEX mission of a MALE MQ-9 in the Spanish Balearic islands, designed for the European Border and Coast Guard Agency. The contingency procedure followed in case of a loss of the C2 link was that the RPAS would fly to its destination according to the initial flight plan. The study concluded that there is limited impact on the ATCo workload. [30]

The results of the simulation carried out under the ERAINT project revealed that the lateral distance flown incurred an increment of 2% when the RPAS was present. This was a result of the ATC heading clearances required to ensure appropriate separation between the RPAS and the surrounding traffic. Moreover, when the number of flights was increased, the non-RPAS flights were not further penalized suggesting that the number of flights does not have a significant impact on the flight inefficiency of interacting traffic. [44] There was no relationship found between fuel cost and delay cost and no clear trend regarding the time spent in the sector by the other flights. [45].

The DEMORPAS project, supported by the Spanish Aviation Safety Agency and the Spanish Air Force, is part of a SESAR Joint Undertaking. The aim of this project is to asses the viability of integrating RPAS in non-segregated airspace across Europe, by conducting real flight trials in which an RPAS interacts with manned aircraft. Two flights were conducted close to the city of Salamanca in Spain, one with a remotely piloted light observation aircraft, ALO, developed by INTA and used in a number of missions for the Spanish Army and another flight with a STEMME S-15 manned aircraft, also owned by INTA. After the flight trials 40% of ATCo believed that it was more difficult to predict the position of the RPAS compared to a manned aircraft. Also, tower control did not perceive the RPAS as a safety risk as much as the area control center did. [3] A data link loss was also simulated. The contingency strategy used was that of flying over a recuperation area where the data link signal was recovered and then the original flight plan was resumed. The conflicts encountered were solved by instructing the manned aircraft to climb. [46]

2.6. Fast Time Simulation Platform

Out of all the different simulators that were analyzed during the literature study part of the project, AirTOp was decided to be the most appropriate tool for this experiment. AirTOp (Air Traffic Optimization)[10] is a modular fast-time simulation platform. It is used by organizations such as DLR, DFS, EUROCONTROL, NATS and NLR[11] for simulating departure, en-route, approach and airport ground movements. AirTOp provides straightforward high fidelity airspace and air traffic which can be used for capacity studies, resectorization projects, reorganization of routes or implementation of free routes. With AirTOp most of the SESAR Key Performance Areas (KPAs) such as capacity, cost effectiveness, efficiency, environment and safety can be measured.

[10] Source: `http://airtopsoft.com/en-route-simulation/` [accessed on 05/04/2017]
[11] Source: `http://airtopsoft.com/our-clients/` [accessed on 05/04/2017]

The module used for this project (both for experiments 1 and 2) is the *En-route Traffic & ATC* one, which supports all key en-route structures and controller tasks. With this module, conflict and resolution rules can be modified such that the RPAS that experiences a failure of the C2 link is excluded from conflict resolution, which simulates the contingency procedure of flying along the initially submitted flight plan. The simulator can generate reports on the number of aircraft movements, conflicts detected, resolutions applied and controller task load, by using the default task load model. [47] The conflict resolution module has not yet been validated for large scale simulations, so for this experiment only the number of blind encounter will be counted, without solving any conflicts. For the second experiment, which focuses on one ATC sector, potential conflicts will be solved using the default AirTOp conflict resolution module.

3

Research Objectives and Questions

This chapter introduces the research objectives, questions and scope of this project. Since there were two different experiments carried out, these are treated separately for the first experiment (Sections 3.1.1 - 3.1.3) and the second one (Sections 3.2.1 - 3.2.3).

3.1. Experiment 1 (country level)

This experiment aims at analyzing how different percentages of flights that are remotely piloted and different C2 link failure rates (failures of the C2 link per flight hour) influence the number of separation losses (blind encounters) on a country level. The experimental set-up is explained in Chapter 4 and the research objective and questions are defined in this section.

3.1.1. Research Objective

As discussed in Section 2.1, 20% of the flights are expected to be remotely piloted by 2050 with the first larger unmanned commercial vehicles expected to begin operations after 2030. Due to the sheer number of RPAS operations, segregation of RPAS flights will not be possible and operations in a mixed environment would be required. Since ATM aims at offering a safe and efficient flight from the moment it departs until it arrives, the main challenge with RPAS operations is to integrate them in the current ATM environment. This should be done by making sure that remotely piloted aircraft emulate themselves to the current operational requirements and procedures and do not expect the existing actors to adapt to RPAS operations in order to ensure safety.

The command and control link was determined in Section 2.2.4 to be critical for safe RPAS operations. This project will contribute to the integration of RPAS in non-segregated airspace by determining how different failure rates of the C2 link impact the ATM Network. Therefore, the research objective is to **establish a methodology for determining the relationship between the number of blind encounters generated by remotely piloted aircraft and the failure rate of the C2 link** by conducting simulations of the Dutch airspace over a period of 24 hours in which different percentages of the manned flights are replaced by RPAS.

3.1.2. Research Questions

Considering the research objectives previously stated, the research questions for this experiment can now be formulated. These are shown below:

1. Will the efficiency of the network be affected by the introduction of RPAS flights?
   (a) What effect would an increase in the percentage of manned flights that are replaced by remotely piloted aircraft have on the number of blind encounters?
   (b) Is there a relationship between the failures per flight hour of the C2 link and the total number of blind encounters?

2. How high can the failure rate of the C2 link be, such that the network capacity is not affected by RPAS flights?

3.1.3. Scope

The scope of this study is twofold. First to determine for a certain failure rate of the C2 link how many remotely piloted flights could potentially be accommodated without impacting the current ATM. And secondly, if a certain percentage of flights are known to be remotely piloted, to determine how high the failure rate could be without impacting the current ATM Network.

3.2. Experiment 2 (sector level)

The aim of this experiment is to establish how an RPAS that experiences a failure of the C2 link right at the moment when it enters an ATC sector influences key ATM performance indicators. The experimental set-up is explained in Chapter 7 and the research objective and questions are defined in this section.

3.2.1. Research Objective

The research objective is to **establish a methodology for determining how an RPAS with a failed C2 link flying alongside manned aircraft influences the flight efficiency of those flights by conducting fast time simulations of an ATC sector** with real flight data in which a percentage of the flights are randomly replaced by a remotely piloted aircraft.

A secondary research objective is to determine how an increasing number of RPAS flights flying alongside manned aircraft will influence the flight efficiency of those flights by conducting fast time simulations of an ATC sector with real flight data in which different percentages of the flights are operated by a remotely piloted aircraft and only one of them experiences a failure of the command and control link.

This experiment is based on a study of a sector in Langen FIR, the busiest flight information region in Germany. The same methodology can be used for other sectors in order to assess the impact of an RPAS flight that experiences a failure of the C2 link.

3.2.2. Research Questions

The research questions are shown below:

1. Will the efficiency of the manned flights be affected when one flight is switched to an RPAS flight which experiences a loss of the C2 link?
   (a) What effect would the introduction of the RPAS flight have on the chosen flight efficiency metrics?
   (b) Is there a relationship between the size of the separation bubble (which is enforced around an RPAS with the failed C2 link) and the flight efficiency of the manned flights?
   (c) Would the choice of the RPAS propulsion system (turbofan/ turboprop) influence the flight efficiency metrics?
2. How would multiple flights being switched to RPAS (with only one experiencing a failure of the C2 link), influence the flight efficiency of manned flights?
3. What relationships exist between the chosen flight efficiency metrics when one or more of the flights are being operated by a remotely piloted aircraft?

3.2.3. Scope

The scope of this study is to understand how different strategies (in terms of the size of the separation bubble enforced around an RPAS once it loses the C2 link) affect key performance indicators of the surrounding flights when dealing with a C2 link loss. This should be used in conjunction with future studies on how ATCos deal with a C2 link loss and what size of the separation bubble is required. The methodology used for this experiment can be applied to other sectors and used to better understand how to plan RPAS operations in order to maintain the same levels of ATM efficiency after a wide scale introduction of RPAS flights.

PART II

EXPERIMENT 1

4

Experimental Set-up: Experiment 1

The aim of this experiment is to determine how different values of the C2 link failure rate influence the number of blind encounters (separation losses). This will be investigated by performing a Monte Carlo analysis for an airspace in which different percentages of flights are replaced by remotely piloted aircraft. The selected airspace, date and time are discussed in Section 4.1. The assumptions that are governing this experiment are the focus of Section 4.2. The selected metric of this experiment is given in Section 4.3. The nine scenarios which will be tested can be found in Section 4.4 and the procedure for carrying out the simulations is addressed in Section 4.5.

4.1. Location, Date and Time

For this experiment the flights in the Dutch airspace during a 24 hour period are considered. The list of flights in the Amsterdam FIR is extracted from DDR, EUROCONTROL's demand data repository. The actual flight data information updated with radar data is used as it contains the most accurate information about the traffic. AIRAC (Aeronautical Information Regulation and Control) cycle 1703 is used, which is the most current data available. The date of March 2^{nd} was selected, as all other week days contained a similar number of flights. An overview of the routes of the 2,969 flights that are considered (between 00:00 - 23:59) can be seen in Figure 4.1.

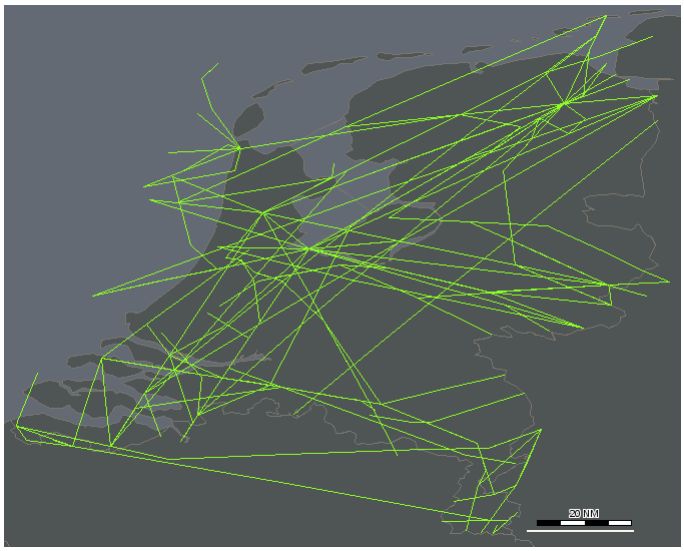

Figure 4.1: Flight Routes in AirTOp

The distribution of the flights during the day is shown in Figure 4.2. On average there are around 200 flights during one hour in the Dutch airspace, the two most busiest periods being between 11 a.m. - 12 p.m. and 6 - 7 p.m.. The least busiest periods are in the late night hours, before 3 a.m.. Half of the flights are only transiting the airspace. One quarter of them are landing at a Dutch airport and 23% of the flights depart from one of the airports in The Netherlands. The remaining 2% of the flights are domestic operations.

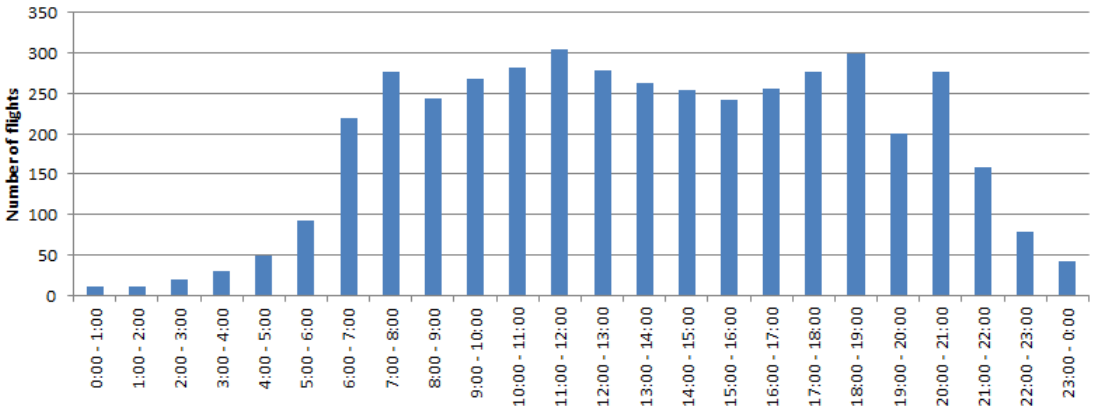

Figure 4.2: Distribution of Flights over Day

Figure 4.3 shows the distribution of aircraft types among the flights. In total, there are 90 different aircraft types. The five most common ones are: Boeing 737-800 (22%), Airbus A320 (16%), A319 (9%), Embraer E190 (7%) and B737-700 (5%). There are also turboprop aircraft such as Bombardier Dash 8 and ATR 45/76. Smaller aircraft such as the Learjet 35 and Pilatus PC-12 are also present.

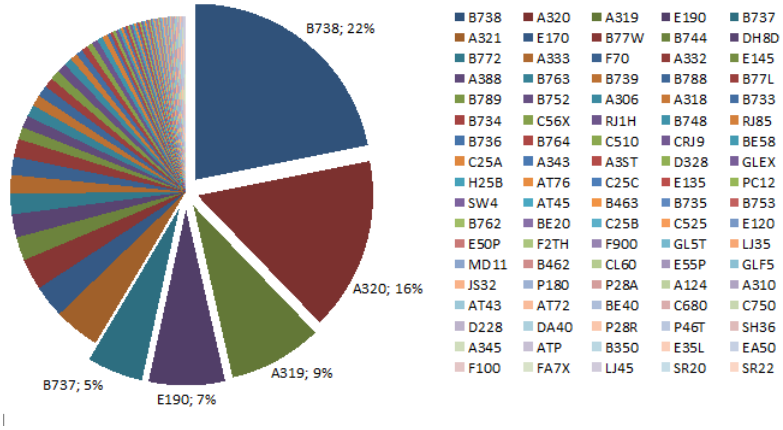

Figure 4.3: Distribution of Aircraft Types among Flights

4.2. Assumptions

The main assumptions that will govern this experiment are summarized below. These assumptions stem from AirTOp limitations and the time-frame of a master thesis project:

1. The C2 link loss occurs immediately after take-off and the RPAS continues its flight to its destination according to the submitted flight plan at departure. Normally a C2 link failure immediately after departure will result in the RPAS returning to its base (see Section 2.2.5). Because the separation bubble around the aircraft could not be created in AirTOp only within a certain time frame (temporal loss of the C2 link), the results of this analysis will provide a "worst-case" view on how RPAS will affect surrounding traffic.

2. The separation bubble around the RPAS will consist of doubling the minimum separation requirements of 5 NM / 1,000 ft enforced by ICAO. [48] This is in line with current studies performed by EUROCONTROL, which envision the integration of RPAS in two stages. The first stage, covering the period up to 2023, deals with creating dedicated corridors and enforcing such separation bubbles around RPAS. [6]
3. The performance of the RPAS will be assumed to be the same as that of the aircraft that it replaced. For instance, if a flight operated by an A320 is switched to RPAS, the same performance model of the A320 will be used in the simulations. This is in line with the requirements of RPAS Class VI as outlined in EUROCONTROL RPAS ATM CONOPS. [6]
4. No weather effects are considered during the simulations, due to AirTOp and run-time limitations.
5. Only IFR/VFR operations are considered for this study. This means that the focus will be on remotely piloted aircraft that share the same airspace with normal transport aircraft, excluding very low level operations (below 500 ft) and very high level operations (above FL600).
6. Only controlled airspace is considered (Classes A - E according to ICAO Annex 11 [49]).

4.3. Selected Key Performance Indicators

The only metric measured in this experiment is the number of blind encounters (losses of separation). A blind encounter occurs when separation drops below 5 NM / 1,000 ft (between two non-RPAS flights) and 10 NM / 2,000 ft (when one of the flights is RPAS). The results obtained are subtracted from the baseline case (when no flights are replaced by an RPAS) in order to determine what is the impact of having remotely piloted aircraft with a C2 link loss.

4.4. Scenarios Tested

The scenarios that will be considered for this experiment are shown in Figure 4.4. As can be seen on the horizontal axis, out of the total number of 2,969 flights in the Dutch airspace, five different percentages of flights will be replaced by an RPAS (10% - 50%). For each percentage of RPAS flights, three different values of the failure rate per flight hour of the C2 link will be considered: 0.01, 0.005 and 0.001. Based on the respective failure rate and the percentage of RPAS flights for a certain simulation, a number of the remotely piloted aircraft will experience an actual failure of the C2 link during the simulation. The exact number of RPAS with a C2 link failure for each case is shown in Figure 4.4 above each of the bars. In total, 9 different scenarios will be simulated which randomly replace between 1 and 15 of the flights with an RPAS that experiences a failure of the C2 link. These scenarios are shown on the vertical axis. For instance, Scenario 3 randomly replaces 3 of the manned flights with an RPAS with C2 link failure. This case is representative for two situations: 10% RPAS flights with a failure rate of 0.01 (first gray bar) and 20% RPAS flights with a failure rate of 0.005 (second blue bar). These scenarios are also summarized in Table 4.1.

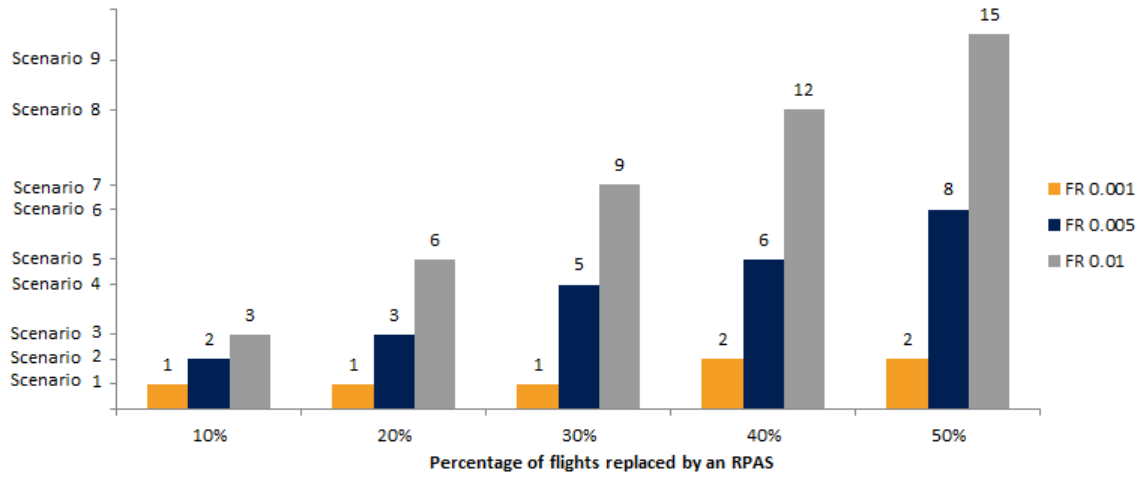

Figure 4.4: Scenarios considered for the AirTOp Simulations (FR = Failure Rate)

Table 4.1: Overview of Simulation Scenarios Considered based on Figure 4.4 (FR = Failure Rate)

Scenario No.	No. RPAS with failed C2 link	Representative for
1	1	10 % RPAS with FR 0.001; 20 % RPAS with FR 0.001; 30 % RPAS with FR 0.001
2	2	10 % RPAS with FR 0.005; 40 % RPAS with FR 0.001; 50 % RPAS with FR 0.001
3	3	10 % RPAS with FR 0.01; 20 % RPAS with FR 0.005
4	5	30 % RPAS with FR 0.005
5	6	20 % RPAS with FR 0.01; 40 % RPAS with FR 0.005
6	8	50 % RPAS with FR 0.005
7	9	30 % RPAS with FR 0.01
8	12	40 % RPAS with FR 0.01
9	15	50 % RPAS with FR 0.01

While JARUS recommends that the failure rate of the C2 link is in the range of 10^{-4} - 10^{-5} failures per hour [33], imposing such values on the number of flights in the Dutch airspace during one day would have resulted in none of the flights being replaced by an RPAS with a failed C2 link. Thus, there is a compromise between running large scale simulations where such a failure rate could be simulated and the number of simulations that can be carried out in the time-frame of a master thesis project considering that larger scale scenarios are more computationally intensive. For instance, according to AirTOp experts at EUROCONTROL Experimental Center in Brétigny, a full one-day simulation of the European airspace takes approximately 8 hours to complete in AirTOp.

4.5. Experiment Outline

The experiment involves three steps:

1. Collecting the input data;
2. Creating the simulation environment;
3. Running the different simulation scenarios.

For the creation of the simulation environment, the following input data is required: GASEL environment, ALL_FT+ traffic files and BADA models. The GASEL environment consists of the locations of airports, waypoints and other navaids. The sector configurations (opening hours, capacity, layers, etc.) and the available ATS routes are also included in the GASEL database. The ALL_FT+ file contains information on all the flights that will be part of the simulation, such as departure and arrival airport and times, aircraft type, airline, registration and route. Both the GASEL and the ALL_FT+ file are downloaded from the Demand Data Repository (DDR) of EUROCONTROL. The BADA files are required in order to have accurate prediction of the aircraft trajectory. Currently there are two BADA versions available. [50] For the purpose of this experiment, BADA 4 was selected because it covers all the aircraft types that will be part of the AirTOp simulations and provides greater precision in the way aircraft performance parameters are estimated over the entire flight envelope. The outline of an ALL_FT+ traffic file is shown in Appendix B, while that of BADA files can be found in Appendix C.

The procedure for creating the simulation environment in AirTOp for this experiment is given in Appendix A.1. There will be two loops when performing the experiments: one in which the selection of aircraft that will be converted to an RPAS type is randomized and another in which the percentage of flights that are switched to an RPAS type is gradually increased. These two loops serve as the basis of the Monte Carlo analysis, because both the flights that are replaced by RPAS and the overall number of RPAS flights in the network will be varied in the simulations.

Depending on the scenario considered, one or more flights are uniformly randomly selected to be replaced by and RPAS with a C2 link loss (the procedure for doing so is outlined in Appendix A.2). The C2 link loss is

simulated by enforcing a new separation standard around the RPAS. The minimum separation standards are defined based on ICAO Doc. 4444 Procedures for Air Navigation Services. [48] For lateral separation Chapter 8 is used, which outlines the procedures and separation minima applicable when radar systems are used. According to paragraph 8.7.4.1, the minimum lateral radar separation shall be 5 NM. The requirement on vertical separation is taken from paragraph 5.3.2, which states that the vertical separation minimum shall be 1000 ft below FL290 and 2000 ft above that level. Following the procedure outlined in Appendix A.3, the separation bubble around the RPAS is created, which is assumed to be double the size of the minimum ICAO values.

The number of runs for each scenario will vary, depending on how quickly the margin of error of the mean number of blind encounters drops to 0.5 when a 95% confidence interval is considered. This will be explained in Chapter 5 which outlines the method of Monte Carlo.

5

The Monte Carlo Method

Monte Carlo methods are usually used to solve problems of probabilistic interpretation. The idea behind it is to make use of randomness when other approaches are impossible, or difficult to use. For the considered experiments, simulating all the possible combinations of flights that could be replaced by RPAS and the different sector entry times would be impossible, hence, the use of the Monte Carlo method. With this method, fractions from a universe of possible outcomes are randomly sampled and based on this, estimates are being made on the entire population. [51]

In probability theory, the "law of large numbers" is a theorem that states that the average of the results obtained from a large number of trials is close to the expected value and that the average will get closer to the actual value as more trials are performed. [52] Assuming that the random variables X_1, X_2, ..., X_N are independent and all drawn from the same distribution, they are called *independent, identically distributed* or i.i.d. random variables. The law of large numbers states that [53]:

$$\mathbb{E}(f(X)) = \lim_{N\to\infty} \frac{1}{N} \sum_{i=1}^{N} f(X_i), \tag{5.1}$$

with probability 1. The Monte Carlo method estimates the expectation $\mathbb{E}(f(X))$ based on the approximation shown in Equation 5.2 (when $(X_i)_{i\in\mathbb{N}}$ are i.i.d and have the same distribution as X).

$$\mathbb{E}(f(X)) \approx \frac{1}{N} \sum_{i=1}^{N} f(X_i) \tag{5.2}$$

For the considered experiments $f(x) = x$, which translates the Monte Carlo estimate in 5.2 to:

$$\mathbb{E}(f(X)) \approx \frac{1}{N} \sum_{i=1}^{N} X_i = Z_N^{MC} \tag{5.3}$$

Equation 5.3 is the usual estimator of the mean that will be used. The mean squared error (MSE) shown in Equation 5.4 is a measure of the variation of the estimator around the parameter's true value (in this case, the mean). Z_N^{MC} is the Monte Carlo estimate for a certain metric after N runs.

$$MSE(Z_N^{MC}) = \frac{\hat{\sigma}^2}{N}, \tag{5.4}$$

where

$$\hat{\sigma}^2 = \frac{1}{N-1} \sum_{i=1}^{N} (X_i - Z_N^{MC})^2 \tag{5.5}$$

is the sample variance of $f(X_1), ..., f(X_N)$. Because the formulation of the mean squared error given in Equation 5.4 provides a squared quantity, the magnitude of the estimate Z_N^{MC} cannot be compared directly with the magnitude of the MSE. Therefore, the root mean square error is considered, which is computed by:

$$RMSE(Z_N^{MC}) = \sqrt{MSE(Z_N^{MC})} = \frac{\hat{\sigma}}{\sqrt{N}} \tag{5.6}$$

Equation 5.6 shows that the Monte Carlo error estimate decreases proportionally to $\frac{1}{\sqrt{N}}$. Because of the square root in the denominator, cutting the error in half requires increasing the number of iterations by a factor of four. This means that increasing the precision of the result with one decimal place would require 100 times as many points. Because of this, the Monte Carlo method represents a trade-off between accuracy and computational cost.

For a finite and at least moderately large N, the estimate of a Monte Carlo analysis can be supplemented with a confidence interval. [51] In Equation 5.7, z_δ denotes the 1 - δ quantile of the standard normal distribution ($\Phi(z_\delta) = 1 - \delta$).

$$\text{Confidence Interval} = (Z_N^{MC} - z_{\delta/2}\frac{\hat{\sigma}}{\sqrt{N}}; \quad Z_N^{MC} + z_{\delta/2}\frac{\hat{\sigma}}{\sqrt{N}}) \tag{5.7}$$

Using 5.6, the upper and lower bounds of the confidence interval can be written as in Equation 5.8. For a 95% confidence interval, δ = 0.05 and $z_{\delta/2} \approx 1.96$. The 95% confidence is a typical value used for Monte Carlo analysis and deciding for a higher value would not necessarily bring added value to the research as is demonstrated in Appendix D.

$$\begin{aligned} \text{Lower bound} &= \overline{X} - z_{\delta/2} \cdot RMSE(Z_N^{MC}) \\ \text{Upper bound} &= \overline{X} + z_{\delta/2} \cdot RMSE(Z_N^{MC}) \end{aligned} \tag{5.8}$$

The margin of error represents how far the lower and upper bounds of the confidence interval are from Z_N^{MC}. The MOE is defined in Equation 5.9.

$$\text{MOE} = z_{\delta/2} \cdot RMSE(Z_N^{MC}) \tag{5.9}$$

6

Results Experiment 1

The results obtained for the first experiment are given in Section 6.1. Section 6.2 summarizes the main findings of this experiment and proposes a new experimental set-up that would offer additional insight on how an RPAS with a failed C2 link affects key ATM performance indicators. This will be the focus of the second experiment (Part III).

6.1. Analysis of Simulation Results

This section contains the results of the first experiment which looked at how different failure rates of the C2 link and different percentages of flights that are switched to an RPAS influence the number of blind encounters. A total of 4,049 simulations have been carried out.

The results of the nine scenarios of the first experiment are shown in Table 6.1. This table includes the number of flights that were replaced by remotely piloted aircraft experiencing a failure of the C2 link for each scenario and the mean number of additional blind encounters that were recorded with respect to the baseline (no flights were replaced by RPAS). The number of blind encounters in the baseline scenario was 1993. The root mean square error (RMSE) and the margin of error (MOE), which were defined in Chapter 5, are also shown in this table. The last column of Table 6.1 includes the percentage increase of blind encounters with respect to the baseline.

Table 6.1: Results of Experiment 1 - Additional Number of Blind Encounters (w.r.t. 1993 in Baseline)

Scenario	**No. RPAS Failed C2 Link**	**Mean** (Z_N^{MC})	**Std. dev.** (σ)	**RMSE**	**MOE**	**Pct. Diff. w.r.t. Baseline**
1	1	1.84	1.95	0.21	0.41	0.09 %
2	2	3.04	2.72	0.23	0.45	0.15 %
3	3	4.67	3.46	0.24	0.47	0.23 %
4	5	7.66	4.35	0.25	0.49	0.38 %
5	6	9.34	4.78	0.25	0.49	0.47 %
6	8	12.45	5.66	0.25	0.49	0.62 %
7	9	14.13	6.09	0.25	0.49	0.71 %
8	12	18.31	7.13	0.25	0.49	0.92 %
9	15	23.58	8.11	0.25	0.49	1.18 %

As can be seen from Table 6.1, having one RPAS with a failed C2 link results in an additional number of 1.84 blind encounters, which represents an increase of 0.09% compared to the baseline situation. This is representative of the case when 10-30% of the flights in the Dutch airspace are switched to RPAS and the failure rate of the C2 link is 0.001 (see Table 4.1). On the opposite spectrum, experiencing 15 failures of the C2 link during one day in the Dutch airspace increased the number of blind encounters with 23.58, or by 1.18% This is representative of the case when 50% of the traffic is RPAS and the failure rate of the C2 link is 0.01. With this

in mind, the values envisioned by JARUS in [33] ($10^{-4} - 10^{-5}$) would increase the number of blind encounters by less than 0.09% when the ATCo would increase separation around the RPA with failed C2 link. The second experiment will zoom in on the C2 link failure and analyze how one RPAS with C2 link failure impacts the non-RPAS flights in a sector that it flies through.

Using the method of least squares, a regression line is fitted to the points from a data set that has the minimal sum of the deviations squared (minimizing sum of squared error). The estimated regression line is given by Equation 6.1, where the estimates $\hat{\beta}_0$ and $\hat{\beta}_1$ are calculated using Equations 6.2 and 6.3. [54] [55]

$$\hat{y} = \hat{\beta}_0 + \hat{\beta}_1 \cdot x \tag{6.1}$$

$$\hat{\beta}_0 = \overline{y} - \hat{\beta}_1 \cdot \overline{x} \tag{6.2}$$

$$\hat{\beta}_1 = \frac{\sum_{i=1}^{N} (x_i - \overline{x}) \cdot (y_i - \overline{y})}{\sum_{i=1}^{N} (x_i - \overline{x})^2} \tag{6.3}$$

As can be seen from Table 6.1, as the number of flights that are switched to RPAS increases, so does the number of blind encounters. Applying the method of least squares , the increase in number of blind encounters is linear as is given be Equation 6.4 (Figure 6.1). This linear relationship is only valid for the area considered for this experiment and under the given assumptions. Expanding the analysis with more RPAS flights and different failure rates might result in a non-linear relationship.

$$\text{Blind Encounters} = 1.55 \cdot \text{RPAS} + 0.04, \quad R^2 = 0.9993 \tag{6.4}$$

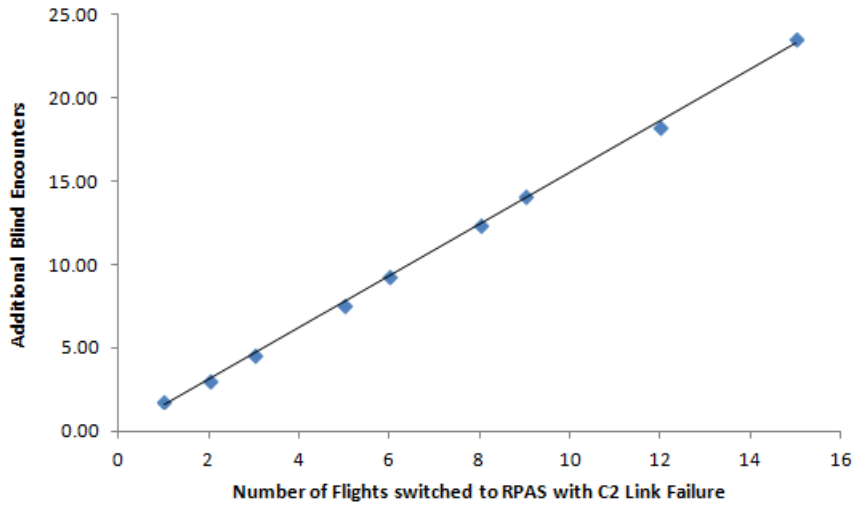

Figure 6.1: Additional Blind Encounters as a Function of Flights switched to RPAS with C2 link Failure

The impact of switching different percentages of flights to RPAS and the different values tested for the failure rate of the C2 link can be analyzed by looking at Figure 6.2. This figure shows how the number of blind encounters varies for the three failure rates that were considered during the experiment. As the failure rate increases, the number of blind encounters during the simulation increases, for all percentages of flights that are switched to RPAS. This is logical since the more often the C2 link fails, there are more situations in which the controller would have to increase the separation around the RPAS and hence, the are more cases in which the separation will be lost between the RPAS and the manned aircraft with which it interacts during the flight.

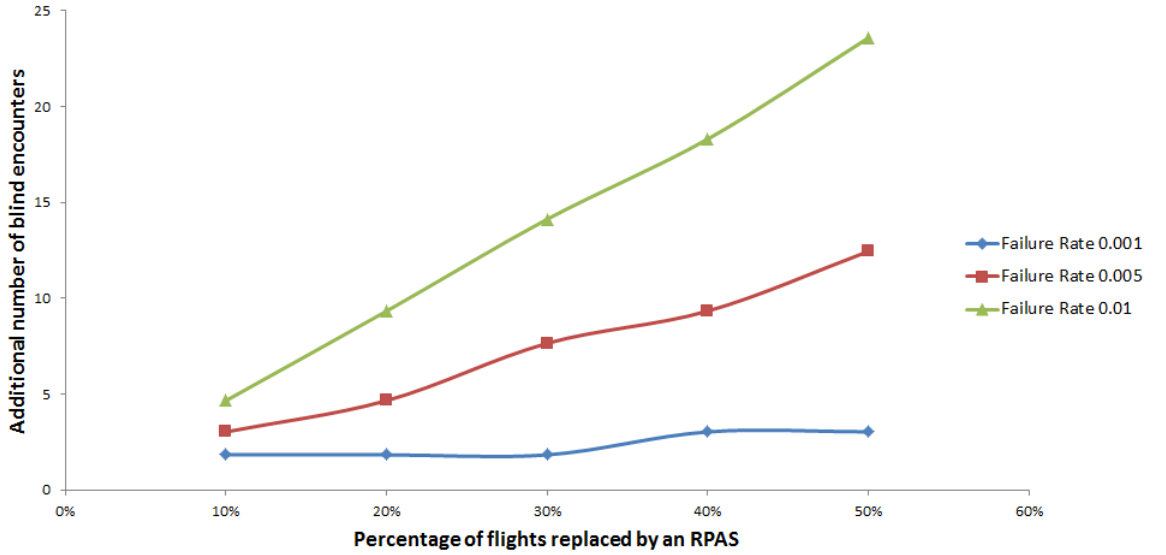

Figure 6.2: Number of additional Blind Encounters VS. Percentage of Flights switched to RPAS for three Failure Rates of the C2 Link

6.2. Conclusion Experiment 1

As explained in Chapter 4 the purpose of this experiment was to investigate how different failure rates of the C2 link affect the capacity of the airspace, by considering the Dutch airspace in which a number of flights would be replaced by an RPAS with a failed command and control link. The number of flights that were switched to RPAS with C2 link failure was determined by multiplying the total number of flights with the percentage of flights that are assumed to be remotely piloted and the failure rate of the C2 link for a particular scenario. Then, the separation around RPAS was doubled and the number of blind encounters was measured (occurrences in which the separation was lost). The blind encounters obtained in the baseline situation (no RPAS flights) was subtracted from the results, such that the impact of the RPAS fights can be analyzed.

Nine different scenarios were considered, in which 1 - 15 flights were switched to an RPAS with a failed C2 link. These corresponded to replacing 10% - 50% of the total flights in the airspace by an RPAS with failure rates of the C2 link of 0.01, 0.005 and 0.001.

Having one RPAS with a failed C2 link resulted in an additional number of 1.84 blind encounters, which represents an increase of 0.09% compared to the baseline situation were there were a total of 1993 blind encounters. On the opposite spectrum, experiencing 15 failures of the C2 link during one day in the Dutch airspace increased the number of blind encounters with 23.58, or by 1.18%. There was a linear relationship found between the number of RPAS flights and number of blind encounters: one additional RPAS flight increasing on average the total number of blind encounters by 0.1%. Also, a lower failure rate of the C2 link reduces the number of blind encounters. A failure rate of 10^{-3} increases the number of blind encounters by up to 0.15% when as many as 50% of the flights are converted to an RPAS. Thus, values of 10^{-4} and 10^{-5} as suggested by JARUS [33] will increase the overall number of blind encounters by an even smaller amount.

Using this approach to test lower failure rates would require a larger population of flights, so an extension of this study would be to increase the simulated area, either by considering a number of adjacent FIRs or the entire European airspace. This study would only offer an indication on how many more blind encounters air traffic controllers would have to handle and would not assess the impact that the RPAS flights have on the flights that it interacts with. This is because in the simulations carried out for this experiment only the conflict detection module of AirTOp was used. Thus, the blind encounters were counted, but not solved. Solving the potential conflicts would require the activation of the conflict resolution module of AirTOp. However, this module has not yet been tested for such large scale experiments and in conjunction with the higher run time required for such a simulation, it was not feasible to also solve the conflicts with the available simulation tools.

In order to better understand what happens with the flights that interact with an RPAS that experiences a

failure of the C2 link, a new experiment is proposed. This experiment would only focus on a sector in which all potential conflicts resulting from an increase in separation around the RPAS are resolved. This way the impact of the RPAS on key ATM performance indicators would be assessed. The second experiment will be the focus of the next part of the thesis report. The new experimental set-up is presented in Chapter 7.

PART III

EXPERIMENT 2

7

Experimental Set-up: Experiment 2

The aim of this experiment is to establish how a remotely piloted aircraft that experiences a failure of the C2 link right at the moment when it enters an ATC sector influences key ATM performance indicators. Section 7.1 introduces the sector that will be considered and Section 7.2 the assumptions which are associated with this experiment. The Key Performance Indicators considered are explained in Section 7.3. The 14 scenarios that are simulated are outlined in Section 7.4. Two RPAS performance models are used for this experiment: the MQ-9 Reaper and RQ-4A Global Hawk. These RPAS are discussed in Section 7.5. The outline of the experiment and how AirTOp and MATLAB are connected to each other is the topic of Section 7.6.

7.1. Sector EDGGPHHM

The ideal sector for this experiment is one that combines cruising, climbing and descending flights and brings together different routes such that the interaction of an RPAS with conventional (manned) flights and the impact of using different performing RPAS models can be better studied. The German airspace is Europe's busiest in terms of IFR movements. [56] This airspace is divided in three Flight Information Regions (FIR) for lower airspace (up to FL245) and two Upper Flight Information Regions (UIR) for the airspace above FL245. [57] The FIRs are: Bremen, Langen and München and are shown in Figure 7.1. The two UIRs are Rhein and Hannover and are shown in Figure 7.2.

Using the same AIRAC cycle as for the first experiment (1703), the entry counts of the three FIRs account for 22%, 41% and 28% of all entries in the German airspace. As Langen FIR is the busiest flight information region, one sector from this FIR will be selected. There are two control areas in Langen FIR: NCTA and SCTA, which are shown in Figures 7.3 and 7.4. SCTA contains mostly traffic arriving and departing from Frankfurt airport (ICAO: EDDF), which is Germany's busiest airport with 1,264 daily flights. [58] Following consultations with the EUROCONTROL Network Manager, sector EDGGPHHM in NCTA was selected as it includes traffic arriving and departing from four German airports: Düsseldorf (EDDL), Dortmund (EDLW), Köln/Bonn (EDDK) and the regional airport of Münster (EDDG). This was the preferred choice because of the different routes and the fact that it also contains climbing and descending traffic and not only cruising flights.

Figures 7.5 and 7.6 show the lateral and top views of sector EDGGPHHM, which only covers flights between FL115 and FL245. The same date as that selected for the first experiment is used (2^{nd} of March 2017) and the flights during the busiest one hour period are considered for the simulation. This corresponds to the time between 6:00 - 7:00 a.m. when there were 53 flights present in the sector. The data is extracted in AirTOp from EUROCONTROL's DDR and the actual flight data information updated with radar data is used as it contains the most accurate information about the traffic.

Out of the 53 flights which are part of the experiment, there are 10 flights departing from and 21 arriving at EDDL, 3 flights departing from EDLW, 3 flights departing from and 4 arriving at EDDK and 2 flights departing from and one arriving at EDDG. The remaining 9 flights are overflying the sector, heading to or originating from Amsterdam, Brussels, Budapest, Eindhoven and Vilnius. Figure 7.7 shows the routes flown by the 53

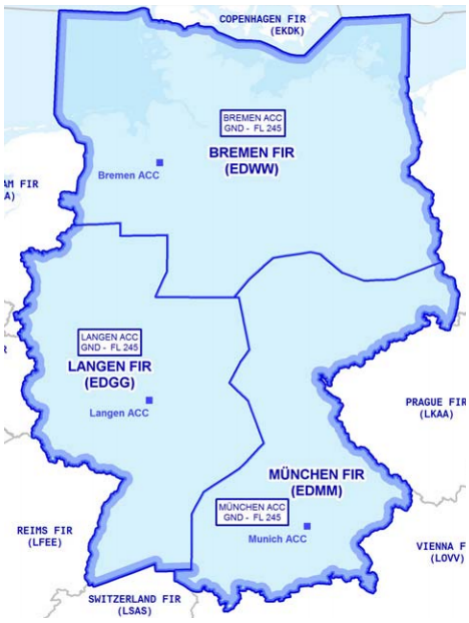

Figure 7.1: Flight Information Regions in Germany [57]

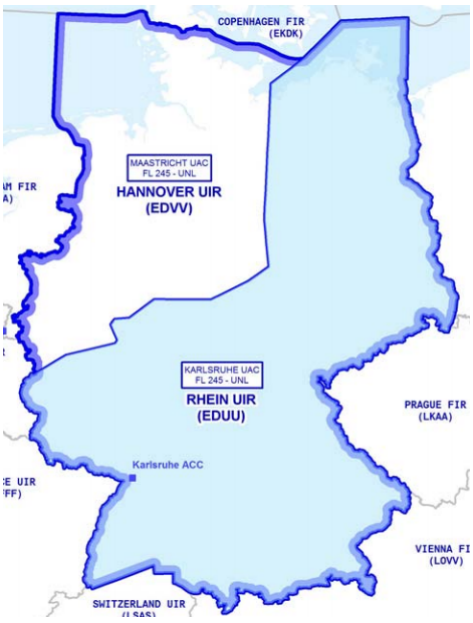

Figure 7.2: Upper Flight Information Regions in Germany [57]

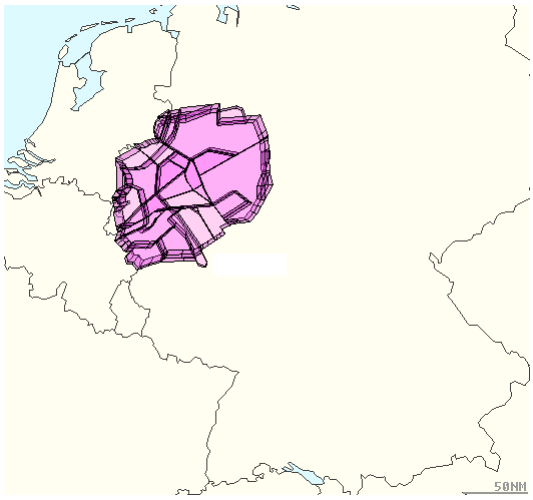

Figure 7.3: Top view EDGGNCTA (NEST)

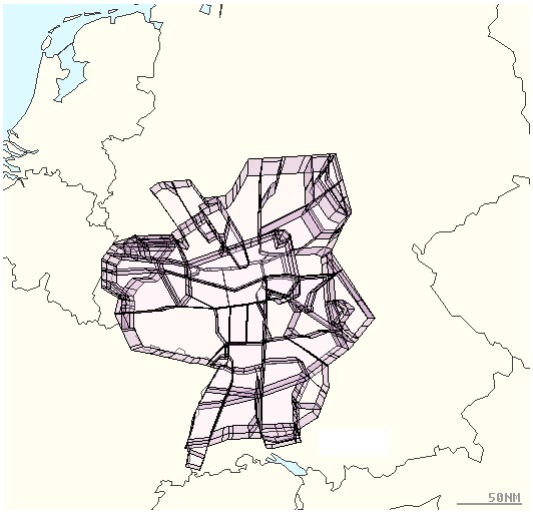

Figure 7.4: Top view EDGGSCTA (NEST)

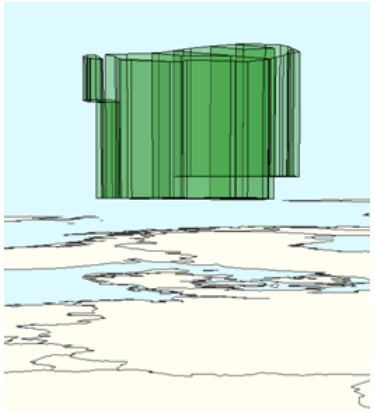

Figure 7.5: Lateral View of Sector EDGGPHHM (FL115 - FL245)

Figure 7.6: Top View of Sector EDGGPHHM

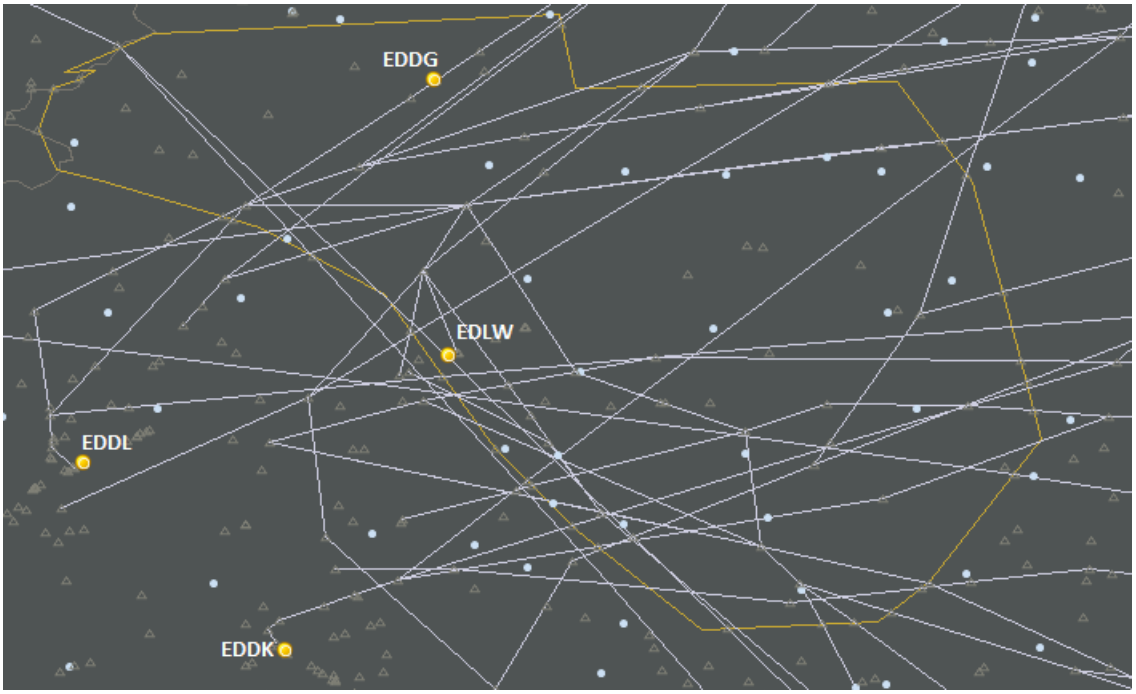

Figure 7.7: Flight Routes in Sector EDGGPHHM between 06:00-07:00 a.m. (AirTOp)

flights in sector EDGGPHHM.

The flights considered are being operated by a mix of turboprop and turbofan aircraft. In total 11 different aircraft types are used, as shown in Table 7.1. This table summarizes the performance of each aircraft type and indicates the number of each units that are part of the simulation. Out of all the flights, 15% are operated by turboprop aircraft such as the DH8D and AT75 and 85% by turbofan aircraft, most of them belonging to the A320 family.

Table 7.1: Specifications of Aircraft used in Simulations (Data collected from: Airbus[59], ATR[60], Boeing [61], Bombardier [62], de Havilland [63], Embraer [64] and British Aerospace [65].)

Aircraft ICAO Code	Manufacturer	Range [km]	Ceiling [ft]	MTOW [kg]	Cruise speed [kt]	Engine Type	No. a/c in simulation
A319	Airbus	6950	40000	75500	448	Turbofan	11
A320	Airbus	6100	40000	78000	448	Turbofan	23
A321	Airbus	5950	40000	93500	448	Turbofan	4
AT75	ATR	1450	25000	22000	275	Turboprop	1
B738	Boeing	5500	41000	75000	452	Turbofan	1
CR9	Bombardier	2880	41000	38300	448	Turbofan	1
DH8D	de Havilland Canada	2040	27000	30500	325	Turboprop	6
E135	Embraer	3240	37000	20000	450	Turbofan	1
E170	Embraer	3980	41000	38600	470	Turbofan	2
E190	Embraer	4540	41000	51800	470	Turbofan	2
JS32	British Aerospace	1260	25000	6950	230	Turboprop	1

7.2. Assumptions

The assumptions that govern this experiment are given below:

1. The C2 link loss occurs at the moment when the RPAS enters the sector and will remain down until the remotely piloted aircraft exists the sector.

2. In case an RPAS experiences a loss of the C2 link, the contingency strategy used is that of proceeding along the initially submitted flight plan. ATCo will enforce a separation bubble around the RPAS.

3. The separation bubble enforced around an RPAS with a C2 link failure is defined as a percentage increase with respect to the minimum separation requirements defined by ICAO in Doc. 4444 Procedures for Air Navigation Services (5 NM lateral/ 1,000 ft vertical). [48]

4. There is no communication delay present between an RPAS with a working C2 link and air traffic controllers. As discussed in Section 2.5 a 1.5 second delay is typically encounters in RPAS operations, but was not part of the AirTOp simulation environment.

5. RPAS are fully integrated in the airspace and a Detect and Avoid (DAA) system is present in the form of the default AirTOp conflict detection and resolution module. This enables the controllers and other aircraft to detect the RPAS and solve potential conflicts.

6. A preliminary airspace assessment has been executed and there are no no-drone zones in the sector considered.

7. No weather effects are considered during the simulations, due to AirTOp and run-time limitations.

8. Only IFR/VFR operations are considered for this study. This means that the focus will be on remotely piloted aircraft that share the same airspace with normal transport aircraft, excluding very low level operations (below 500 ft) and very high level operations (above FL600).

7.3. Selected Key Performance Indicators

This section introduces the 9 metrics that will be measured during the experiment. These metrics are summarized in Table 7.2 which includes the abbreviations used throughout the remaining of the report and the units in which they are measured.

Table 7.2: Overview of KPIs considered for Experiment 2

Key Performance Indicator	Abbreviation	Measurement Unit
Number of Potential Conflicts	KPI_1	[-]
ATCo Task Load	KPI_2	[Pct. time active/10-min. interval]
Sector Occupancy	KPI_3	[Aircraft/min]
Distance	KPI_4	[NM/flight]
Flight Time	KPI_5	[sec/flight]
Fuel Consumption	KPI_6	[kg/flight]
Lost Altitude	KPI_7	[ft/desc_flight]
Gained Altitude	KPI_8	[ft/climb_flight]
Altitude Deviation	KPI_9	[ft/flight_changing_level]

Number of potential conflicts (KPI_1)

A blind encounter occurs in the moment when the minimum separation requirements (both lateral and vertical) between two aircraft are no longer met. A potential conflict is defined as the violation of the minimum separation between the pseudo radar controllers' prediction of the future position of a pair of aircraft. This metric measures the number of potential conflicts that are encountered in the sector per run.

In AirTOp a "ghost" aircraft departs at every step from the "real" aircraft and flies ahead for 10 minutes. This is similar to the simulator running ahead 10 minutes for every flight at every step of the simulation in order to determine if there will be any separation losses along the way. A potential conflict is detected 5 minutes ahead of the time when the real conflict would take place. When a potential conflict is detected the radar controllers will request the aircraft (either one, or both) to perform a series of resolution actions (see Section 8.1), such that an actual conflict is avoided. If the conflict is between an RPAS and another aircraft, the RPAS will be excluded from the conflict resolution strategies in order to simulate the loss of the C2 link, during

which the remotely piloted vehicle would be uncontrollable and would fly along the initially defined route (in accordance with the project assumption in Section 7.2).

Controller Task Load (KPI_2)

While in real time simulations the term controller workload is used, in fast time simulations this is referred to as controller task load. This comprises two elements: task-based and monitoring-based workload. The unit of measurement is the percentage of time a controller is active during a 10-minute interval.

Examples of task-based workload are: altitude change clearances, resolving conflicts, checking speed, maintaining separation and updating flight strip. For instance if in a 10-minute time interval there are 10 altitude change instructions and for each the controller spends 6 seconds, the task-based workload associated with the altitude change manoeuvers is $10 \cdot 6/600 = 10\%$. Monitoring-based workload encompasses tasks which span a certain period of time, such as monitoring an aircraft from the moment it enters the sector until it is handed off in the next sector. For example, if an ATCo spends 12 seconds on average to monitor a flight and during a 10-minute interval there are two flights to be monitored, one for 2 minutes and another for 7, the total monitoring time is 9 minutes. This means $9 \cdot 12 = 1.8$ minutes spent on monitoring the aircraft, or a monitoring-based workload of 18%.

AirTOp assigns by default an average work duration for each ATCo task. During the simulated period (6:00-07:00 am) there will be 6 10-minute time-blocks which contain the total ATCo task load. Taking the average of the 6 task load values gives the average controller task load during one run. It should be borne in mind when interpreting the results, that for this experiment AirTOp assumes a single controller for the sector.

Sector Occupancy (KPI_3)

The sector occupancy is defined as the number of flights that are present (handled by ATC) in the sector during one minute. After each run is completed the average occupancy for the 60 minutes of the simulation is calculated.

Distance flown (KPI_4)

The distance flown by a flight is defined as the number of nautical miles that a flight has travelled while within the boundaries of the sector. This value is computed every time a flight leaves the sector. After the completion of each run, the average distance flown is calculated for all non-RPAS flights.

Flight Time (KPI_5)

For each flight, the flight time is defined as the interval of time, in seconds, during which the flight is within the boundaries of the sector (both the lateral and vertical boundaries). This metric is calculated by taking the difference between the sector exit and entry times, which are recorded by the simulator every time a flight enters/leaves one of the ATC sectors. For each run, the average flight time is computed by dividing the sum of all non-RPAS flight times to the number of non-RPAS flights.

Fuel Consumption (KPI_6)

The fuel consumption (in kilograms) of a flight is measured only during the time interval when the aircraft is within the boundaries of the sector. It depends on the type of aircraft, its altitude and its state (cruising/descending/climbing). This is done automatically by AirTOp with information from the BADA file of each aircraft. Appendix G explains the procedure for calculating fuel consumption. This metric records the average fuel consumption of all non-RPAS flights.

Each time a flight enters the sector its altitude (in ft.) will be recorded as the entry altitude. Once it leaves the sector, the current altitude will represent the exit altitude (in ft.). In order to analyze the variation of the flights' flight level over the simulation (if solving the potential conflicts resulted in flights to descend/climb), three different metrics will be used: lost altitude, gained altitude and altitude deviation. These metrics are

defined below:

Lost Altitude (KPI_7)

When a flight leaves the sector at a lower altitude than at the one it entered, the difference between the exit and entry altitudes is added to the altitude lost variable (in ft, absolute value). This variable sums up the altitude changes of the flights that are descending during the simulation. After each run is completed, this metric will record the average altitude that was dropped by the descending flights (only applied to non-RPAS flights).

Gained Altitude (KPI_8)

When a flight leaves the sector at a higher altitude than at the one it entered, the difference between the exit and entry altitudes is added to the altitude gained variable (in ft). This variable sums up the altitude changes of the flights that are climbing during the simulation. After each run is completed, this metric will record the average altitude that was gained by the climbing flights (only applied to non-RPAS flights).

Altitude Deviation (KPI_9)

This metric represents the average of KPIs 7 and 8 and is used to analyze the total overall altitude changes that occurred during a simulation.

7.4. Scenarios Tested

This experiment consists of 14 scenarios, which consider two cases: only one RPAS present in the sector and multiple RPAS are present in the sector. Scenarios 1_1 - 1_8 replace one of the flights with an RPAS with a C2 link failure. Two RPAS performance models are used (MQ-9 Reaper and RQ-4A Global Hawk as will be discussed in Section 7.5) and 4 separation strategies are tested: no separation increase (same as for the other flights in the sector - Scenarios 1_1 and 1_5), 20% separation increase (6 NM/ 1,200 ft - Scenarios 1_2 and 1_6), 40% separation increase (7 NM/ 1,400 ft - Scenarios 1_3 and 1_7) and 60% separation increase (8 NM/ 1,600 ft - Scenarios 1_4 and 1_8). In the second part of the experiment (Scenarios 2_1 - 2_5) 10 - 20% of the flights are replaced by a MQ-9 Reaper and tests larger values of the separation bubble (60 - 200% increase compared to the minimum 5 NM/ 1,000 ft ICAO requirement). Scenario 0 represents the baseline, in which no flights were switched to RPAS. Table 7.3 summarized the situations which are tested for this experiment.

Table 7.3: Scenarios for Experiment 2

Scenario	RPAS C2 Failure	Other RPAS	Separation Bubble Increase	Separation Value RPAS C2 Failure
0 (Baseline)	No	No	No	No
1_1	1 x RQ-4A	No	0%	5 NM / 1,000 ft
1_2	1 x RQ-4A	No	20%	6 NM / 1,200 ft
1_3	1 x RQ-4A	No	40%	7 NM / 1,400 ft
1_4	1 x RQ-4A	No	60%	8 NM / 1,600 ft
1_5	1 x MQ-9	No	0%	5 NM / 1,000 ft
1_6	1 x MQ-9	No	20%	6 NM / 1,200 ft
1_7	1 x MQ-9	No	40%	7 NM / 1,400 ft
1_8	1 x MQ-9	No	60%	8 NM / 1,600 ft
2_1	1 x MQ-9	9 x MQ-9 (20% of flights)	60%	8 NM / 1,600 ft
2_2	1 x MQ-9	9 x MQ-9 (20% of flights)	100%	10 NM / 2,000 ft
2_3	1 x MQ-9	9 x MQ-9 (20% of flights)	200%	15 NM / 3,000 ft
2_4	1 x MQ-9	4 x MQ-9 (10% of flights)	100%	10 NM / 2,000 ft
2_5	1 x MQ-9	14 x MQ-9 (30% of flights)	100%	10 NM / 2,000 ft

7.5. Selected RPAS Models

Depending on the scenario that is considered (Section 7.4), one or more flights are randomly switched to an RPAS. Out of the RPAS flights only one will experience a failure of the C2 link, which is simulated by enforcing a special separation bubble around it that is larger than that for the other aircraft, Also, this RPAS is excluded from any conflict resolution strategies.

The current EUROCONTROL BADA 3 RPAS package contains the performance model for four RPAS types: RQ-4A Global Hawk, MQ-9 Reaper, Generic Tactical RPAS and RQ-2A Pioneer. [66] However, only the first two models can be used for this experiment as the Tactical and RQ-2A RPAS cannot fly at the altitudes which are considered for the EDGGPHHM sector. The Global Hawk (Figure 7.8[1]) is an unmanned surveillance aircraft developed by Northrop Grumman and is used by the United States Air Force in worldwide military operations. [67]. Powered by a turbofan engine, the RQ-4A can fly up to 28 hours or 14000 km. The MQ-9 Reaper is a turboprop unmanned aerial vehicle used in long endurance or medium altitude surveillance missions. Both NASA [2] and the US Customs and Border Protection [22] make use of this RPAS for missions such as monitoring wildfire and illegal cross-border activities. Table 7.4 summarizes the performance of the two RPAS types that will be used for the experiment.

Figure 7.8: Northrop Grumman RQ-4A Global Hawk

Figure 7.9: General Atomics MQ-9 Reaper

Table 7.4: Specifications of RPAS used in Simulations [66]

BADA Code	Aircraft Name	Range [km]	Endurance [h]	Ceiling [ft]	MTOW [kg]	Cruise speed [kt]	Engine Type
RP01	RQ-4A Global Hawk	14000	28	60000	14628	335	Turbofan
RP02	MQ-9 Reaper	1852	14	50000	4760	200	Turboprop

When compared to the other aircraft in the experiment, apart from the differences in cruise speeds between RPAS and commercial manned aircraft (Tables 7.4 and 7.1), there are also differences in the climb and descent performances of the RPAS models that are considered. The equation for rate of climb (RC) is derived from the equations of motion assuming an unsteady quasi-rectilinear climbing flight. [68] RC is calculated by Equation 7.1, where RC_{st} represents the rate of climb during steady flight ($\frac{dV}{dt} = 0$), which is given in Equation 7.2. V represents the true airspeed, W the weight of the aircraft, T its trust, D the drag, P_a and P_r available and required power and g the standard acceleration due to gravity.

$$RC = \frac{RC_{st}}{1 + \frac{V}{g} \cdot \frac{dV}{dh}} \tag{7.1}$$

$$RC_{st} = \frac{V \cdot (T - D)}{W} = \frac{P_a - P_r}{W} \tag{7.2}$$

[1] Source: http://www.northropgrumman.com/MediaResources/Pages/Photo.aspx?pid%3DGH-10020_021%26rel%3D%2F%26name%3DPhotos [accessed on: 22/08/2017]

[2] Source: https://www.nasa.gov/centers/armstrong/news/FactSheets/FS-097-DFRC.html [accessed on 23/08/2017]

As typical climb manoeuvers are performed at constant indicated airspeed and constant power setting, true airspeed increases with increasing altitude, which is reflected in different rate of climb values depending on each flight level. Figures 7.10 and 7.11 show the typical rates of climb and descent for the RQ-4A and MQ-9 RPAS as well as for the commercial civil aircraft most frequently used in this experiment. These figures are based on the BADA performance table file (PTF). The values for the Global Hawk and Reaper are validated with those in [69] and [70].

From figure 7.10 it can be seen that the MQ-9 has a lower climbing performance than all the other aircraft, with the exception of the ATR-75. Only one of the 53 flights in the simulation is operated by and ATR aircraft, which means that in most cases the Reaper will be the aircraft with the lowest climbing performance. On the other hand, the RQ-4A can climb faster than any other commercial aircraft. However, from Figure 7.11 one can see that the Global Hawk has the lowest descent performance out of all aircraft considered, with descent rates between 1200 - 1600 fpm for the flight levels which are part of the sector. Up to FL180 the MQ-9 has a similar performance with the ATR-75 and above that level its performance deteriorates. The DH8D is unlike any of the other aircraft considered, with an overall decrease in descent performance as flight level increases and three local peaks at FL120, FL150 and FL180. These differences in climb and descent performances should be kept in mind when analyzing the results of the simulations.

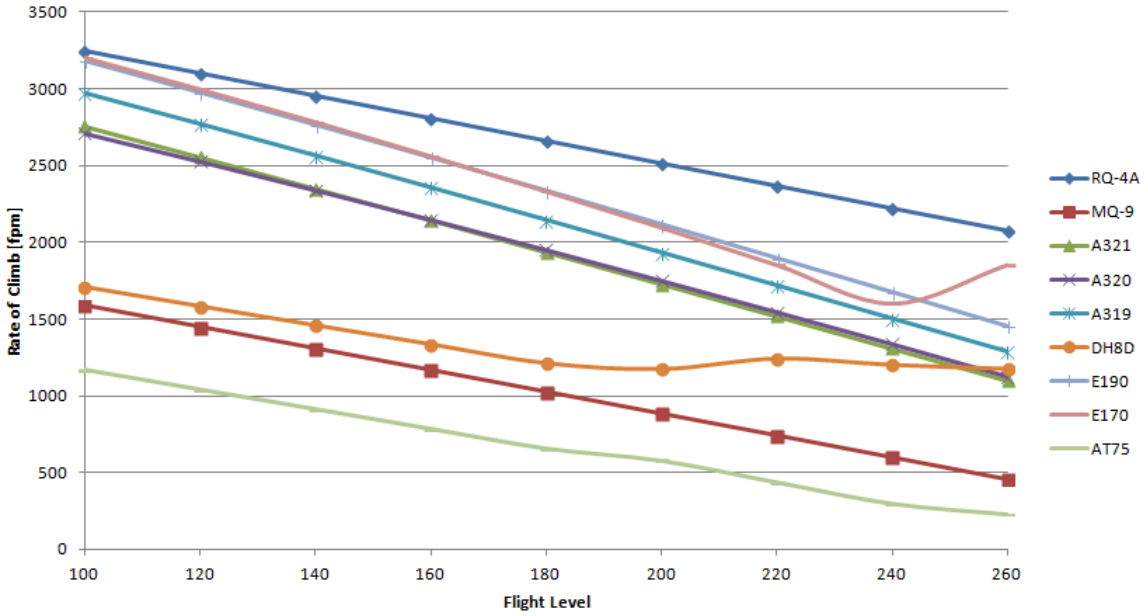

Figure 7.10: Typical Rate of Climb Values (RPAS and Commercial Civil Aircraft) - Based on BADA data

7.6. Experiment Outline

This experiment uses MATLAB for the creation of AirTOp project files, randomization of flights that are switched to RPAS, extracting the results and calculating all KPIs. AirTOp is used for running the simulation itself and for randomizing the sector entry times of all flights. Microsoft Powershell is used for extracting the AirTOp output files into the MATLAB directory. Figure 7.12 shows the interaction between the three programs.

The coordinates of the sector are used in AirTOp to create a polygon and then from this polygon a sector block is defined. This block is divided in three ATC sectors: SECT-DN (0 - FL115), SECT (FL115 - FL245) which is the sector on which the analysis will be focusing and SECT-UP (FL245+). Two additional ATC sectors (SECT-EAST and SECT-WEST) are created in the same way around SECT, such that the flights can be simulated a few minutes before entering sector EDGGPHHM. The detailed procedure associated with creating a simulation environment is explained in Appendix H.

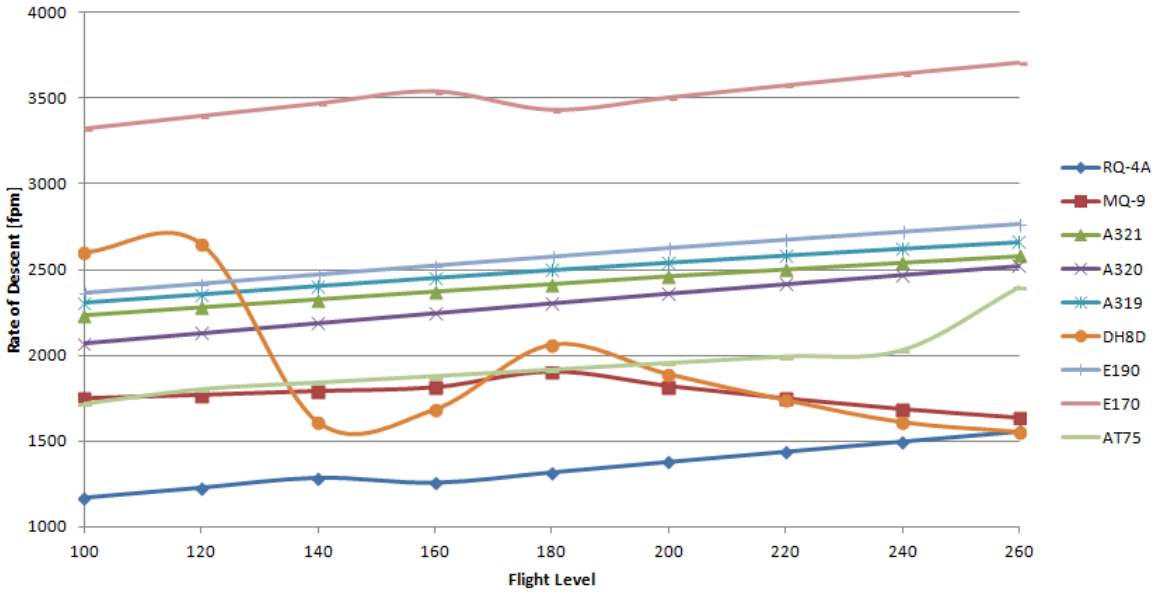

Figure 7.11: Typical Rate of Descent Values (RPAS and Commercial Civil Aircraft) - Based on BADA data

For each run the sector entry time, is uniformly randomly varied between -60 and + 60 seconds around the original value. This ensures a variability in the sector entry times of the flights, which could occur due to the weather or delays in a previous ATC sector. The Monte Carlo algorithm that will be used in this case is summarized below:

input:
- set of sector entry times $X_i, i = \overline{1,53}$ for each flight in the simulation;
- separation value used in case of C2 link failure;
- type of RPAS;
- number of runs N, $N \in \mathbb{N}$;

randomness used:
- uniformly vary $(X_{i,j})_{j \in \mathbb{N}}$ for each i = $\overline{1,53}$ around +/- 60 seconds of actual sector entry time;
- flight that will be switched to RPAS;

output:
- an estimate Z_N^{MC} after N runs for each of the 9 metrics calculated as explained in Chapter 5;

The next chapter focuses on the AirTOp default conflict detection and resolution adapter and analyzes the frequency of resolution actions taken to solve the conflicts for one of the scenarios of this experiment. The complete results of the 14 scenarios are given in Chapter 9 and a statistical analysis on them is performed in Chapters 10 and 11.

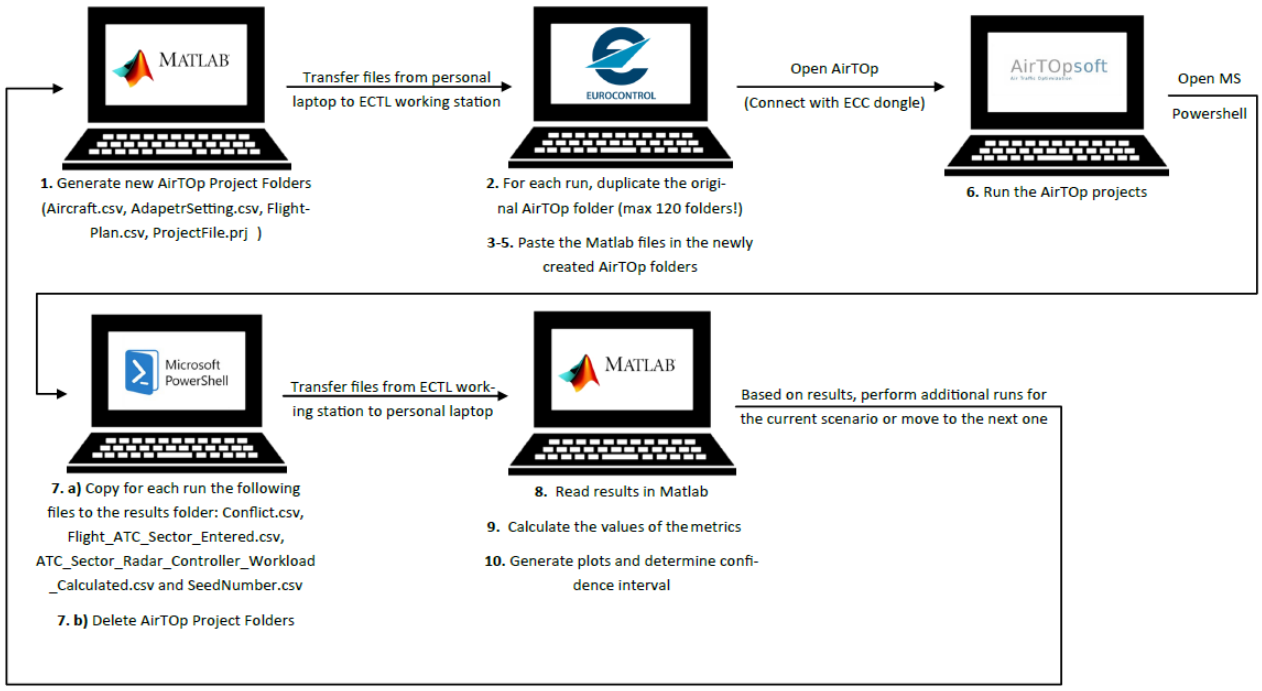

Figure 7.12: Experiment 2 combines the use of MATLAB, AirTOp and MS Powershell

8

Detecting and Resolving Potential Conflicts in AirTOp

One of the advantages of the second experiment over the first one was its ability to solve the potential conflicts that were generated by an increase in separation around an RPAS that experienced a failure of the C2 link. For this, the default AirTOp Conflict Resolution Rule Base Tree is used which is explained in Section 8.1. An example on how a conflict is detected and solved is given in Section 8.2. Section 8.3 considers all the runs of Scenario 2_2 (which replaced 20% of the flights by an MQ-9 Reaper) and analyzes the distribution of the conflict resolution actions that were selected. The complete results of all scenarios are given in Chapter 9.

8.1. The AirTOp Conflict Resolution Rule Base Tree

In order to avoid a potential loss of separation that has been identified to happen between two aircraft at a certain point in the future, a conflict resolution rule base (CRRB) is followed by the air traffic controller. At each moment and from each aircraft, a "ghost" aircraft departs which flies ahead of the flight for 10 minutes. In other words, the simulator runs ahead the upcoming 10 minutes in order to identify any situations in which a loss of separation could occur. A potential conflict begins 5 minutes before the actual separation would be lost. This is the time when the ATCo would instruct one (or both) aircraft to perform a conflict resolution action.

In order for the ATCo to determine what action to perform such that a conflict is avoided, the Conflict Resolution Rule Base Tree is followed. The default AirTOp Conflict Resolution Rule Base Tree is shown in Figure 8.1. The branches of this tree are represented by the type of the conflict and the leaves by the resolution action that has to be taken. The way in which the ATCo deals with a potential conflict is the following:

1. It takes the root node of the CRRB and tests whether the conflict condition is met (if the vertical and lateral separation requirements are violated). If this condition is false (so no conflict), the ATCo leaves the CRRB. Otherwise, the controller moves on to the next step.

2. If the condition is true, the first child of the root node is examined.

    (a) If it is a resolution action (and it is enabled) and if by applying it to the ghost aircraft the conflict is avoided, then that resolution action is applied to the actual aircraft and the ATCo leaves the CRRB. In case the resolution action would not solve the conflict, the next resolution action is tested.
    (b) If it is a conflict condition node, the ATCo applies that condition to the conflict (similar to Step 1) and if it is true it moves to the child of that conflict condition node. If the condition is false, then the ATCo goes back to the last node that was true and repeats this step with its next child node.

The CRRB tree has five levels and the controller performs a depth-first search in order to determine which resolution action to apply. The first level tests whether the conflict condition is met (if both the lateral and vertical separation distances are not met). Based on whether the aircraft is an RPAS (with a C2 link failure)

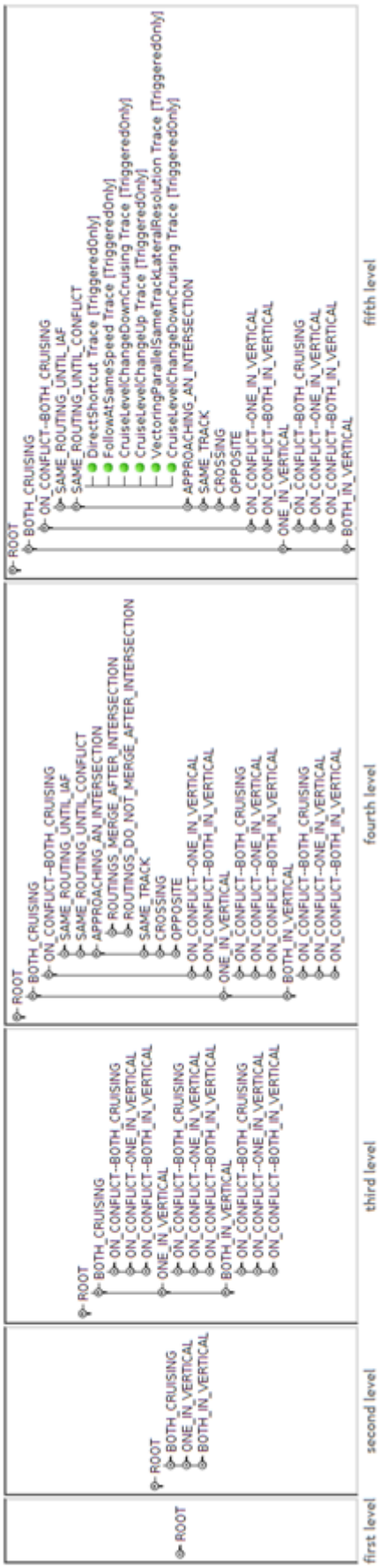

Figure 8.1: Default AirTOp Conflict Resolution Rule Base Tree [47]

or not, different separation standards are applied compared to the other aircraft in the simulation. The separation around the RPAS depends on the scenario that is being tested. The second level checks whether the two aircraft are currently cruising or performing an altitude change manoeuver. The third step looks at the vertical state of the aircraft at the time of the conflict: both aircraft are in cruise, one is climbing/descending, or both climbing/descending. The fourth level looks at the directions that the flights are heading to (whether they fly on the same track towards an initial approach fix, or if they approach an intersection), such that specific resolution actions can be tested. On the fifth level of the CRRB the conflict resolution actions are located. The order in which these actions are added to the CRRB depends on their impact on the ATCo task load and on how much it would cause a flight to deviate from its original flight plan. [47]

The 10 resolution actions that can be taken in AirTOp to solve a potential conflict are summarized in Appendix F. Section 8.2 shows how a conflict is detected and solved for one of the runs that were simulated.

8.2. A Conflict Resolution Example

This section presents the procedure followed in order to detect a potential conflict and illustrates how the Closest Point of Approach (CPA) and conflict start and end time are calculated for one of the conflicts encountered. This analysis considers a run of Scenario 5, in which one of the flights is replaced by a MQ-9 Reaper and no additional separation increase is imposed on the separation bubble around the RPAS. Thus, the lateral separation requirement is 5 NM and the vertical one 1000 ft. The same procedure is used when a larger separation bubble around the RPAS is enforced.

During the run that was considered, flight PNX501 between Münster and Stuttgart was randomly selected to be switched to a MQ-9 Reaper. In the original situation (when the flight was operated by a British Aerospace Jetstream 32), there were 2 conflicts: one between this flight and a Lufthansa A320 descending towards Dusseldorf airport (Figure 8.2) and another one with a German Wings A319 heading to Cologne. Three heading changes were applied to flight PNX501 that instructed it to fly parallel to the initial trajectory, before bringing it back to the original trajectory (Figure 8.3). This resolution action also solved the second conflict with the A319.

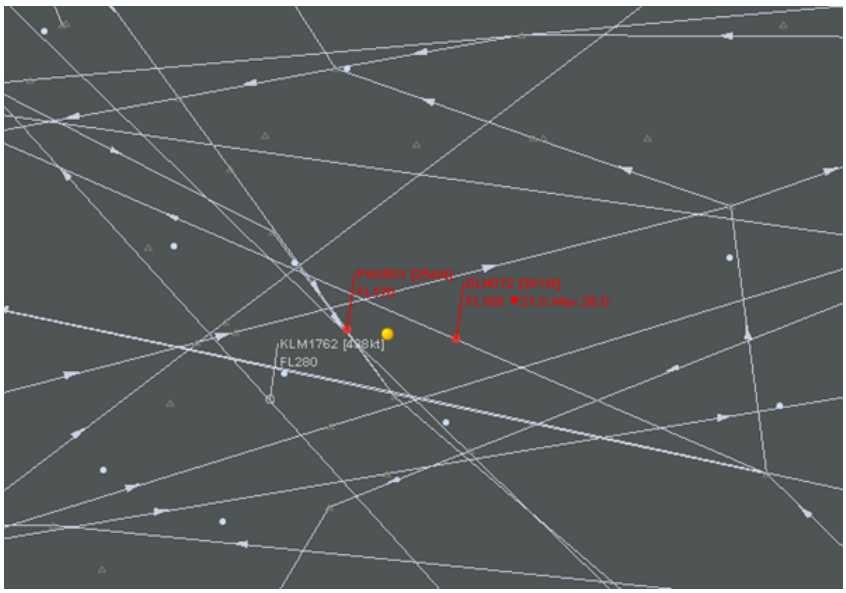

Figure 8.2: Conflict PNX501-DLH072 (before PNX501 is switched to RPAS)

Once flight PNX501 is switched to a MQ-9 Reaper (and keeping the same sector entry times for all flights), the number of conflicts increases to 4. The procedure to determine the CPA and conflict time will be presented in this section for the situation shown in Table 8.1. This situation is also illustrated in Figure 8.4 and summarized by the sketch in Figure 8.5.

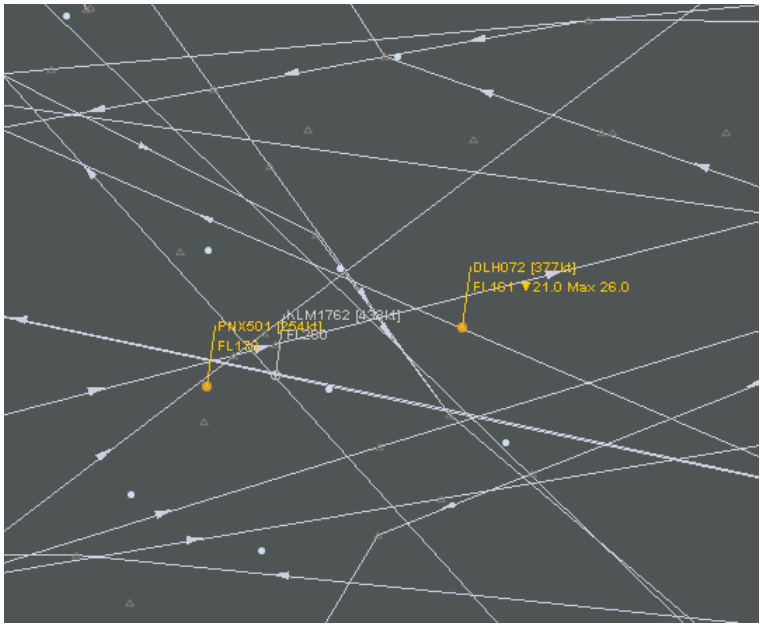

Figure 8.3: Vectoring PNX501 parallel to its original route (before flight is switched to RPAS)

Table 8.1: Flights PNX501 and BER509 at 06:28:00

	PNX501	**BER509**
Time	06:28:00	
Aircraft Type	MQ-9 Reaper	Airbus A321
Position	N51.3858 E7.7708	N51.0267 E8.5525
Altitude	FL170 (level)	FL231 (desc. with 2500 fpm)
Ground Speed	194 kts	405 kts
Track Angle	160.55	289.76

Assuming flat earth approximations, the relative position vector is obtained from equation 8.1, where R is the earth radius (R=6371km).

$$\begin{aligned} \Delta x &= R \cdot \frac{\pi}{180} \cdot \begin{bmatrix} (lon_b \text{ - } lon_a) \cdot cosd(0.5 \cdot (lat_b + lat_a)) \\ (lat_b \text{ - } lat_a) \end{bmatrix} \quad [71] \\ \Delta x &= \begin{bmatrix} 54457 \\ -39930 \end{bmatrix} \quad \text{m} \end{aligned} \tag{8.1}$$

From geometry (Figure 8.6), the relative velocity vector is given by Equation 8.2. The time until CPA is calculated from the relative geometry shown in Figure 8.7 and is derived in Equation 8.3.

$$\overline{v}_{rel} = \overline{v}_a - \overline{v}_b = 194 \cdot \begin{bmatrix} sind(160.55) \\ cosd(160.55) \end{bmatrix} - 405 \cdot \begin{bmatrix} sind(289.76) \\ cosd(289.76) \end{bmatrix} = \begin{bmatrix} 445 \\ -319 \end{bmatrix} \quad \text{kts} \tag{8.2}$$

$$t_{CPA} = \frac{dx'}{|v_{rel}|} = \frac{1}{|v_{rel}|} \cdot \frac{|v_{rel}| \cdot \Delta x}{|v_{rel}|} = 123.07 \quad \text{sec} \tag{8.3}$$

Also from the geometry in Figure 8.7, the minimum passage distance, CPA, is determined. This is calculated in Equation 8.4.

$$CPA^2 = \Delta x^2 - \frac{(v_{rel} \cdot \Delta x)^2}{v_{rel}^2} = 0.37 \quad \text{NM} \tag{8.4}$$

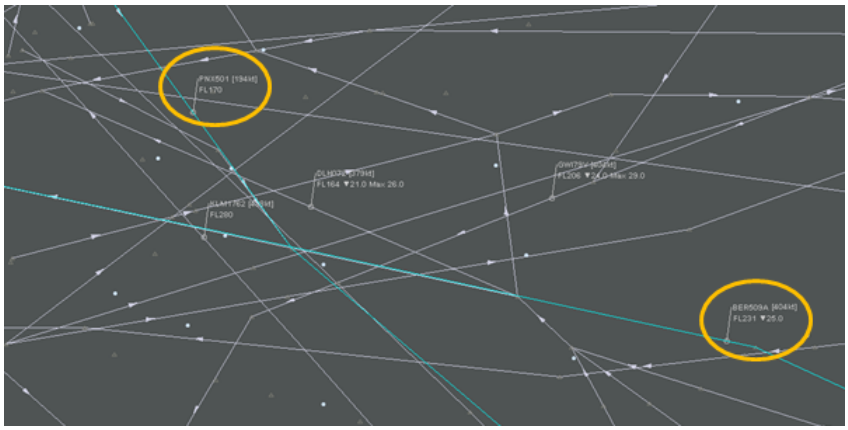

Figure 8.4: Flights PNX501 and BER509 at 06:28:00

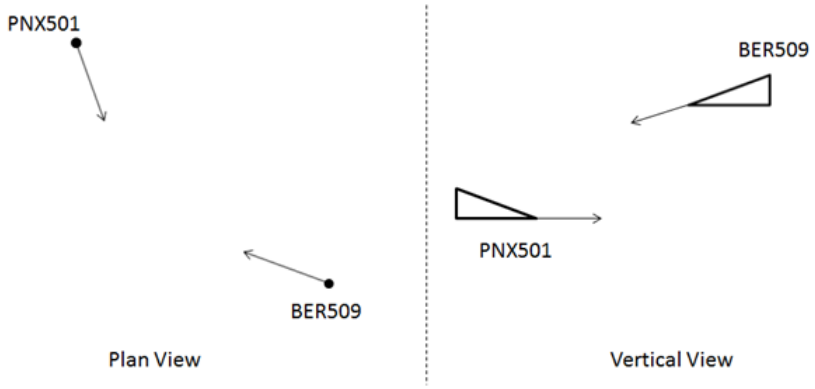

Figure 8.5: Sketch of situation shown in Figure 8.4

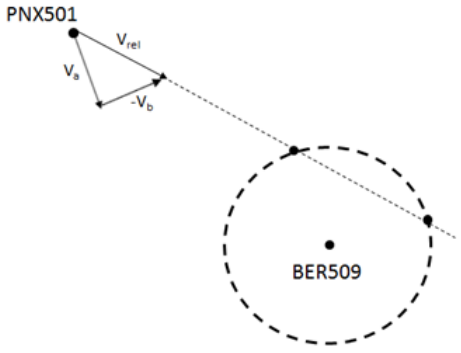

Figure 8.6: Geometry for the Determination of the Relative Velocity Vector

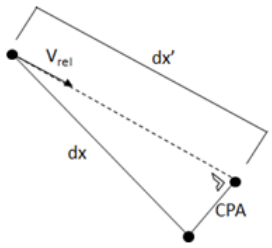

Figure 8.7: Geometry for the Determination of the Time until CPA

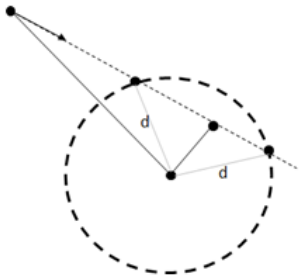

Figure 8.8: Geometry for the Determination of Entry/ Exit Points

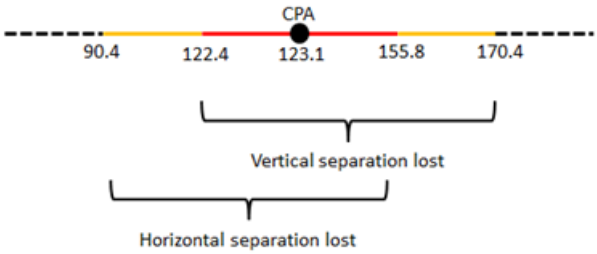

Figure 8.9: Time line of Conflict between flights PNX501 and BER509

Considering that the required lateral separation is 5 NM, Equation 8.5 is used to calculate the intrusion severity.

$$\text{Intrusion Severity} = \left(1 - \frac{0.37}{5}\right) \cdot 100 = 92.6\% \tag{8.5}$$

Using Pythagoras theorem (Figure 8.8), the points where the aircraft would enter and exit the protected area are calculated with Equation 8.6, where d is the radius of the separation bubble (5 NM).

$$(t_{in,out})_{hor} = t_{CPA} \pm \frac{\sqrt{d^2 - CPA^2}}{\overline{v}_{rel}} = 123.07 \pm 32.72 \quad \text{sec} \tag{8.6}$$

The vertical separation is a one dimensional problem, for which the entry and exit times are calculated by Equation 8.7, where VS is the vertical speed of flight BER509.

$$(t_{in,out})_{vert} = \frac{ALT_2 - ALT_1 \pm 1000}{VS} = 146.4 \pm 24 \quad \text{sec} \tag{8.7}$$

Having obtained the times at which both the vertical and horizontal separations are lost and then recovered, the diagram in Figure 8.9 shows how the conflict occurred. The time below the axis is in seconds with respect to the time considered at the beginning of the exercise (6:28:00). As can be seen in this figure, the horizontal separation is the first one to be lost at 6:29:30 and then the vertical separation drops below 1000 ft at 6:30:02. This is also the time at which the conflict begins. Then, one second later the closest point of approach is reached. At 06:30:35 the horizontal separation is regained, which marks the ending time of the conflict. The duration of the conflict was 32 seconds. As flight BER509 is still descending, at 06:30:50 the vertical separation between the two flights exceeds the minimum requirement of 1000 ft.

Activating the conflict resolution module of AirTOp solved this conflict by accelerating the descent of flight BER509. Following the structure of the Conflict Resolution Rule Base Tree discussed in Section 8.1 and shown in Figure 8.1, the following nodes of the CRRBT were followed: *Root* > *One in Vertical* > *On Conflict One in Vertical* > *Approaching an Intersection* > *Routes do not merge after Intersection* > *Accelerate Descent.* The resolution action began at 6:27:00, when the A321 was instructed to descent at a rate of 5000 fpm for 1 minute, before resuming its previous descent rate of 2500 fpm. Performing this manoeuver ensured that the vertical separation between the two flights was 1000 ft at the time when their routes were crossing, as can be seen in Figure 8.10. Table 8.2 summarizes the conflicts that were encountered during this run, both between the RPAS flight (PNX501) and other non-RPAS flights as well as between two non-RPAS flights. The resolution actions that were taken and the conflict types are also mentioned in Table 8.2.

The conflict type looks at both the vertical state of the flights, as well as the difference between their headings. For instance, if both flights are climbing or descending, then the vertical type of the conflict will be “both in vertical”. Similarly, if only one flight is climbing or descending, then the vertical type of the conflict will be “one in vertical”. Otherwise, the conflict will be between two cruising flights. If the heading difference between the two flights is smaller than 45 degrees, then the lateral state of the conflict will be “following”. If the heading difference is greater than 135 degrees, the lateral state will be “crossing”. All other cases are included in the “opposite” case. Section 8.3 analyzes which conflict resolution strategies are most frequently used during a scenario and whether there are any differences in strategies between aircraft types (RPAS/non-RPAS).

Table 8.2: Conflicts encountered during the Run considered for this Example

Flights (a/c types)	Conflict Type	Lateral Sep. [NM]	Vertical Sep. [ft]	Resolution Start Time	CPA Time	Action
GWI55F (A319) – GWI29T (A319)	Crossing, both in vertical	2.3	682	05:57	06:02	Stop Climb
CSA2MZ (AT75) – GWI55F (A319)	Crossing, both cruising	4.6	0	05:58	06:03	Cruise level change down
BER312G (A321) – BER818D (DH8D)	Crossing, both in vertical	3.4	669	06:03	06:08	Vectoring behind
PNX501 (MQ9) – BER509 (A321)	Crossing, one in vertical	0.4	975	06:27	06:30	Accelerate descent
PNX501 (MQ9) – BER191J (A320)	Opposite, one in vertical	2.2	980	06:28	06:33	Accelerate descent
PNX501 (MQ9) – EWG4156 (A319)	Crossing, one in vertical	3.6	957	06:29	06:34	Accelerate descent
PNX501 (MQ9) – WZZ283 (A320)	Crossing, one in vertical	4.1	984	06:33	06:37	Accelerate descent
GWI9F (A319) – GWI47Y (A319)	Opposite, one in vertical	0.2	100	06:52	06:56	Vectoring parallel

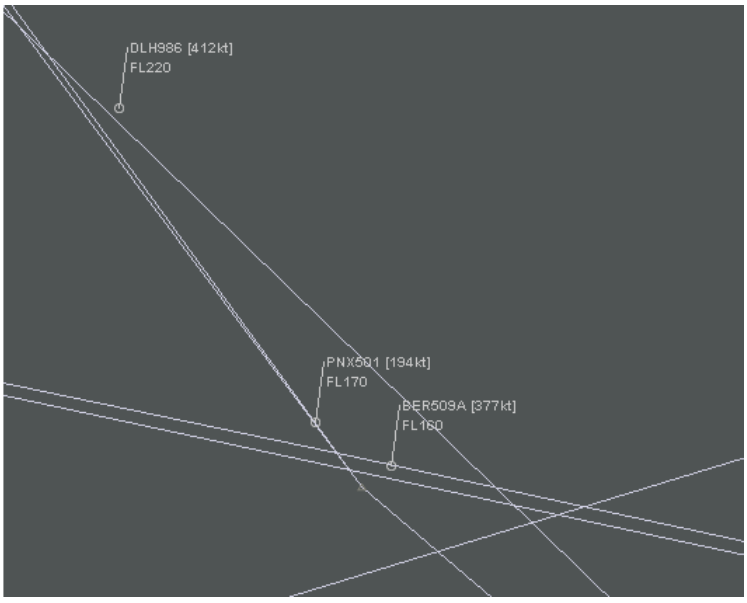

Figure 8.10: Accelerating Descent of BER509 solves Conflict with PNX501 (RPAS)

8.3. Distribution of Conflict Resolution Strategies

This section presents the conflict resolution actions that were taken to solve any potential conflicts that were encountered for the scenario in which 20% of the flights were replaced with a MQ9 Reaper (SCN_2_2) (1 experiencing a failure of the C2 link and doubling the separation around it, plus 9 other Reapers with a working data link that participated in conflict resolution and no additional increase in separation). This scenario was chosen in order to identify any differences in the strategies that were used to solve conflicts between manned-manned, manned-RPAS and RPAS-RPAS aircraft. In the presented statistics the total number of conflicts recorded during the 1060 different runs is considered. For this experiment the default AirTOp conflict detection and resolution module was used and in the case of RPAS that were active participants in conflict resolution (no failure of the C2 link), the assumption of no communication delay was present. The results are compared against the baseline case which is shown in Figure 8.11.

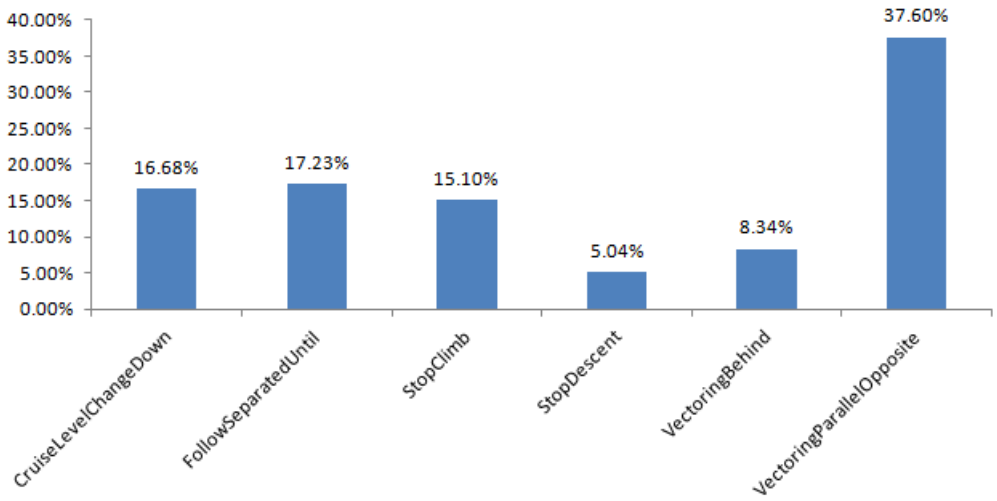

Figure 8.11: Distribution of Conflict Resolution Strategies in Baseline Scenario

Figure 8.11 shows how frequent the resolutions actions were used when potential conflicts had to be solved in the baseline. Horizontal resolution actions were used in 46% of the cases (vectoring behind or parallel vectoring). Out of the vertical resolution actions the option that matches the descend rate of the aircraft flying behind was most popular (FollowSeparated). Stopping a flight from climbing occurred more frequently than stopping a descent manoeuver (15% vs. 5%).

When scenario 2_2 is considered, potential conflicts are no longer only between manned flights. Figure 8.12 shows how the potential conflicts are distributed between the different aircraft types that are considered. The largest percentage of conflicts is between manned and manned aircraft (48%), while the conflicts between two RPAS with a working C2 link is of only (3%). The second biggest category of conflicts is that between a manned aircraft and an RPAS (33%), which is not surprising since the two most common aircraft types in the simulation are manned aircraft and Reapers with a functioning C2 link. 16% of the conflicts involved the one RPAS that experienced a C2 link failure. Furthermore, this can be divided into 12% with manned aircraft and 4% with another Reaper. Considering the conflicts with a manned aircraft and the fact that one RPAS with C2 link failure accounted for 12% of them while 9 RPAS without C2 link failure for 33%, this means that on average the RPAS with C2 failure generated 3.3 times more conflicts. This can be attributed to the different separation standard that is enforced around the Reaper once it loses its C2 link (double than than between the other flights).

Figures 8.13 and 8.14 show the distribution of the resolution actions that were applied when an aircraft was in a potential conflict with the RPAS with the C2 link failure. The results are shown for both the situation in which the RPAS interacts with a regular (manned) aircraft and the one in which it interacts with another RPAS. To improve the readability of the results, a different axis scale was used in Figure 8.14 than in Figure 8.13. In 38.6% of the times lateral resolution was selected when the manned aircraft solved the potential conflict with

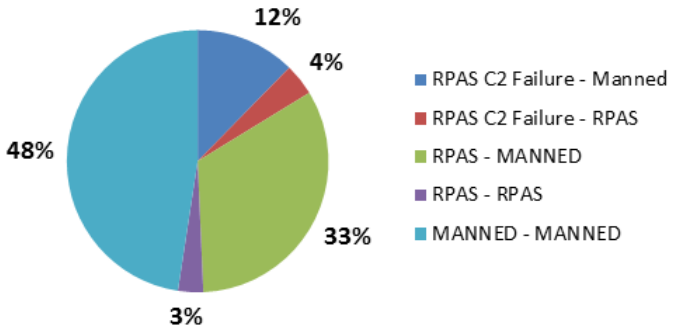

Figure 8.12: Distribution of Conflicts Based on Aircraft Type (SCN_2_2)

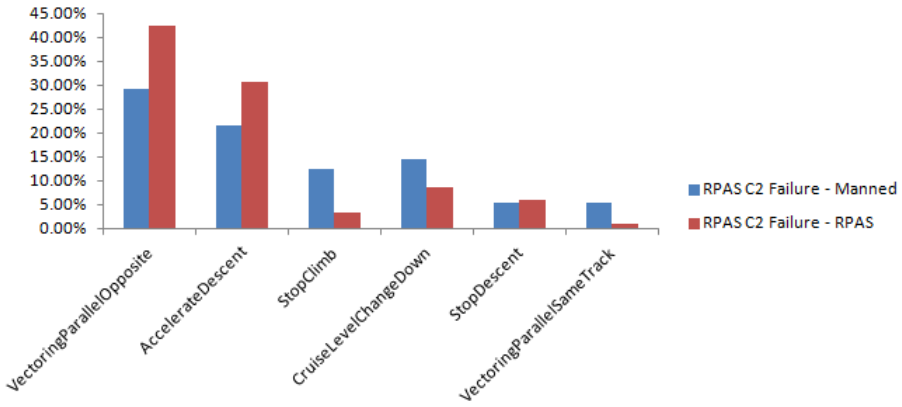

Figure 8.13: Resolution Strategies Used in Conflicts with the RPAS with C2 link failure (1/2) (SCN_2_2)

the RPAS and 45.5% when another RPAS was involved. Compared to the baseline, having the MQ-9 Reaper with C2 link failure resulted in more vertical resolution actions to be taken.

In both cases, the most common resolution action was parallel vectoring (29.3% with manned aircraft and 42.4% with another RPAS). This meant that the aircraft that was in a potential conflict with the RPAS with C2 failure had to perform three heading changes, first moving towards a point behind the CPA, and then flying parallel to its original route before heading back on the original trajectory. The second most frequently used resolution action was in both cases to accelerate descent (21.6% with manned and 30.6% with RPAS). Instructing the cooperative flight to cruise at a lower flight level was the third most popular option in both cases: 14.5% of the time with a manned aircraft and 8.7% with another RPAS. The decision to stop the climbing manoeuver was more frequently used when a conflict with a manned aircraft was encountered (12.5%), whereas for the RPAS case this option was only used in 3.3% of the cases.

If the frequencies of using the stop climb and stop descent actions are compared, another difference is observed between the RPAS and manned aircraft cases. When the conflict involved another RPAS the stop descent instruction was more frequently used compered to its climbing counterpart (5.9% vs. 3.3%). On the contrary, when a manned aircraft was involved, it stopped its climbing manoeuver more often than its descent one (12.5% vs. 5.3%). This is likely to be a consequence of the different performance of the MQ-9 Reaper compared to the other aircraft used in the experiment.

Figure 8.15 shows the six most common resolution actions that were used to solve conflicts not involving the RPAS with a C2 link failure. The results are broken down in conflicts that were between two RPAS (with a working C2 link), two manned aircraft or one RPAS and a manned aircraft. When compared with the baseline (Figure 8.11 one can see that the manned-manned conflicts follow the same distribution for this scenario. This means that the differences between the other categories are likely to be a result of the MQ-9 Reapers that were introduced in the simulations.

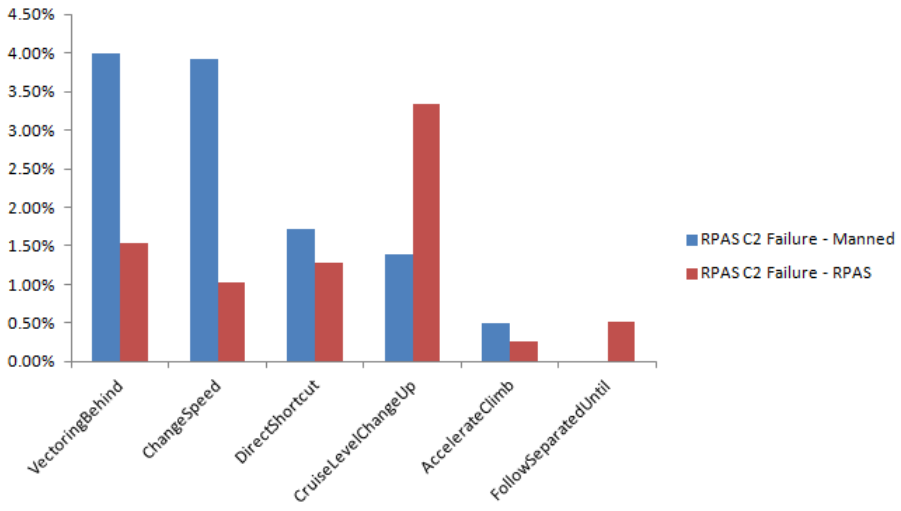

Figure 8.14: Resolution Strategies Used in Conflicts with the RPAS with C2 link failure (2/2) (SCN_2_2)

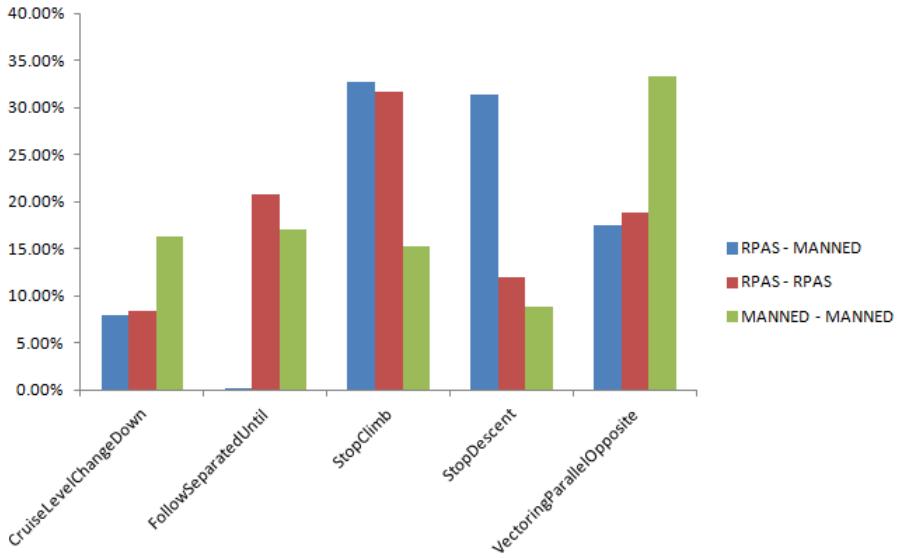

Figure 8.15: Resolution Strategies Used in Conflicts not involving the RPAS with C2 link failure (SCN_2_2)

While parallel vectoring was the most frequently used resolution action to solve conflicts between manned aircraft (33.9%), when a conflict occurred between an RPAS and a manned aircraft stopping the climb manoeuver of one of the flights was the most common action (32.8%). Also, the stop descent action was widely used for this case (31.4%), suggesting that more than 60% of the conflicts between an RPAS and a manned aircraft were solved in a vertical manner. Stopping the descent of a flight was also the most used resolution action for conflicts between two Reapers (31.7%). However, stopping the descent manoeuver was only the 4^{th} most popular option in the manned-manned case.

The follow separated until action was not used in the cases between RPAS and manned flights, whereas for the other two situations this option was used for 17.1% of the conflicts (manned-manned) and 20.7% (RPAS-RPAS). Since this resolution action tries to match the descent rates of the two aircraft, this suggests that such an action is only possible between aircraft with similar performances. Chaining the cruising level to a lower one by asking one of the aircraft to descent, was used as frequent in both cases involving an RPAS, whereas it was used twice as much for solving conflicts between manned aircraft (16.3%).

The next chapter summarizes the results obtained for all 14 scenarios of this experiment. These results are analyzed using ANOVA and MANOVA tests in Chapters 10 and 11.

9

Results Experiment 2

The experimental set-up was discussed in Chapter 7. The 9 KPIs that are of interest were explained in Section 7.3 and the 14 scenarios considered were introduced in Section 7.4. These scenarios were divided in two: only one flight switched to RPAS (with a C2 link failure) and multiple flights switched to RPAS (one with a C2 link failure, the other not). These scenarios were summarized in Table 7.3. An example on how a conflict is detected and solved using the default AirTOp conflict detection and resolution module and the distribution of the conflict resolution actions that were selected for one of the scenarios was the topic of Chapter 8. This chapter shows the procedure followed in order to establish whether the results of the simulations converged (Section 9.1 and then presents the results that were obtained for this experiment (Section 9.2).

9.1. Checking for Convergence

Each scenario was initially run 1060 times, with each of the 53 flights being replaced by an RPAS with a failed C2 link 20 times. Each flight was replaced the same number of times by an RPAS because the probability of either flight being an RPAS is assumed to be equal. Then the sector entry times of each of the flights are varied with a random value between +/- 60 seconds of the original sector entry time.

Once the 1060 runs for a scenario are completed, the results for all the metrics are processed in MATLAB. For each KPI and each scenario the mean value of the KPI from all the previous runs is plotted against the number of runs. Figure 9.1 shows how the mean number of potential conflicts changes as the number of runs increases. From top to bottom there are 5 scenarios shown in Figure 9.1, the first one being the baseline. Figure 9.2 shows how the mean air traffic controller task load varies as more runs are performed for 4 of the scenarios.

As can be seen in Figures 9.1 and 9.2 the initial 1060 simulations were sufficient for ensuring the convergence of KPIs 1 and 2. A similar check was performed for the other KPIs and scenarios and it was determined that no additional runs are necessary. This was complemented by the calculation of the 95% confidence interval (as explained in Chapter 5) which was suitable for all KPIs. The values of the results and the confidence intervals for each key performance indicators can be found in Section 9.2.

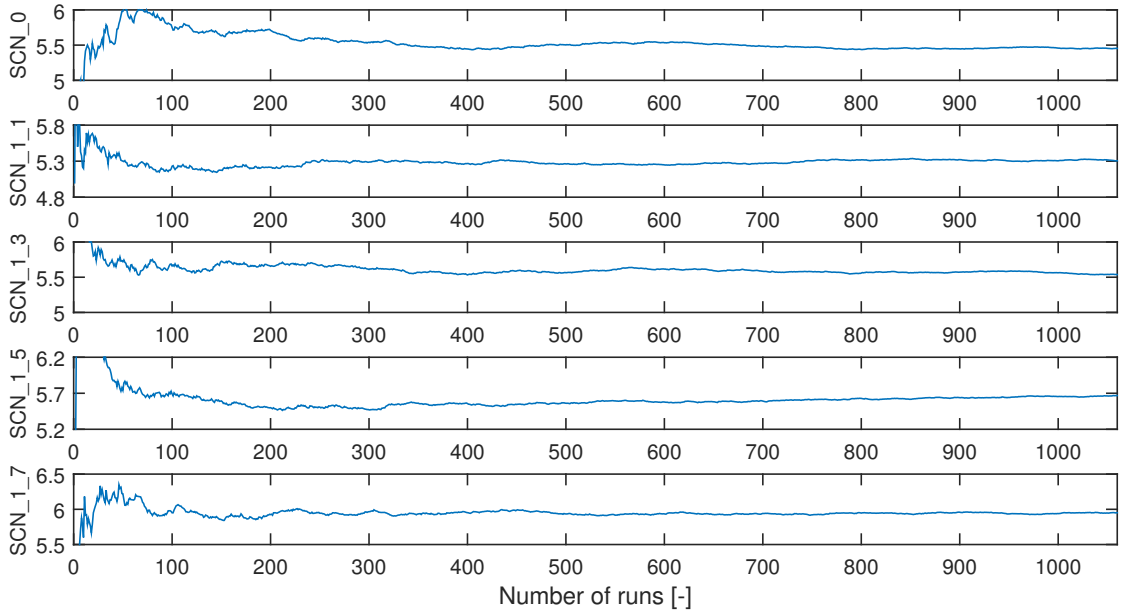

Figure 9.1: KPI_1 (Potential Conflicts) as a Function of Number of Runs for Scenarios 0, 1_1, 1_3, 1_5 and 1_7

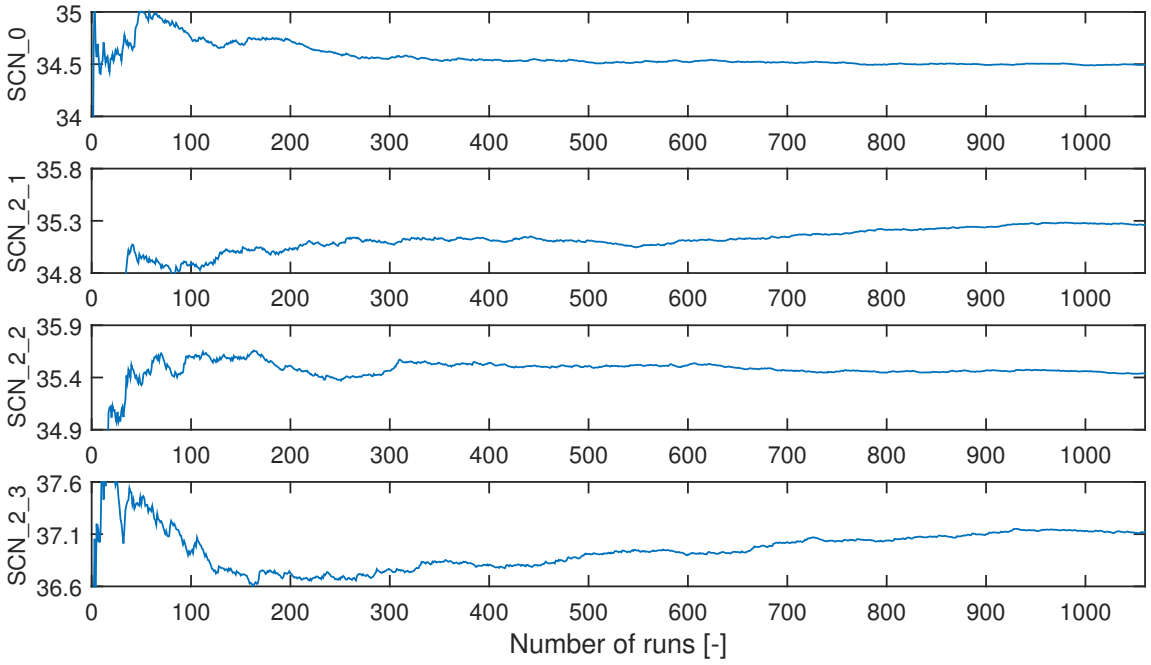

Figure 9.2: KPI_2 (ATCo task load) as a Function of Number of Runs for Scenarios 0, 2_1, 2_2 and 2_3

9.2. Results of Simulations

The results of 14,840 simulations grouped in 14 scenarios are shown in this section. They are grouped in 9 tables (9.1-9.9), one for each KPI. The tables contain the mean value of the KPI, the standard deviation (calculated by taking the square root of Equation 5.5), the root mean square error (RMSE, from Equation 5.6) and

the margin of error (MOE, Equation 5.9) which is a measure of how far apart the lower and upper bounds of the 95% confidence interval are from the mean value. To improve readability, the table distinguishes between the following cases: baseline, Global Hawk, Reaper and multiple RPAS. In Table 9.1, for instance, one can see that there were 5.45 potential conflicts recorded in the baseline, with the 95% confidence interval of 5.34 - 5.56 (MOE is 0.11).

As the differences between the scenarios are very small, the results will be analyzed from a statistical point of view. This will be done in Chapter 10 where the means are compared with each other using ANOVA tests to determine whether the differences are due to the experimental conditions (RPAS performance/ increase in separation) and not by chance alone. Thus, the results will not be analyzed any further in this section.

Table 9.1: Results KPI_1 (Potential Conflicts [-])

Scenario	Mean	σ	RMSE	MOE
0 (Baseline)	5.45	1.78	0.05	0.11
1_1	5.31	1.68	0.05	0.10
1_2	5.38	1.82	0.06	0.11
1_3	5.54	1.79	0.06	0.11
1_4	5.63	1.78	0.05	0.11
1_5	5.67	1.89	0.06	0.11
1_6	5.91	1.97	0.06	0.12
1_7	5.95	2.07	0.06	0.12
1_8	6.10	2.03	0.06	0.12
2_1	8.06	2.95	0.09	0.18
2_2	8.55	3.02	0.09	0.18
2_3	11.43	4.25	0.13	0.26
2_4	7.62	2.67	0.08	0.16
2_5	9.43	3.18	0.10	0.19

Table 9.2: Results KPI_2 (ATCo Task Load [pct. time active/10min])

Scenario	Mean	Sigma	RMSE	MOE
0 (Baseline)	34.50	1.40	0.04	0.08
1_1	34.34	1.34	0.04	0.08
1_2	34.34	1.41	0.04	0.08
1_3	34.43	1.42	0.04	0.09
1_4	34.37	1.35	0.04	0.08
1_5	34.62	1.50	0.05	0.09
1_6	34.66	1.49	0.05	0.09
1_7	34.66	1.54	0.05	0.09
1_8	34.64	1.46	0.04	0.09
2_1	35.26	2.06	0.06	0.12
2_2	35.44	2.08	0.06	0.13
2_3	37.12	3.10	0.10	0.19
2_4	35.20	1.85	0.06	0.11
2_5	35.69	2.13	0.07	0.13

Table 9.3: Results KPI_3 (Sector Occupancy [a.c/min])

Scenario	Mean	Sigma	RMSE	MOE
0 (Baseline)	5.47	0.07	0.00	0.00
1_1	5.49	0.08	0.00	0.00
1_2	5.49	0.08	0.00	0.00
1_3	5.49	0.08	0.00	0.00
1_4	5.49	0.08	0.00	0.00
1_5	5.51	0.09	0.00	0.01
1_6	5.51	0.09	0.00	0.01
1_7	5.52	0.09	0.00	0.01
1_8	5.52	0.09	0.00	0.01
2_1	5.88	0.21	0.01	0.01
2_2	5.87	0.21	0.01	0.01
2_3	5.89	0.22	0.01	0.01
2_4	5.67	0.16	0.01	0.01
2_5	6.09	0.23	0.01	0.01

Table 9.4: Results KPI_4 (Distance [NM/flight])

Scenario	Mean	Sigma	RMSE	MOE
0 (Baseline)	33.77	0.23	0.01	0.01
1_1	33.77	0.35	0.01	0.02
1_2	33.76	0.36	0.01	0.02
1_3	33.76	0.36	0.01	0.02
1_4	33.77	0.38	0.01	0.02
1_5	33.80	0.35	0.01	0.02
1_6	33.79	0.36	0.01	0.02
1_7	33.80	0.36	0.01	0.02
1_8	33.80	0.38	0.01	0.02
2_1	33.92	0.93	0.03	0.06
2_2	33.97	0.93	0.03	0.06
2_3	33.96	1.11	0.03	0.07
2_4	33.93	0.69	0.02	0.04
2_5	34.01	1.21	0.04	0.07

Table 9.5: Results KPI_5 (Flight Time [sec/flight])

Scenario	Mean	Sigma	RMSE	MOE
0 (Baseline)	319.53	2.79	0.09	0.17
1_1	319.62	3.88	0.12	0.23
1_2	319.48	3.81	0.12	0.23
1_3	319.42	3.78	0.12	0.23
1_4	319.67	4.00	0.12	0.24
1_5	319.92	3.83	0.12	0.23
1_6	319.85	3.85	0.12	0.23
1_7	319.83	3.84	0.12	0.23
1_8	319.90	4.14	0.13	0.25
2_1	322.10	9.92	0.30	0.60
2_2	322.84	9.64	0.30	0.58
2_3	322.88	11.25	0.35	0.68
2_4	321.79	6.97	0.21	0.42
2_5	323.96	12.57	0.39	0.76

Table 9.6: Results KPI_6 (Fuel Consumption [kg/flight])

Scenario	Mean	Sigma	RMSE	MOE
0 (Baseline)	151.58	0.75	0.02	0.05
1_1	151.59	2.71	0.08	0.16
1_2	151.52	2.85	0.09	0.17
1_3	151.53	2.91	0.09	0.18
1_4	151.57	2.97	0.09	0.18
1_5	151.70	2.77	0.08	0.17
1_6	151.72	2.87	0.09	0.17
1_7	151.83	2.89	0.09	0.17
1_8	151.87	3.02	0.09	0.18
2_1	152.79	9.03	0.28	0.54
2_2	152.84	9.20	0.28	0.55
2_3	153.84	10.56	0.32	0.64
2_4	152.70	6.76	0.21	0.41
2_5	153.12	12.14	0.37	0.73

Table 9.7: Results KPI_7 (Lost Altitude [ft/desc. flight])

Scenario	Mean	Sigma	RMSE	MOE
0 (Baseline)	10004.87	98.54	3.03	5.93
1_1	10000.44	113.48	3.49	6.83
1_2	10001.10	118.31	3.63	7.12
1_3	9999.16	116.14	3.57	6.99
1_4	9994.12	126.17	3.88	7.60
1_5	9998.18	119.39	3.67	7.19
1_6	9995.63	126.02	3.87	7.59
1_7	9994.05	128.70	3.95	7.75
1_8	9987.90	129.95	3.99	7.82
2_1	9895.53	291.82	8.96	17.57
2_2	9885.52	282.36	8.67	17.00
2_3	9833.31	374.61	11.51	22.55
2_4	9940.42	204.10	6.27	12.29
2_5	9848.87	360.39	11.07	21.70

Table 9.8: Results KPI_8 (Gained Altitude [ft/climb. flight])

Scenario	Mean	Sigma	RMSE	MOE
0 (Baseline)	4390.66	72.35	2.22	4.36
1_1	4392.06	133.00	4.09	8.01
1_2	4390.73	133.61	4.10	8.04
1_3	4394.79	129.07	3.96	7.77
1_4	4389.21	129.90	3.99	7.82
1_5	4394.98	129.34	3.97	7.79
1_6	4390.04	132.84	4.08	8.00
1_7	4392.25	139.68	4.29	8.41
1_8	4390.07	145.57	4.47	8.76
2_1	5104.14	396.39	12.17	23.86
2_2	5095.32	411.93	12.65	24.80
2_3	5114.84	436.41	13.40	26.27
2_4	5080.61	300.02	9.22	18.06
2_5	5111.34	516.42	15.86	31.09

Table 9.9: Results KPI_9 (Altitude Deviation [ft/flight chg. lvl.])

Scenario	Mean	Sigma	RMSE	MOE
0 (Baseline)	8134.91	70.39	2.16	4.24
1_1	8132.86	103.26	3.17	6.22
1_2	8128.89	104.13	3.20	6.27
1_3	8129.81	103.82	3.19	6.25
1_4	8122.74	106.81	3.28	6.43
1_5	8132.61	103.25	3.17	6.22
1_6	8127.65	105.44	3.24	6.35
1_7	8128.32	110.65	3.40	6.66
1_8	8124.20	117.86	3.62	7.10
2_1	8079.47	292.48	8.98	17.61
2_2	8069.17	286.31	8.79	17.24
2_3	8040.67	318.02	9.77	19.14
2_4	8091.14	198.72	6.10	11.96
2_5	8050.65	364.16	11.19	21.92

PART IV

STATISTICAL ANALYSIS OF EXPERIMENT 2 RESULTS

10

Analyzing Simulation Results using ANOVA tests

The results of the simulations were given in Section 9.2 (Tables 9.1 - 9.9). This chapter presents a statistical analysis of the results using the method of ANOVA (analysis of variance). For this, the 14 scenarios are divided in 5 cases in order to determine whether there are any significant differences between the Reaper and Global Hawk simulations (and if the performance of the RPAS plays a role in how the other flights are affected), if the size of the separation bubble enforced around the RPAS with C2 link failure affects the 9 KPIs and how an environment with increasing number of RPAS flights (in which one experiences a loss of the C2 link) impacts the considered metrics. Section 10.1 introduces the ANOVA test and the procedure that was followed in order to compare the scenarios from a statistical point of view. The results of the ANOVA tests, which are obtained using IBM SPSS, are presented in Sections 10.2 - 10.6 and conclusions are drawn in Section 10.7.

10.1. Theory on Analysis of Variance (ANOVA)

Chapter 5 defines the statistical estimators that are used to obtain the mean values of the key performance indicators selected in Section 7.3. As was noticed in Tables 9.1 - 9.9, which show the simulation results of the second experiment, some KPIs have values which are very close between the scenarios. For instance, the number of potential conflicts in scenario 1_1 is 5.31, whereas in scenario 1_2 is 5.38. In order to determine whether the difference of 0.07 is due to the increase of 20% in separation around the RPAS, a statistical analysis of the means of each KPI will be conducted. For this, the scenarios will be split in 5 cases:

1. **Case 1:** scenarios 1_5 - 1_8 and baseline to determine the impact of the MQ-9 Reaper on the key performance indicators (Section 10.2).
2. **Case 2:** scenarios 1_1 - 1_4 and baseline to determine the impact of the RQ-4A Global Hawk on the KPIs (Section 10.3).
3. **Case 3:** scenarios 2_2, 2_4, 2_5 and baseline to determine whether other RPAS flights, in addition to the one MQ-9 Reaper that experiences a failure of the C2 link significantly penalize the KPIs (Section 10.4).
4. **Case 4:** scenarios 2_1, 2_2, 2_3 and baseline to determine whether increasing the separation around the RPAS flight that experiences a failure of the C2 link, in an environment with multiple RPAS flights, significantly penalizes the KPIs (Section 10.5).
5. **Case 5:** scenarios 1_1 - 1_8 to determine whether the performance of the RPAS that experiences the failure of the C2 link affects the KPIs (Section 10.6).

The ANOVA test (analysis of variance) analyzes the differences between the scenarios and indicates whether they are different for a certain significance level. [72] The assumptions of the ANOVA test are summarized below:

1. Variances between the groups shall be similar
2. Observations shall be independent

3. The dependent variable (the KPIs) shall be measured on at least an interval scale and shall be normally distributed within the groups.

The second assumption is true from the way the experiment was set up: the sector entry times of the flights were randomized by +/- 60 seconds around the original entry time and the flight that was switched to the RPAS with C2 link failure was randomly selected. The ANOVA test is still accurate if the third assumption is violated, provided that there are at least 40 runs and all scenarios have an equal number of measurements. [73] [74] Since there were 1060 runs performed for each scenario, violating the third assumption will not influence the results. Having an equal sample size ensures robustness also in the case when the first assumption is violated (homogeneity of variance). In this case, Welch's ANOVA will be used instead of the one-way ANOVA, as it has more power and a lower error rate. [72]

The hypothesis tested by ANOVA is that of equal means. If k scenarios are considered and μ represents the mean of KPI$_i$, the ANOVA hypothesis is formulated below.

$$\begin{aligned} &H_0 : \mu_1 = \mu_2 = ... = \mu_k \\ &H_1 : \text{at least one of the means is different} \end{aligned} \tag{10.1}$$

According to APA, who sets standards on how statistical results should be reported, the results of an ANOVA test shall be presented as follows: $F(df_M, df_R)$ = F-ratio, p = p-value. [72]

The p-value is the significant output that has to be analyzed in order to determine whether the null hypothesis H_0 is accepted or not. The p-value represents the smallest level of significance that would force the rejection of H_0 and is represented by 0.05. [55] If the p-value is larger than 0.05 then the null hypothesis is accepted and it can be concluded that the groups that were compared have equal means. Having a p-value lower than 0.05 rejects H_0 and means that the mean of at least one of the groups is different.

The F-ratio is an output of the test that specifies whether the group means are different. A value grater than one suggests that the experimental conditions had some effect on the results (the means differ), but cannot specify what the effect was. The procedure to determine the F-ratio will be described in the remainder of this section.

The following three sum of squares are calculated: SS_T (which assesses the variability within the data), SS_M (the variability that can be explained by the model - different data points belonging to different groups) and SS_R (a measure of how much error there is in the model).

SS_T is calculated by taking the difference between each data point in the observations and the grand mean for that variable, squaring this difference and adding them up as shown in Equation 10.2. [72] The degrees of freedom (df_T) are one less than the sample size (N-1).

$$SS_T = \sum_{i}^{N} (x_i - \overline{x}_{grand})^2 \tag{10.2}$$

SS_M is obtained by taking the difference between the mean of each group and the grand mean, squaring this difference and multiplying it by the number of observations for that scenario (n_k). Then the values of the groups are added together as shown in Equation 10.3. [72] The degrees of freedom, df_M, are one less than the number of groups that are considered (k-1).

$$SS_M = \sum_{k} n_k \cdot (\overline{x}_k - \overline{x}_{grand})^2 \tag{10.3}$$

SS_R is calculated by summing up the squares of the difference between each data point and the mean of the group that it originated from, for all the groups that are considered (Equation 10.4). [72] The degrees of freedom are the difference between the total degrees of freedom and those of the model ($df_R = df_T - df_M$), or the difference between the sample size and the number of groups (N - k).

$$SS_R = \sum_{k} \sum_{i}^{N} (x_{i,k} - \overline{x}_k)^2 = SS_T - SS_M \tag{10.4}$$

In order to eliminate the bias resulted from the number of results that were summed, the average sum of squares is calculated in Equations 10.5 and 10.6. MS_M is a measure of systematic variation (amount of variation that can be explained by the model), whereas MS_R represents unsystematic variation.

$$MS_M = \frac{SS_M}{df_M} \tag{10.5}$$

$$MS_R = \frac{SS_R}{df_R} \tag{10.6}$$

For determining how much error there is in the model, the F-ratio is calculated (Equation 10.7). This is the ratio of the variation explained by the model and the unsystematic variation.

$$F = \frac{MS_M}{MS_R} \tag{10.7}$$

The assumption of homogeneity of variance is checked with Levene's test. The null hypothesis of this test is $H_0 : \sigma_1^2 = \sigma_2^2 = ... = \sigma_k^2$, which tests that the variances of all the groups are the same. A p-value larger than 0.05 means that the null hypothesis is accepted, variances are homogeneous and the one-way ANOVA can be reported. A p-value below 0.05 means that $H_1 : \sigma_1^2 \neq \sigma_2^2 \neq ... \neq \sigma_k^2$ is accepted (variances are not equal between the groups) and Welch's ANOVA will be used. The procedure to find Welch's F_{ratio} is described below. [75]

For the determination of Welch's F_{ratio}, a weight, w_k is first computed for each group by Equation 10.8, where n_k represents the sample size and σ_k^2 the variance of a certain group.

$$w_k = \frac{n_k}{\sigma_k^2} \tag{10.8}$$

Then, the grand mean of each group is adjusted using w_k as shown in Equation 10.9.

$$\overline{x}_{grand}^{Welch} = \frac{\sum_k w_k \cdot \overline{x_k}}{\sum_k w_k} \tag{10.9}$$

Instead of using Equation 10.3 to calculate SS_M, Equation 10.10 will be used. The mean squares is calculated as in Equation 10.5 of the one-way ANOVA and is shown for the Welch case in Equation 10.11.

$$SS_M^{Welch} = \sum_k w_k \cdot (\overline{x}_k - \overline{x}_{grand}^{Welch})^2 \tag{10.10}$$

$$MS_M^{Welch} = \frac{SS_M^{Welch}}{df_M} \tag{10.11}$$

Based on the sample size of each group (n_k), the weight (w_k) and the total number of groups (k) the value of Λ is calculated (Equation 10.12). This is then used in Equation 10.13 to determine the F_{ratio} for Welch's ANOVA, F_W.

$$\Lambda = \frac{3 \sum \frac{(1 - \frac{w_k}{\sum w_k})^2}{n_k - 1}}{k^2 - 1} \tag{10.12}$$

$$F_W = \frac{MS_W^{Welch}}{1 + \frac{2\Lambda \cdot (k-2)}{3}} \tag{10.13}$$

The model degrees of freedom, df_M, remain the same (k-1), but the residual degrees of freedom, df_R, is calculated by Equation 10.14. [75]

$$df_R = \frac{1}{\Lambda} \tag{10.14}$$

Once the ANOVA test has been performed and the result is significant (and thus the null hypothesis has been rejected) further tests need to be carried out in order to determine how the scenarios differ. This is required because the H_1 hypothesis of ANOVA only states that at least one of the group means is different, but it does not give any information about which group.

For the cases in which the ANOVA test was significant, a planned comparison test will be performed. This breaks down the variance of the model in component parts, without inflating the Type I error rate (incorrect rejection of H_0). [72] Planned comparison tests are one-tailed, testing a certain hypothesis, such as: *"Does an increase of 20% in separation increase the number of potential conflicts?"*, or *"Does increasing the percentage of RPAS flight increase ATCo task load?"*. The rules below should be followed when performing a planned comparison test. [72] This is illustrated in Figure 10.1 by an example of a planned contrast test for Case 1 (determining the impact of the MQ-9 Reaper with C2 link failure on a certain KPI_i).

- If a group is singled out in one comparison, it should not be used for another comparison.
- Each contrast should only compare two pieces of variance.
- Once a piece of variance has been split from a larger piece it cannot be attached to another piece of variance.
- There should always be one less contrasts than the number of groups.
- The first group should always compare the experimental groups with the baseline situation.

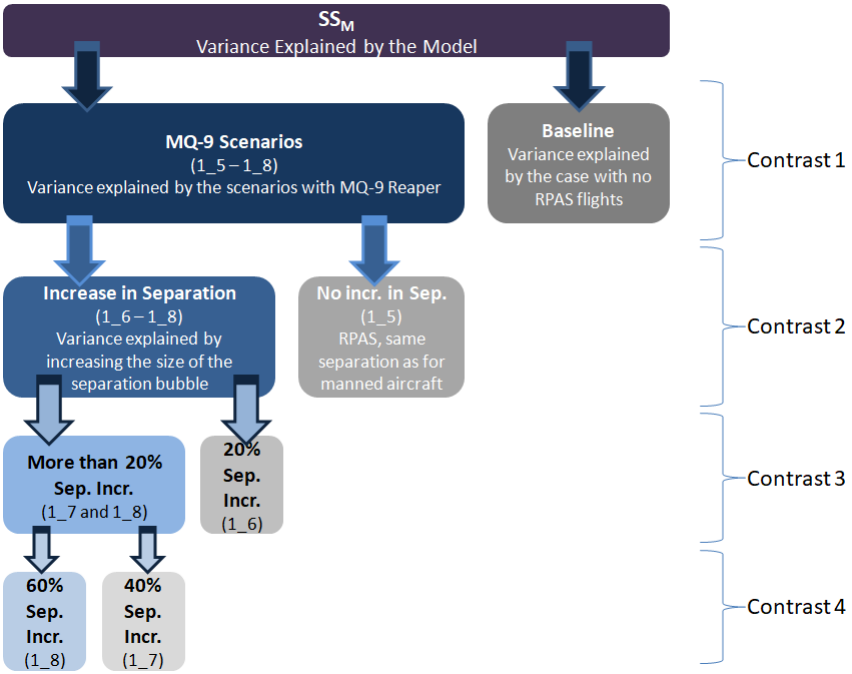

Figure 10.1: Example of Planned Comparison Test for Case 1

Performing a planned comparison in ANOVA is similar with conducting a t-test in which the mean of one piece of variance is compared to the mean of a another piece of variance. The procedure to determine the t-value is calculated below. [76] First the weighted sum $\hat{\psi}$ is calculated (Equation 10.15) where w_i represents the contrast weight and $\overline{x}_i$ the mean of group i. The procedure for establishing the contrast weights is beyond the scope of this project, but can be found in [72].

$$\hat{\psi} = \sum_{i=1}^{k} w_i \cdot \overline{x}_i \tag{10.15}$$

The standard error, $S_{\hat{\psi}}$ is then calculated by Equation 10.16, where $MS_{s/A}$ is the mean-square error obtained from the ANOVA test. The t value is then computed by Equation 10.17.

$$S_{\hat{\psi}} = \sqrt{MS_{s/A} \cdot \sum_{i=1}^{k} \frac{w_i^2}{N}} \tag{10.16}$$

$$t_{contrast} = \frac{\hat{\psi}}{S_{\hat{\psi}}} \tag{10.17}$$

As can be seen from Figure 10.1 this method compares more scenarios at once. For instance, the first contrast tell us whether the Reaper flight increased KPI_i, but it does not tell us which separation values are actually responsible for the increase. Similarly, contrasts 2 and 3 compare multiple scenarios as well. In order to be sure of the differences between scenarios themselves, post hoc tests will be conducted if a certain planned comparison test is found to be significant.

Depending on whether the groups have equal variances or not (which was previously checked with Levene's test), either a Tukey or a Games-Howell test is carried out. If the groups have homogeneous variances (non-significant Levene's test) Tukey's post hoc is used because it has the highest control over Type I error when group sizes are equal. [77] For unequal variances (significant Levene's test and Welch's ANOVA), a Games-Howell post hoc test is performed. The post hoc tests compare the differences in means between two scenarios only. [72]

In accordance with APA standards, the planned comparison results will be reported as follows: t(df) = t_value, p = p_value (1-tailed). For the post hoc tests, only the p-value (significance) is reported. [72]

10.2. Case 1: MQ-9 Reaper Scenarios

The focus of this section is to determine whether a MQ-9 Reaper experiencing a failure of the C2 link right at the moment when it enters an ATC sector significantly penalizes key ATM performance indicators. Also, the effect of increasing the size of the separation bubble that is enforced around the RPAS is assessed from a statistical point of view. The scenarios that are considered are: 1_5 - 1_8 which are first compared against the baseline case (no RPAS) and then between each other.

The hypothesis tested by ANOVA will be in this case: *"Are the mean results of the KPIs equal between the 5 scenarios?"* A significant result ($p < 0.05$) would mean that the hypothesis is rejected and that at least one scenario is different from the others for that particular KPI. A non-significant result ($p > 0.05$) would mean that the differences between scenarios for a certain KPI are too small to be considered significant and it can be concluded that the Reaper with a failed C2 link did not influence that KPI (mean values are equal).

Table 10.1 shows the ANOVA results for this case. There are three KPIs for which the null hypothesis of the ANOVA was not rejected, meaning that the means of the 5 scenarios that were considered are not significantly different. Therefore, it can be concluded that the distance flown, the gained altitude and the altitude deviation of the flights (KPIs 4, 8 and 9) did not change significantly with respect to the baseline case, where there was no RPAS present in the sector. For all the other metrics the ANOVA revealed that the means are significantly different between the groups. In order to determine the exact way in which the scenarios differ between them, planned contrast and post-hoc tests will be performed. Since the assumption of equal variance between groups is violated for all the metrics (Levene's test was significant for all KPIs, meaning that the null hypothesis of equal variances between groups has been rejected), the results of Welch's ANOVA were considered. If post hoc analysis is required, Games-Howell test will be used because it offers the best performance when the variances of the scenario results are not equal.

Results of Planned Comparison Test

The results of the planned comparison are shown in Table 10.2. The one-tailed significance is used because the following hypothesis is tested: *"Will increasing the separation around the Reaper increase KPIs 1, 2, 3, 5 and 6 and reduce KPI 7?"* There are four contrasts that are applied which exclude scenarios one by one and compare the groups as follows:

Table 10.1: ANOVA Results (Case 1)

KPI	Levene's Significance	ANOVA Type	ANOVA Result	H_0 Rejected?	Post hoc
KPI_1	0.00	Welch's ANOVA	[F(4,2645.44) = 19.49, p = 0]	Yes	G-H
KPI_2	0.01	Welch's ANOVA	[F(4,2646.77) = 2.48, p = 0.04]	Yes	G-H
KPI_3	0.00	Welch's ANOVA	[F(4,2634.03) = 62.26, p = 0]	Yes	G-H
KPI_4	0.00	Welch's ANOVA	[F(4,2613.85) = 2.06, p = 0.08]	No	No
KPI_5	0.00	Welch's ANOVA	[F(4,2629.84) = 2.85, p = 0.02]	Yes	G-H
KPI_6	0.00	Welch's ANOVA	[F(4,2333.95) = 4.61, p = 0]	Yes	G-H
KPI_7	0.00	Welch's ANOVA	[F(4,2638.76) = 3.18, p = 0.01]	Yes	G-H
KPI_8	0.00	Welch's ANOVA	[F(4,2573.43) = 0.29, p = 0.88]	No	No
KPI_9	0.00	Welch's ANOVA	[F(4,2615.68) = 2.18, p = 0.07]	No	No

Table 10.2: Planned Comparison Results (Case 1)

KPI / Contrast	0 vs (5,6,7,8)			5 vs. (6,7,8)			6 vs. (7,8)			7 vs. 8		
	t	df	Sig.	t	df	Sig.	t	df	Sig.	t	df	Sig.
KPI_1	7.26	1783.42	0.00	4.68	1928.71	0.00	1.62	2195.10	0.05	1.71	2117.31	0.04
KPI_2	3.07	1719.70	0.00	0.64	1810.74	0.26	-0.14	2132.48	0.44	-0.40	2111.90	0.35
KPI_3	15.74	2140.23	0.00	0.16	1797.60	0.43	1.14	2121.76	0.13	0.10	2116.97	0.46
KPI_5	3.32	2227.45	0.00	-0.44	1861.43	0.33	0.15	2187.35	0.44	0.41	2106.16	0.34
KPI_6	4.06	5273.38	0.00	1.06	1908.33	0.14	1.19	2175.64	0.12	0.33	2113.99	0.37
KPI_7	-3.04	2018.51	0.00	-1.31	1934.63	0.10	-0.97	2167.44	0.17	-1.09	2117.80	0.14

1. The baseline with respect to the other 4 scenarios (*"Was there any significant impact of having a Reaper with a failed C2 link in the sector?"*)
2. Scenario 1_5 with respect to scenarios 1_6 - 1_8 (*"Was there any significant impact of enforcing a larger separation bubble around the Reaper with C2 link failure?"*)
3. Scenario 1_6 with respect to scenarios 1_7 and 1_8 (*"Was there any significant impact of increasing separation around the Reaper by 40 or 60% compared to the 20% case?"*)
4. Scenario 1_7 with respect to scenario 1_8 (*"Was there any significant impact of increasing separation around the Reaper by 60% compared to the 40% increase case?"*)

As discussed in the previous section, the standard for reporting the results of a planned contrast test are: t(df) = t_value, p = p_value. For example the results of the first contrast test for KPI_1 shall be reported as follows: *Planned contrasts revealed that there is a significant impact of having a Reaper with C2 link loss on the number of potential conflicts, t(1783.42) = 7.26, p = 0.0.* The t-value is calculated by Equation 10.17 using IBM SPSS and is shown in the first column of each contrast in Table 10.2. Using the statistical software the value of the degrees of freedom and significance level (p-value) are also derived (columns 2 and 3 of each contrast in Table 10.2). As Levene's test was significant for all KPIs in this case, df is calculated using Equation 10.14 which explains why the values are not discrete. As a comparison, in Section 10.3, KPI_2 had a non-significant Levene's test (Table 10.4) and the df values of the contrasts in Table 10.5 are discrete for this KPI (N - k).

The planned comparison test in Table 10.2 revealed that there was a significant impact of having an MQ-9 Reaper in the sector for the 6 KPIs that were considered (p = 0 for the first contrast of all KPIs). All other contrast were non-significant (p > 0.05) for all KPIs with the exception of KPI_1 (potential conflicts). The p-values for the second and fourth contrasts are less than 0.05 meaning that there was a significant increase in the number of potential conflicts when a different separation bubble was enforced around the MQ-9 and that there was a significant increase in the number of potential conflicts when separation was increased by 60% compared to the 40% case.

The non-significance of the other contrasts for the remaining KPIs means that increasing the separating bubble by up to 60% does not affect these metrics. This means that if ATCos determine that a separation standard of 8 NM/1,600 ft is acceptable to handle a C2 link loss, there will be no impact on KPIs 2, 3, 5, 6 and 7 in their sector for remotely piloted aircraft with performances similar to those of the MQ-9 Reaper.

Table 10.3: Post hoc tests (Case 1)

KPI	0 vs. 1_5		0 vs. 1_6		0 vs. 1_7		0 vs. 1_8	
	Mean Difference	Sig.	Mean Difference	Sig.	Mean Difference	Sig.	Mean Difference	Sig.
KPI_1	-0.22	0.05	-0.45	0.00	-0.50	0.00	-0.65	0.00
KPI_2	-0.12	0.28	-0.16	0.07	-0.17	0.07	-0.14	0.15
KPI_3	-0.04	0.00	-0.04	0.00	-0.04	0.00	-0.04	0.00
KPI_5	-0.39	0.05	-0.32	0.19	-0.30	0.23	-0.38	0.10
KPI_6	-0.12	0.62	-0.14	0.52	-0.25	0.05	-0.29	0.02
KPI_7	6.69	0.62	9.24	0.33	10.82	0.19	16.97	0.01

Because the first contrast of the planned comparison was significant for all KPIs, a post hoc test is performed in which the four scenarios are compared against the baseline. The results are summarized in Table 10.3 and are discussed in the remainder of this section.

Number of Potential Conflicts (KPI_1)

The simulation results obtained for this KPI can be found in Table 9.1. The post hoc results for KPI_1 show that the increase in the number of potential conflicts is significant for the scenarios in which separation is larger than 6NM/1200ft ($p < 0.05$ for KPI_1 for scenarios 1_6 - 1_8 in Table 10.3). The non-significant comparison between the baseline and scenario 1_5 revealed that having a Reaper with a failed C2 link for which the same separation standard is enforced as for manned aircraft does not results in more conflicts. Since contrasts 2 and 4 of the planned comparison were significant for this metric, a further Games-Howell test is conducted in which scenarios 1_6, 7 and 8 are compared against scenario 1_5. These tests showed that increasing separation by 20, 40 and 60% resulted in a significant increase in number of potential conflicts by 4.2%, 5.0% and 7.7% compared to the case with one RPAS and same separation as for manned aircraft ($p = 0.04$, 0.01 and 0.00 respectively).

Therefore, as having a smaller separation bubble is beneficial in terms of limiting the number of potential conflicts, if ATCos would require larger separation bubbles to handle remotely piloted aircraft with performances similar to that of the MQ-9 Reaper and to ensure the safety of the airspace, they should take into account the increase in the number of potential conflicts which will have to be handled.

ATCo Task Load (KPI_2)

The simulation results obtained for this KPI can be found in Table 9.2. Controller task load did not vary significantly when the four scenarios are compared with the baseline individually ($p > 0.05$ for KPI_2 in Table 10.3). While this may seem counter intuitive because the increase in number of potential conflicts was significant when the separation bubble was larger than 5 NM/ 1,000 ft, this shows that task load is dependent on other KPIs as well such as sector occupancy, flight time and altitude change manoeuvers. It can also be explained through the fact that since the RPAS was excluded from conflict resolution in AirTOp, the task load "saved" by the ATCo who could not give any instructions to the RPAS might have been replaced by that generated from solving the other conflicts. In real life, however, the remote pilot would contact the ATCo and inform the controller about the C2 link failure and the resolution action, which would generate additional task load. This dimension was not captured in the experiments that were carried out.

Sector Occupancy (KPI_3)

The simulation results obtained for this KPI can be found in Table 9.3. The sector became more agglomerated in the four scenarios compared to the baseline (an additional 0.04 aircraft per minute). This increase is significant when compared to the baseline ($p = 0$ for KPI_3 in Table 10.3). However, since the three other contrast in Table 10.2 are non-significant (and the mean difference is the same between each scenario and the baseline), increasing separation by up to 60% does not influence the occupancy of the sector in this case.

Flight Time (KPI_5)

The simulation results obtained for this KPI can be found in Table 9.5. Regarding the time spent in the sector, the post hoc test revealed that increasing separation around the RPAS does not significantly change the flight times of the manned flights in any of the scenarios when they are compared directly to the baseline ($p > 0.05$ for KPI_5 in Table 10.3). This means that increases in flight times in the order of 0.3 seconds are not the result of increasing the separation around the RPAS. Therefore, because of the first contrast of the planned comparison being significant (Table 10.2), it can be concluded that flight time is influenced by the Reaper that experiences a C2 link failure, but increasing the size of the separation bubble by up to 60% does not affect this metric.

Fuel Consumption (KPI_6)

The simulation results obtained for this KPI can be found in Table 9.6. The only significant increase in fuel consumption by non-RPAS flights compared to the baseline was when separation was increased by 60% ($p < 0.05$ for KPI_6 for scenario 1_8 in Table 10.3). In this case fuel consumption went up by 0.19%, or an additional 0.3 kg per flight. This suggest that if the separation bubble around an RPAS with performance similar to that of an MQ-9 Reaper increases up to 8NM/1600ft, the flights would not consume more fuel. Exceeding this threshold would result in more fuel being burnt, which translates to higher costs for the airlines and an increased impact on the environment.

Lost Altitude (KPI_7)

The simulation results obtained for this KPI can be found in Table 9.7. The Games-Howell post hoc test for lost altitude (the average flight level difference of the descending flights) revealed that the difference with respect to the baseline is only significant when the size of the separation bubble is increased by 60% ($p < 0.05$ for KPI_7 for scenario 1_8 in Table 10.3). The lost altitude decreases in this case by 0.17%. This means that for separation bubbles smaller than 8NM/1600ft the descending flights were not impacted; whereas a separation of 8NM/1600ft forced the other flights to stop or reduce their descent rates (the value for this KPI is lower than in the baseline).

10.3. Case 2: RQ-4A Global Hawk Scenarios

The focus of this section is to determine whether a RQ-4A Global Hawk experiencing a failure of the C2 link right at the moment when it enters an ATC sector significantly penalizes key ATM performance indicators. Also, the effect of increasing the size of the separation bubble that is enforced around the RPAS is assessed from a statistical point of view. The scenarios that are considered are: 1_1 - 1_4 which are first compared against the baseline case (no RPAS) and then between each other.

The hypothesis tested by ANOVA will be in this case: *"Are the mean results of the KPIs equal between the 5 scenarios?"* A significant result ($p < 0.05$) would mean that the hypothesis is rejected and that at least one scenario is different from the others for that particular KPI. A non-significant result ($p > 0.05$) would mean that the differences between scenarios for a certain KPI are too small to be considered significant and it can be concluded that the Global Hawk with a failed C2 link did not influence that KPI (mean values are equal).

Table 10.4 shows the ANOVA results for this case. The hypothesis of equal means was not rejected for KPIs 4 - 8. This means that having a Global Hawk did not change the distance flown, flight time, fuel consumption or lost/gained altitude of the manned flights. However, having a Global Hawk with a failed C2 link did influence the number of potential conflicts, controller task load, capacity and overall altitude deviation (at least one mean is significantly different). Levene's test was non-significant (equal variance between groups) in the case of controller task load, so the one-way ANOVA is used. For all other KPIs Welch's ANOVA is reported. For the KPIs that rejected the null hypothesis of the ANOVA, a planned contrast test will be carried out in order to determine the exact way in which the scenarios differ between them.

Table 10.4: ANOVA Results (Case 2)

KPI	Levene's Significance	ANOVA Type	ANOVA Result	H_0 Rejected?	Post hoc
KPI_1	0.04	Welch's ANOVA	[F(4,2646.93) = 5.64, p = 0]	Yes	G-H
KPI_2	0.28	One-way ANOVA	[F(4,5295) = 2.61, p = 0.03]	Yes	Tukey
KPI_3	0.00	Welch's ANOVA	[F(4,2645.98) = 13.8, p = 0]	Yes	G-H
KPI_4	0.00	Welch's ANOVA	[F(4,2614.36) = 0.66, p = 0.62]	No	No
KPI_5	0.00	Welch's ANOVA	[F(4,2631.33) = 0.69, p = 0.6]	No	No
KPI_6	0.00	Welch's ANOVA	[F(4,2336.72) = 0.21, p = 0.94]	No	No
KPI_7	0.00	Welch's ANOVA	[F(4,2642.52) = 1.24, p = 0.29]	No	No
KPI_8	0.00	Welch's ANOVA	[F(4,2583.49) = 0.3, p = 0.88]	No	No
KPI_9	0.00	Welch's ANOVA	[F(4,2622.78) = 2.63, p = 0.03]	Yes	G-H

Results of Planned Comparison Test

The results of the planned comparison are shown in Table 10.5. The one-tailed significance is used because the following hypothesis is tested: *"Will increasing the separation around the Global Hawk increase KPIs 1, 2 and 3 and reduce KPI 9?"* There are four contrasts that are applied which exclude scenarios one by one and compare the groups as follows:

1. The baseline with respect to the other 4 scenarios (*"Was there any significant impact of having a Global Hawk with a failed C2 link in the sector?"*)
2. Scenario 1_1 with respect to scenarios 1_2 - 1_4 (*"Was there any significant impact of enforcing a larger separation bubble around the Global Hawk with C2 link failure?"*)
3. Scenario 1_2 with respect to scenarios 1_3 and 1_4 (*"Was there any significant impact of increasing separation around the Global Hawk by 40 or 60% compared to the 20% case?"*)
4. Scenario 1_3 with respect to scenario 1_4 (*"Was there any significant impact of increasing separation around the Global Hawk by 60% compared to the 40% increase case?"*)

Table 10.5: Planned Comparison Results (Case 2)

KPI	0 vs (1,2,3,4)			1 vs. (2,3,4)			2 vs. (3,4)			3 vs. 4		
	t	df	Sig.	t	df	Sig.	t	df	Sig.	t	df	Sig.
KPI_1	0.20	1621.77	0.42	3.50	1933.21	0.00	2.93	2083.72	0.00	1.20	2117.96	0.11
KPI_2	-2.64	5295.00	0.00	0.93	5295.00	0.18	1.29	5295.00	0.10	-0.96	5295.00	0.17
KPI_3	7.19	1774.85	0.00	0.25	1863.86	0.40	0.16	2150.05	0.44	1.93	2116.30	0.03
KPI_9	-2.35	2368.07	0.01	-1.55	1840.73	0.06	-0.66	2139.50	0.25	-1.54	2116.30	0.06

The first contrast is significant for KPIs 2, 3 and 9 for which a post hot test is performed with respect to the baseline. The results are given in Table 10.6.

Number of Potential Conflicts (KPI_1)

The simulation results obtained for this KPI can be found in Table 9.1. The non-significant result for the first contrast (Table 10.5) means that, compared to the baseline, an RPAS with a performance similar to that of a

Table 10.6: Post Hoc Tests with respect to Baseline (Case 2)

KPI	0 vs. 1		0 vs. 2		0 vs. 3		0 vs. 4	
	Mean Difference	Sig.	Mean Difference	Sig.	Mean Difference	Sig.	Mean Difference	Sig.
KPI_2	0.12	0.14	-0.04	0.91	-0.04	0.92	0.06	0.74
KPI_3	-0.02	0.00	-0.02	0.00	-0.01	0.00	-0.02	0.00
KPI_9	2.05	0.98	6.02	0.52	5.10	0.68	12.16	0.02

Table 10.7: Post Hoc Tests KPI_1 (Case 2)

KPI	1 vs. 2		1 vs. 3		1 vs. 4		2 vs. 3		2 vs. 4	
	Mean Difference	Sig.	Mean Difference	Sig.	Mean Difference	Sig.	Mean Difference	Sig.	Mean Difference	Sig.
KPI_1	-0.08	0.84	-0.23	0.02	-0.33	0.00	-0.15	0.29	-0.25	0.01

Global Hawk does not impact the number of potential conflicts in the airspace when the separation bubble enforced around it is up to 8 NM/ 1,600 ft. However, the second contrast is significant ($p < 0.05$) which means that the increase in the number of conflicts measured between scenario 1_1 (same separation as for manned aircraft) and the scenarios 1_2 - 1_4 (an increase in separation around the RPAS) was significant (0.21 conflicts or 3.95%). Furthermore, as the third contrast is also significant, the additional 0.20 conflicts or 3.71% increase is significant when separation increases of 40 and 60% are used compared to the 20% case. The last contrast of KPI_1 is not significant which means that there is no impact on the number of potential conflicts when separation is increased from 7NM/1400ft to 8NM/1600ft (40% - 60% increase).

In order to determine whether there are any differences between the scenarios 1_1 - 1_4, a Games-Howell post hoc test is performed for this KPI. The results are shown in Table 10.7. The Games-Howell post hoc test revealed that increasing the separation by 20% does not increase the number of conflicts ($p > 0.05$ for 1_1 vs. 1_2, 1_2 vs. 1_3). This supports the findings of the last planned comparison from Table 10.5 which showed no significant difference between scenarios 1_3 and 1_4. On the other hand, increasing separation by 40% did result in a significant increase in number of potential conflicts ($p < 0.05$ when the following scenarios are compared: 1_1 - 1_3 and 1_2 - 1_4). Also increasing separation by 60% resulted in a significant increase in number of potential conflicts ($p < 0.05$ when scenarios 1_1 and 1_4 are compared). These differences can be explained by the fact that the sector considered is not neatly packed with aircraft, each 5 miles apart. Thus, it is possible that a small increase of 1 NM / 200 ft (which represents a 20% increase) can have little impact on the metrics.

These results suggest that if an RPAS with a performance similar to that of the RQ-4A Global Hawk experiences a failure of the C2 link there will be no impact on the number of potential conflicts if ATCo establish that a separation standard equal to that currently in place is sufficient to handle such a situation. If, however, ATCos would require a larger separation around the RPAS in order to have a buffer for the situations in which the remotely piloted aircraft deviates from its flights route or starts to behave unexpectedly, then the number of potential conflicts would increase. In order to experience a significant increase, the increase in separation around the RPAS should be of at least 40%.

ATCo Task Load (KPI_2)

The simulation results obtained for this KPI can be found in Table 9.2. Controller task load decreased by 0.13% when the four scenarios are compared against the baseline ($p < 0.05$ for contrast 1 of KPI_2 in Table 10.5). There are two possible causes for the counter-intuitive decrease in task load when an RPAS is present in the sector. One explanation is that because of the high climb performance of the Global Hawk (Figure 7.10), when one of the climbing flights was replaced with the RQ-4A, the RPAS spent less time in the sector and, therefore, the monitoring task load of the controller went down (it is directly proportional to the time a flight spends in the sector). Another possibility is that that because of the difference in performance compared to the aircraft that it replaced, the Global Hawk interacted with less aircraft than in the baseline (the number of potential conflicts first goes below that of the baseline for scenarios 1 and 2 and then it increases for scenarios 3 and 4) which meant that controller task load went down as fewer conflict resolution actions were required. Increasing the separation around the RPAS did not affect controller task load as the remaining three contrasts are not significant ($p > 0.05$).

In order to determine whether there are any differences between each individual scenario and the baseline, a Tukey post hoc test will be performed for this KPI. The results are shown in Table 10.6. All Tukey post hoc test were non-significant ($p > 0.05$) which means task load remained constant with respect to the baseline when different separation values were tested.

Sector Occupancy (KPI_3)

The simulation results obtained for this KPI can be found in Table 9.3. Regarding sector occupancy, the planned comparison analysis in Table 10.5 revealed that the difference of 0.02 aircraft per minute (5.47 in baseline vs. 5.49 in scenarios 1_1 - 1_4) is significant ($p < 0.05$ for contrast 1 of KPI_3). Moreover, each scenario significantly increased sector occupancy compared to the baseline (Table 10.6). However, increasing the size of the separation bubble did not influence this KPI (contrasts 2 and 3 in Table 10.5 are non-significant). The only significant increase in agglomeration is when scenario 1_4 is compared against 1_3 (contrast 4 in Table 10.5 is significant).

Altitude Deviation (KPI_9)

The simulation results obtained for this KPI can be found in Table 9.9. Having a Global Hawk with a failed C2 link did reduce the altitude deviations of manned flights compared to the baseline ($p < 0.05$ for contrast 1 for KPI_9 in Table 10.5). If the four scenarios with RQ-4A are compared with the baseline, altitude deviation went down by 0.08%. Increasing the separation around the RPAS did not penalize in a significant way the climb and descent manoeuvers of the remaining flights ($p > 0.05$ for contrasts 2 - 4 for KPI_9). The post hoc tests in Table 10.6 showed that the only significant difference is between the baseline and scenario 1_4, which means that increasing separation by 20% or 40% does not impact the climb / descent manoeuvers of the remaining flights. Since neither the lost altitude nor the gained altitude metric were significant in the ANOVA test (Table 10.4), it cannot be ascertained whether the Global Hawk penalized more climbing or descending flights.

10.4. Case 3: Increasing Percentage of RPAS Flights

The focus of this section is to determine whether other RPAS flights, in addition to the one MQ-9 Reaper that experiences a failure of the C2 link right at the moment when it enters an ATC sector, significantly penalize key ATM performance indicators. This will be tested by replacing 4, 9 and 14 of the other flights with MQ-9 Reapers (10, 20 and 30% of the total flights) which do not experience any failure and are active participants in conflict resolution. The size of the separation bubble that is enforced around the RPAS with C2 link failure is 10 NM/ 2,000 ft, which corresponds to doubling the minimum ICAO standards. The scenarios that are considered are 2_2, 2_4 and 2_5 which are first compared against the baseline case (no RPAS) and then between each other.

The hypothesis tested by ANOVA will be in this case: *"Are the mean results of the KPIs equal between the 4 scenarios?"* A significant result ($p < 0.05$) would mean that the hypothesis is rejected and that at least one scenario is different from the others for that particular KPI. A non-significant result ($p > 0.05$) would mean that the differences between scenarios for a certain KPI are not a result of adding different percentages of RPAS flights in the simulations (mean values are equal).

The ANOVA results for this case are shown in Table 10.8. As can be seen in this table, the hypothesis of equal means was rejected for all KPIs. The results of Welch's ANOVA were considered as Levene's test was significant for all KPIs.

Results of Planned Comparison Test

In order to determine the exact way in which the scenarios differ between them, a planned contrast analysis will be performed. The results of the planned comparison are shown in Table 10.9. The one-tailed significance is used because the following hypothesis is tested: *"Will an increase in the percentage of RPAS flights increase the values of KPIs 1, 2, 3, 4, 5, 6 and 8 and reduce KPIs 7 and 9?"* There were three contrasts that were applied which exclude scenarios one by one and compare the groups as follows:

1. The baseline with respect to the other 3 scenarios (*"Did the value of KPI_i increase when different percentages of flights are replaced by RPAS?"*)
2. Scenario 2_4 with respect to scenarios 2_2 and 2_5 (*"Did the value of KPI_i increase as more than 10% of the flights are switched to RPAS?"*)

Table 10.8: ANOVA Results (Case 3)

KPI	Levene's Significance	ANOVA Type	ANOVA Result	H_0 Rejected?	Post hoc
KPI_1	0.00	Welch's ANOVA	[F(3,2282.61) = 583.84, p = 0]	Yes	G-H
KPI_2	0.00	Welch's ANOVA	[F(3,2317.15) = 101.83, p = 0]	Yes	G-H
KPI_3	0.00	Welch's ANOVA	[F(3,2074.62) = 3384.01, p = 0]	Yes	G-H
KPI_4	0.00	Welch's ANOVA	[F(3,1967.16) = 41.43, p = 0]	Yes	G-H
KPI_5	0.00	Welch's ANOVA	[F(3,2021.49) = 96.99, p = 0]	Yes	G-H
KPI_6	0.00	Welch's ANOVA	[F(3,1791.25) = 21.52, p = 0]	Yes	G-H
KPI_7	0.00	Welch's ANOVA	[F(3,2096.32) = 121.24, p = 0]	Yes	G-H
KPI_8	0.00	Welch's ANOVA	[F(3,1879.35) = 3236.66, p = 0]	Yes	G-H
KPI_9	0.00	Welch's ANOVA	[F(3,1974.14) = 45.38, p = 0]	Yes	G-H

Table 10.9: Planned Comparison Results (Case 3)

KPI	Base. vs. (10%,20%,30% RPAS)			10% vs. (20%, 30% RPAS)			20% vs. 30% RPAS		
	t	df	Sig.	t	df	Sig.	t	df	Sig.
KPI_1	40.59	3040.12	0.00	12.89	2422.62	0.00	6.53	2112.55	0.00
KPI_2	16.92	2624.65	0.00	4.95	2372.66	0.00	2.73	2116.89	0.00
KPI_3	97.25	4034.11	0.00	44.38	2693.15	0.00	22.27	2093.56	0.00
KPI_4	10.87	3424.67	0.00	2.01	2915.92	0.02	0.86	1990.35	0.20
KPI_5	16.95	3538.36	0.00	4.96	2942.34	0.00	2.29	1984.78	0.01
KPI_6	7.59	2732.08	0.00	0.89	2926.15	0.19	0.59	1974.25	0.28
KPI_7	-19.01	3725.78	0.00	-7.77	2939.91	0.00	-2.61	2003.30	0.00
KPI_8	90.94	3159.60	0.00	1.66	2926.22	0.05	0.79	2018.28	0.21
KPI_9	-11.54	3391.51	0.00	-3.33	2983.92	0.00	-1.30	2006.29	0.10

3. Scenario 2_2 with respect to scenarios 2_5 (*"Did the value of KPI_i increase as more than 20% of the flights are switched to RPAS?"*)

As can be seen in Table 10.9, all KPIs increased significantly compared to the baseline situation (lost altitude and altitude deviation decreased). This is supported by the fact that the first contrast for all KPIs had a significance value lower than 0.05. Therefore, a Games-Howell post hoc test will be performed on all KPIs in order to determine how the individual scenarios differ from the baseline situation. The results are shown in Table 10.10. Furthermore, for KPIs 1, 2, 3, 5 and 7 a further post hoc test is performed to establish the differences between then 10 - 20% and 10 - 30% cases. These results are shown in Table 10.11.

Number of potential conflicts (KPI_1)

The simulation results obtained for this KPI can be found in Table 9.1. Switching more than 10% of the flights to RPAS significantly increased the number of potential conflicts by 18% ($p < 0.05$ for contrast 2 of this KPI in Table 10.9 which compares the 20 and 30% scenarios against the 10% one). Also, switching more than 20% of the flights to RPAS significantly increased the number of potential conflicts by 10.3% ($p < 0.05$ for contrast 3 of this KPI in Table 10.9 which compares the 30% scenario against the 20% one).

The increase in number of potential conflicts is significant both with respect to the baseline and as more flights were switched to RPAS. With respect to the baseline, each scenario significantly increased the number of potential conflicts by 39.7%, 56.8% and 72.9% ($p < 0.05$ for all post hoc tests in Table 10.10). The comparison between the scenarios themselves can be seen in Table 10.11 and in the fourth contrast in Table 10.9 which was found to be significant for all cases.

Controller Task Load (KPI_2)

The simulation results obtained for this KPI can be found in Table 9.2. Switching more than 10% of the flights to RPAS significantly increased the controller task load with 0.36% ($p < 0.05$ for contrast 2 of this KPI in Table

Table 10.10: Post Hoc Tests with respect to Baseline (Case 3)

KPI	Base. vs. 10% RPAS Flights		Base. vs. 20% RPAS Flights		Base. vs. 30% RPAS Flights	
	Mean Difference	Sig.	Mean Difference	Sig.	Mean Difference	Sig.
KPI_1	-2.17	0.00	-3.09	0.00	-3.97	0.00
KPI_2	-0.71	0.00	-0.94	0.00	-1.19	0.00
KPI_3	-0.20	0.00	-0.40	0.00	-0.61	0.00
KPI_4	-0.16	0.00	-0.20	0.00	-0.24	0.00
KPI_5	-2.26	0.00	-3.31	0.00	-4.43	0.00
KPI_6	-1.12	0.00	-1.26	0.00	-1.54	0.00
KPI_7	64.45	0.00	119.35	0.00	156.00	0.00
KPI_8	-689.95	0.00	-704.66	0.00	-720.69	0.00
KPI_9	43.77	0.00	65.74	0.00	84.26	0.00

Table 10.11: Post Hoc Tests (Case 3)

KPI	10% vs. 20% RPAS flights		10% vs. 30% RPAS flights	
	Mean Difference	Sig.	Mean Difference	Sig.
KPI_1	-0.93	0.00	-1.81	0.00
KPI_2	-0.24	0.03	-0.49	0.00
KPI_3	-0.20	0.00	-0.41	0.00
KPI_5	-1.05	0.02	-2.17	0.00
KPI_7	54.90	0.00	91.55	0.00

10.9 which compares the 20 and 30% scenarios against the 10% one). Also, switching more than 20% of the flights to RPAS significantly increased ATCo task load with 0.25% ($p < 0.05$ for contrast 3 of this KPI in Table 10.9 which compares the 30% scenario against the 20% one).

The increase in task load is significant both with respect to the baseline and as more flights were switched to RPAS. With respect to the baseline, each scenario significantly increased controller task load with 0.7%, 0.9% and 1.2% ($p < 0.05$ for all post hoc tests in Table 10.10). The comparison between the scenarios themselves can be seen in Table 10.11 and in the fourth contrast in Table 10.9 which was found to be significant for all cases.

Sector Occupancy (KPI_3)

The simulation results obtained for this KPI can be found in Table 9.3. Switching more than 10% of the flights to RPAS significantly increased the agglomeration of the sector by 5.5% ($p < 0.05$ for contrast 2 of this KPI in Table 10.9 which compares the 20 and 30% scenarios against the 10% one). Also, switching more than 20% of the flights to RPAS significantly increased sector occupancy by 3.6% ($p < 0.05$ for contrast 3 of this KPI in Table 10.9 which compares the 30% scenario against the 20% one).

The increase in sector occupancy is significant both with respect to the baseline and as more flights were switched to RPAS. With respect to the baseline, each scenario significantly increased sector occupancy by 3.6%, 7.3% and 11.2% ($p < 0.05$ for all post hoc tests in Table 10.10). The comparison between the scenarios themselves can be seen in Table 10.11 and in the fourth contrast in Table 10.9 which was found to be significant for all cases.

Distance flown (KPI_4)

The simulation results obtained for this KPI can be found in Table 9.4. Switching more than 10% of the flights

to RPAS significantly increased the distance flown by the non-RPAS flights by 0.17% ($p < 0.05$ for contrast 2 of this KPI in Table 10.9 which compares the 20 and 30% scenarios against the 10% one). However, switching more than 20% of the flights to RPAS did not affect this metric ($p > 0.05$ for contrast 3 of this KPI in Table 10.9). The post hoc tests in Table 10.10 are significant, which means that increases of 0.5%, 0.6% and 0.7% in flight distances with respect to the baseline are significant when 10%, 20% and 30% of the flights are switched to an RPAS.

Flight Time (KPI_5)

The simulation results obtained for this KPI can be found in Table 9.5. Switching more than 10% of the flights to RPAS significantly increased the flight time of non-RPAS flights by 0.5% ($p < 0.05$ for contrast 2 of this KPI in Table 10.9 which compares the 20 and 30% scenarios against the 10% one). Also, switching more than 20% of the flights to RPAS significantly increased flight time by 0.3% ($p < 0.05$ for contrast 3 of this KPI in Table 10.9 which compares the 30% scenario against the 20% one).

The increase in flight time is significant both with respect to the baseline and as more flights were switched to RPAS. With respect to the baseline, each scenario significantly increased flight time by 0.7%, 1.0% and 1.4% ($p < 0.05$ for all post hoc tests in Table 10.10). The comparison between the scenarios themselves can be seen in Table 10.11 and in the fourth contrast in Table 10.9 which was found to be significant for all cases.

Fuel Consumption (KPI_6)

The simulation results obtained for this KPI can be found in Table 9.6. The fuel consumption increase of 0.9% compared to the baseline when the three RPAS scenarios are considered is significant ($p < 0.05$ for contrast 1 of this KPI in Table 10.9). However, varying the percentage of RPAS flights did not influence the fuel consumption of non-RPAS flights ($p < 0.05$ for contrast 2 and 3 of this KPI in Table 10.9).

Lost Altitude (KPI_7)

The simulation results obtained for this KPI can be found in Table 9.7. Switching more than 10% of the flights to RPAS significantly reduced the altitude that was descended by the non-RPAS flights by 0.7% ($p < 0.05$ for contrast 2 of this KPI in Table 10.9 which compares the 20 and 30% scenarios against the 10% one). Also, switching more than 20% of the flights to RPAS significantly reduced lost altitude by 0.4% ($p < 0.05$ for contrast 3 of this KPI in Table 10.9 which compares the 30% scenario against the 20% one).

The decrease in lost altitude is significant both with respect to the baseline and as more flights were switched to RPAS. With respect to the baseline, each scenario significantly decreased lost altitude by 0.6%, 1.2% and 1.6% ($p < 0.05$ for all post hoc tests in Table 10.10). The comparison between the scenarios themselves can be seen in Table 10.11 and in the fourth contrast in Table 10.9 which was found to be significant for all cases. A decrease in this metric means that the flights descent procedures have been stopped during conflict resolution, having a negative effect on their descent performance. The significance of this result is also supported by the fact that for scenario 2_2 31% of the conflicts between a manned aircraft and an RPAS were solved by stopping the descent manoeuver (Section 8.3).

Gained Altitude (KPI_8)

The simulation results obtained for this KPI can be found in Table 9.8. Switching more than 10% or 20% of the flights to RPAS did not affect the gained altitude ($p > 0.05$ for contrast 2 and 3 of this KPI in Table 10.9). The post hoc tests in Table 10.10 are significant, which means that increases of 15.7%, 16.1% and 16.4% in gained altitude with respect to the baseline are significant when 10%, 20% and 30% of the flights are switched to an RPAS.

Graphical Interpretation of ANOVA Results for Case 3

The results of the ANOVA analysis that were presented in this section can be summarized by looking at Figures 10.2 and 10.3 which plot the percentage change of each KPI with respect to the baseline scenario for

the three situations that were considered: 10%, 20% and 30% of the flights are replaced by a MQ-9 Reaper. Different scales of the vertical axis are used to improve the readability of the graphs.

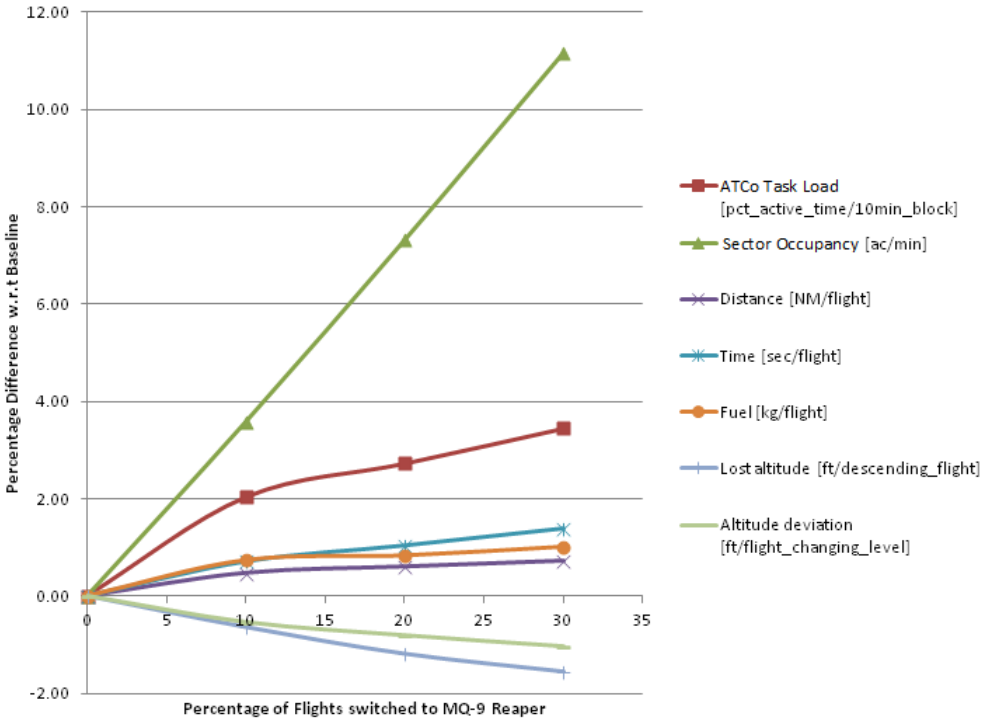

Figure 10.2: Percentage Change of KPIs 2 - 7 and 9 with respect to Baseline

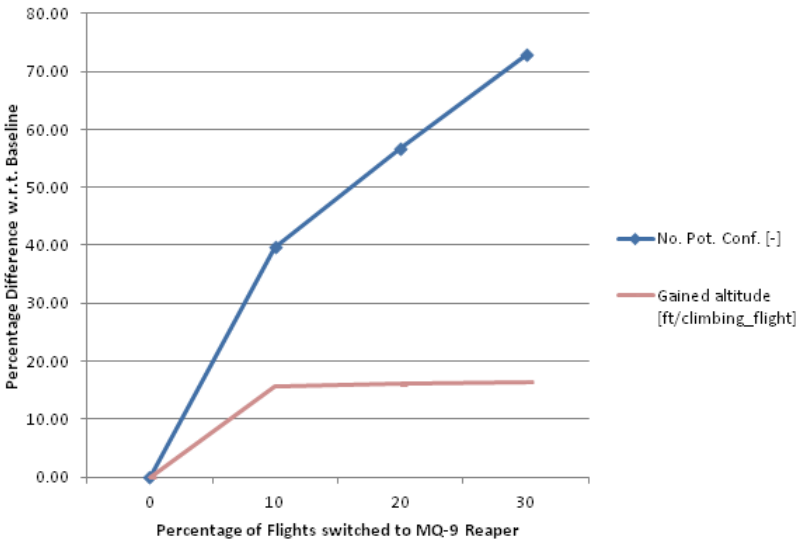

Figure 10.3: Percentage Change of KPIs 1 and 8 with respect to Baseline

Switching 10 – 30% of the flights to RPAS has significantly increased all KPIs (lost altitude and altitude deviation decreased). The small slope of distance flown, altitude deviation, fuel consumption, and gained altitude confirms that varying the percentage of RPAS flights between 10 – 30% did not affect these metrics. In the case of potential conflicts, ATCo task load, capacity, flight time and lost altitude, these metrics were also influenced by the different percentages of flights that were switched to a MQ-9 as can be seen by their positive slopes (negative for lost altitude). Using the method of least squares (which was discussed in Section 6.1) the

trend lines in Equations 10.18 - 10.22 are obtained. Having 5% RPAS flights for instance and using these equations, the number of potential conflicts in the sector would be approximately 6.5 and the sector occupancy 5.6 aircraft per minute. At the same time, the average flight time in the sector is estimated to be 320.6 seconds and the controller would be active for 34.8% of his/her time.

$$\text{Potential Conflicts [-]} = 0.1285 \cdot \text{RPAS Flights [\%]} + 5.8342, \quad R^2 = 0.9445 \tag{10.18}$$

$$\text{ATCo Task Load [\% time active]} = 0.0381 \cdot \text{RPAS Flights [\%]} + 34.633, \quad R^2 = 0.9199 \tag{10.19}$$

$$\text{Sector Occupancy [ac/min]} = 0.0204 \cdot \text{RPAS Flights [\%]} + 5.47, \quad R^2 = 0.9997 \tag{10.20}$$

$$\text{Flight Time [sec]} = 0.1434 \cdot \text{RPAS Flights [\%]} + 319.88, \quad R^2 = 0.9616 \tag{10.21}$$

$$\text{Lost Altitude [ft]} = -5.2289 \cdot \text{RPAS Flights [\%]} + 9998.4, \quad R^2 = 0.9858 \tag{10.22}$$

10.5. Case 4: Increasing Separation around RPAS

The focus of this section is to determine whether increasing the separation around the RPAS flights that experiences a failure of the C2 link in an environment with multiple RPAS flights (9 other MQ-9 flights without a failed C2 link) significantly penalizes key ATM performance indicators. This will be tested by replacing the size of the separation bubble with 8 NM / 1,600 ft, 10 NM / 2, 000 ft and 15 NM / 3,000 ft (60%, 100% and 200% increase compared to the minimum 5 NM / 1,000 ft ICAO standards). The scenarios which are considered are 2_1, 2_2 and 2_3 which are first compared against the baseline case (no RPAS) and then between each other in order to assess the impact of increasing the size of the separation bubble.

The hypothesis tested by ANOVA will be in this case: *"Are the mean results of the KPIs equal between the 4 scenarios?"* A significant result ($p < 0.05$) would mean that the hypothesis is rejected and that having different separations affected the KPIs. However, in order to understand the exact way in which the scenarios differ, a planned comparison and post hoc analysis will have to be carried out. A non-significant result ($p > 0.05$) would mean that the differences between scenarios for a certain KPI are not a result of increasing the size of the separation bubble.

The results of the ANOVA tests for this case can be seen in Table 10.12. The hypothesis of equal means was rejected for all KPIs. The results of Welch's ANOVA were considered as Levene's test was significant for all KPIs. In order to determine the exact way in which the scenarios differ between them, a planned contrast analysis will be performed. If all contrasts are significant for a particular KPI, an additional Games-Howell post hoc test will be carried out for that metric.

Table 10.12: ANOVA Results (Case 4)

KPI	Levene's Significance	ANOVA Type	ANOVA Result	H_0 Rejected?	Post hoc
KPI_1	0.00	Welch's ANOVA	[F(3,2242.83) = 787.29, p = 0]	Yes	G-H
KPI_2	0.00	Welch's ANOVA	[F(3,2276.53) = 227.28, p = 0]	Yes	G-H
KPI_3	0.00	Welch's ANOVA	[F(3,2043.41) = 3024.54, p = 0]	Yes	G-H
KPI_4	0.00	Welch's ANOVA	[F(3,1932.31) = 30.34, p = 0]	Yes	G-H
KPI_5	0.00	Welch's ANOVA	[F(3,1976.55) = 79.29, p = 0]	Yes	G-H
KPI_6	0.00	Welch's ANOVA	[F(3,1786.51) = 28.72, p = 0]	Yes	G-H
KPI_7	0.00	Welch's ANOVA	[F(3,2031.57) = 144.61, p = 0]	Yes	G-H
KPI_8	0.00	Welch's ANOVA	[F(3,1863.45) = 2885.03, p = 0]	Yes	G-H
KPI_9	0.00	Welch's ANOVA	[F(3,1931.96) = 53.8, p = 0]	Yes	G-H

Results of Planned Comparison Test

The results of the planned comparison are shown in Table 10.13. The one-tailed significance is used because the following hypothesis is tested: *"Will an increase in separation around the RPAS with a failed C2 link increase KPIs 1, 2, 3, 4, 5, 6 and 8 and decrease KPIs 7 and 9?"* There were three contrasts that were applied which exclude scenarios one by one and compare the groups as follows:

1. The baseline with respect to the other 3 scenarios (*"Did the value of KPI_i increase when different sizes of the separation bubble were tested?"*)
2. Scenario 2_1 with respect to scenarios 2_2 and 2_3 (*"Did separation bubbles larger than 8 NM / 1,600 ft increase the value of KPI_i?"*)
3. Scenario 2_2 with respect to scenario 2_3 (*"Did separation bubbles larger than 10 NM / 2,000 ft increase the value of KPI_i?"*)

Table 10.13: Planned Comparison Results (Case 4)

KPI	Base. vs. (60%, 100%, 200% Sep. Incr.)			60% vs. (100%, 200% Sep. Incr.)			100% vs. 200% Sep. Incr.		
	t	df	Sig.	t	df	Sig.	t	df	Sig.
KPI_1	47.37	3384.95	0.00	15.95	2510.41	0.00	18.00	1913.09	0.00
KPI_2	23.57	3093.04	0.00	11.92	2530.95	0.00	14.66	1852.72	0.00
KPI_3	95.22	4220.37	0.00	0.35	2186.92	0.36	1.98	2107.80	0.02
KPI_4	9.37	3873.27	0.00	1.38	2291.08	0.08	-0.33	2055.38	0.37
KPI_5	15.27	4060.65	0.00	2.01	2216.60	0.02	0.08	2069.59	0.47
KPI_6	9.17	3222.65	0.00	1.56	2293.59	0.06	2.32	2078.96	0.01
KPI_7	-20.80	3987.29	0.00	-3.14	2343.22	0.00	-3.62	1968.68	0.00
KPI_8	92.84	3667.52	0.00	0.06	2249.80	0.48	1.06	2110.98	0.14
KPI_9	-12.53	3957.90	0.00	-2.21	2180.10	0.01	-2.17	2095.07	0.02

The first contrast was significant for all KPIs ($p < 0.05$), meaning that the increase / decrease that was measured between the three scenarios with respect to the baseline is significant. As this contrast considered the three scenarios together, a Games-Howell post hoc test is required in order to establish how the scenarios differ from each other. The results are given in Tables 10.14 and 10.15.

Table 10.14: Post Hoc Tests with respect to Baseline (Case 4)

KPI	Base vs. 60% Sep. Incr.		Base vs. 100% Sep. Incr.		Base vs. 200% Sep. Incr.	
	Mean Difference	Sig.	Mean Difference	Sig.	Mean Difference	Sig.
KPI_1	-2.61	0.00	-3.09	0.00	-5.98	0.00
KPI_2	-0.76	0.00	-0.94	0.00	-2.62	0.00
KPI_3	-0.41	0.00	-0.40	0.00	-0.42	0.00
KPI_4	-0.14	0.00	-0.20	0.00	-0.19	0.00
KPI_5	-2.57	0.00	-3.31	0.00	-3.35	0.00
KPI_6	-1.21	0.00	-1.26	0.00	-2.26	0.00
KPI_7	109.34	0.00	119.35	0.00	171.56	0.00
KPI_8	-713.48	0.00	-704.66	0.00	-724.19	0.00
KPI_9	55.44	0.00	65.74	0.00	94.24	0.00

Number of potential conflicts (KPI_1)

The simulation results obtained for this KPI can be found in Table 9.1. Enforcing separations larger than 8 NM / 1,600 ft around the Reaper with C2 link failure significantly increased the number of potential conflicts by 24.0% ($p < 0.05$ for contrast 2 of this KPI in Table 10.13 which compared the 60% separation increase case with the other two situations). Also, enforcing separations larger than 10 NM / 2,000 ft around the RPAS significantly increased the number of potential conflicts by 33.7% ($p < 0.05$ for contrast 3 of this KPI in Table

Table 10.15: Post Hoc Tests (Case 4)

KPI	60% vs. 100% Sep. Incr.		60% vs. 200% Sep. Incr.	
	Mean Difference	Sig.	Mean Difference	Sig.
KPI_1	-0.49	0.00	-3.37	0.00
KPI_2	-0.18	0.19	-1.86	0.00
KPI_5	-0.74	0.30	-0.78	0.32
KPI_7	10.01	0.85	62.22	0.00

10.13 which compared the 100 and 200% separation increase cases).

The increase in number of potential conflicts is significant both with respect to the baseline and as the size of the separation bubble increases. With respect to the baseline, each scenario significantly increased the number of potential conflicts by 47.8%, 56.8% and 109.6% ($p < 0.05$ for all post hoc tests in Table 10.14). The comparison between the scenarios themselves can be seen in Table 10.15 and in the fourth contrast in Table 10.13 which were found to be significant for all cases.

Controller Task Load (KPI_2)

The simulation results obtained for this KPI can be found in Table 9.2. Enforcing separations larger than 8 NM / 1,600 ft around the Reaper with C2 link failure significantly increased the controller task load with 1.0% ($p < 0.05$ for contrast 2 of this KPI in Table 10.13 which compared the 60% separation increase case with the other two situations). Also, enforcing separations larger than 10 NM / 2,000 ft around the RPAS significantly increased ATCo task load with 1.7% ($p < 0.05$ for contrast 3 of this KPI in Table 10.13 which compared the 100 and 200% separation increase cases).

The increase in task load is significant both with respect to the baseline and as the size of the separation bubble increases. With respect to the baseline, each scenario significantly increased controller task load with 0.8%, 0.9% and 2.6% ($p < 0.05$ for all post hoc tests in Table 10.14). Table 10.15 shows that there is no significant difference in ATCo task load between the 60% and 100% scenarios, which means that doubling the size of the separation bubble has the same impact to task load as increasing it by 60%.

Sector Occupancy (KPI_3)

The simulation results obtained for this KPI can be found in Table 9.3. Enforcing separations larger than 8 NM / 1,600 ft around the Reaper with C2 link failure did not increase the agglomeration of the sector significantly ($p > 0.05$ for contrast 2 of this KPI in Table 10.13). However, enforcing separations larger than 10 NM / 2,000 ft around the RPAS significantly increased sector occupancy by 0.31% ($p < 0.05$ for contrast 3 of this KPI in Table 10.13 which compared the 100 and 200% separation increase cases). With respect to the baseline, each scenario significantly increases sector occupancy by 7.4%, 7.3% and 7.6% ($p < 0.05$ for all post hoc tests in Table 10.14), but the differences between the scenarios themselves are not significant.

Distance flown (KPI_4)

The simulation results obtained for this KPI can be found in Table 9.4. With respect to the baseline, each scenario significantly increased the distance flown by non-RPAS flights by 0.4%, 0.6% and 0.6% ($p < 0.05$ for post hoc tests in Table 10.14). However, enforcing separations larger than 8 NM / 1,600 ft around the Reaper with C2 link failure did not increase the the distances flown ($p > 0.05$ for contrast 2 and 3 of this KPI in Table 10.13), therefore the size of the separation bubble did not play a role for this metric.

Flight Time (KPI_5)

The simulation results obtained for this KPI can be found in Table 9.5. Enforcing separations larger than 8 NM / 1,600 ft around the Reaper with C2 link failure resulted in an increase in flight time of non-RPAS flights

of 0.24% (or 0.24 seconds) which is significant ($p < 0.05$ for contrast 2 of this KPI in Table 10.13 which compared the 60% separation increase case with the other two situations). However, enforcing separations larger than 10 NM / 2,000 ft around the RPAS does not influence the results significantly ($p > 0.05$ for contrast 3 of this KPI in Table 10.13). The differences with respect to the baseline are significant for all three scenarios as indicated by the post hoc tests in Table 10.14, but when compared with each other, the differences between the scenarios are not significant (Table 10.15). Therefore, the size of the separation bubble did not play a role for this metric.

Fuel Consumption (KPI_6)

The simulation results obtained for this KPI can be found in Table 9.6. Enforcing separations larger than 8 NM / 1,600 ft around the Reaper with C2 link failure did not increase the fuel consumption of non-RPAS flights ($p > 0.05$ for contrast 2 of this KPI in Table 10.13). However, enforcing separations larger than 10 NM / 2,000 ft around the RPAS significantly increased fuel consumption by 0.7% ($p < 0.05$ for contrast 3 of this KPI in Table 10.13 which compared the 100 and 200% separation increase cases). With respect to the baseline, each scenario significantly increases fuel consumption by 0.8%, 0.8% and 1.5% ($p < 0.05$ for all post hoc tests in Table 10.14).

Lost Altitude (KPI_7)

The simulation results obtained for this KPI can be found in Table 9.7. Enforcing separations larger than 8 NM / 1,600 ft around the Reaper with C2 link failure significantly reduced the altitude that was descended by the non-RPAS flights by 0.4% ($p < 0.05$ for contrast 2 of this KPI in Table 10.13 which compared the 60% separation increase case with the other two situations). Also, enforcing separations larger than 10 NM / 2,000 ft around the RPAS significantly reduced lost altitude by 0.5% ($p < 0.05$ for contrast 3 of this KPI in Table 10.13 which compared the 100 and 200% separation increase cases).

The decrease in lost altitude is significant both with respect to the baseline and as the size of the separation bubble increases. With respect to the baseline, each scenario significantly decreased lost altitude by 1.1%, 1.2% and 1.7% ($p < 0.05$ for all post hoc tests in Table 10.14). Table 10.15 shows that there is no significant difference in lost altitude between the 60% and 100% scenarios, which means that doubling the size of the separation bubble has the same impact on this metric as increasing it by 60%.

Gained Altitude (KPI_8)

The simulation results obtained for this KPI can be found in Table 9.8. With respect to the baseline, each scenario significantly increased the gained altitude of non-RPAS flights by 16.3%, 16.1% and 16.5% ($p < 0.05$ for post hoc tests in Table 10.14). However, enforcing separations larger than 8 NM / 1,600 ft around the Reaper with C2 link failure did not increase this KPI ($p > 0.05$ for contrast 2 and 3 of this KPI in Table 10.13), so the size of the separation bubble did not play a role for the gained altitude metric.

Graphical Interpretation of ANOVA Results for Case 4

The results of the ANOVA analysis that were presented in this section can be summarized by looking at Figures 10.4 and 10.5 which plot the percentage change of each KPI with respect to the baseline scenario for the three situations that were considered: 60%, 100% and 200% separation increase around the MQ-9 Reaper that experienced a failure of the C2 link. Different scales of the vertical axis are used to improve the readability of the graphs.

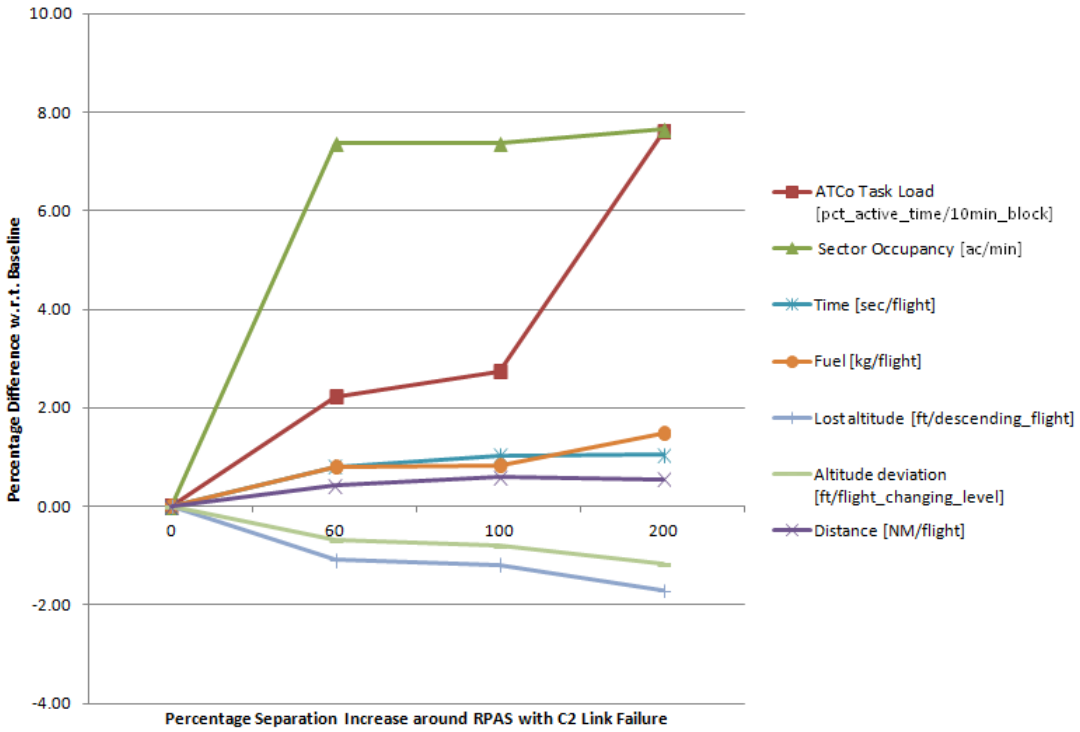

Figure 10.4: Percentage Change of KPIs 2 - 7 and 9 with respect to Baseline

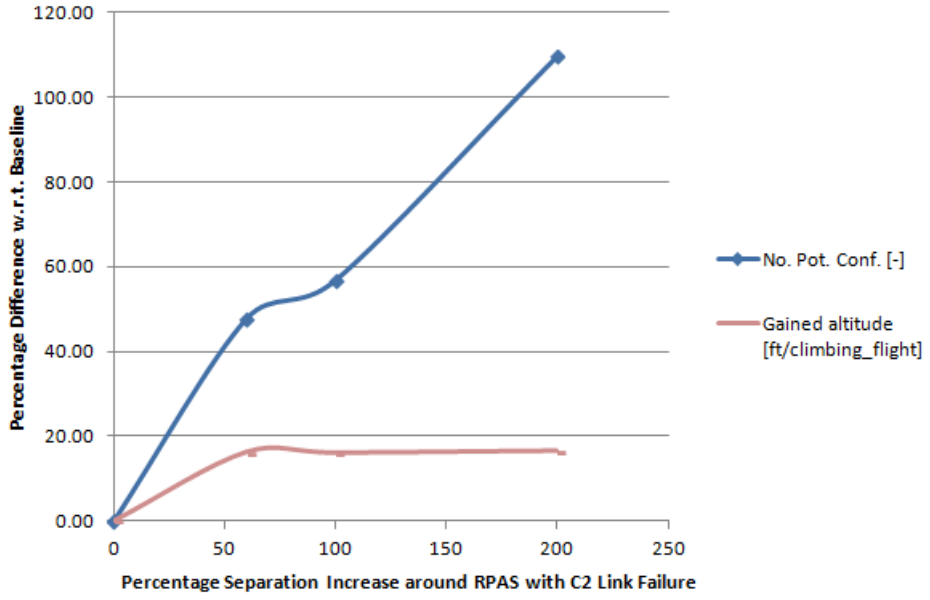

Figure 10.5: Percentage Change of KPIs 1 and 8 with respect to Baseline

As can be seen in Figures 10.4 and 10.5, all KPIs increased with respect to the baseline (altitude deviation and lost altitude decreased). Distance flown, gained altitude and capacity are not influenced by the increase in separation (slope is zero). Flight time is not influenced when separation is increased by more than 100% and fuel consumption and controller task load are affected only when separation is more than double. As the change in gained altitude was not significant, the choice to drop the altitude deviation metric was appropriate, as one can see that its line follows that of the lost altitude.

Furthermore, as can be seen in Figure 10.5, the number of potential conflicts increased as separation in-

creases. Equations 10.23 shows the linear trend lines that is obtained for KPI_1 using the method of least squares (Section 6.1). For instance, increasing the separation bubble by 10% would result in 6.10 potential conflicts while a 50% increase would result in 7.22 potential conflicts.

$$\text{Potential Conflicts [-]} = 0.0288 \cdot \text{Sep. Incr. [\%]} + 5.7816, \quad R^2 = 0.9758 \tag{10.23}$$

10.6. Case 5: Difference in Performance (MQ-9 Vs. RQ-4A)

The focus of this analysis is to determine whether the performance of the RPAS that experiences the failure of the C2 link affects key ATM performance indicators. The analysis will consider an RQ-4A Global Hawk (turbofan) and an MQ-9 Reaper (turboprop) and will compare the results obtained during the experiments for four values of the separation bubble around the RPAS: 5 NM / 1,000 ft, 6 NM / 1,200 ft, 7 NM / 1,400 ft and 8 NM / 1,600 ft (or 0%, 20%, 40% and 60% increase with respect to the minimum separation imposed by ICAO).

The hypothesis tested by ANOVA will be in this case: *"Are the mean results of the KPIs equal for the two different RPAS and for the separation value considered?"* A significant result ($p < 0.05$) would mean that the hypothesis is rejected and that the performance of the RPAS resulted in a significant difference for the KPI that was considered. A non-significant result ($p > 0.05$) would mean that any difference measured during the experiment was not due to the difference in RPAS performance and the considered KPI scored equally in both cases.

The results of the ANOVA tests between scenarios 1_1 – 1_5, 1_2 – 1_6, 1_3 – 1_7 and 1_4 – 1_8 are shown in Tables I.1 - I.4 of Appendix I. The following observations can be drawn:

- The number of potential conflicts, controller task load and sector occupancy were significantly different between the RQ-4A and MQ-9 scenarios ($p < 0.05$ for KPIs 1, 2 and 3 for all values of separation). Table 10.16 summarizes the percentage increase with respect to the RQ-4A scenarios for the four separation values. Having a turbofan RPAS with a lower overall performance resulted in a significant increase for all the three metrics. Therefore, for these metrics, it can be said that the Reaper penalized more the other flights than the Global Hawk.

Table 10.16: Differences KPIs 1 - 3 (RQ-4A Vs. MQ-9)

KPI / Scenario	**0% Sep. Incr. (Scn. 1_1 vs. 1_5)**	**20% Sep. Incr. (Scn. 1_2 vs. 1_6)**	**40% Sep. Incr. (Scn. 1_3 vs. 1_7)**	**60% Sep. Incr. (Scn. 1_4 vs. 1_8)**
KPI_1	6.83%	9.69%	7.48%	8.41%
KPI_2	0.83%	0.94%	0.67%	0.76%
KPI_3	0.42%	0.37%	0.49%	0.38%

- The only case in which the difference between the two RPAS cases was significant for the flight distance was when a separation increase of 40% was used. In this case the Reaper increased flight distance by 0.04 NM (0.1% compared to the Global Hawk case).
- Flight time was also higher in the Reaper case when 20% and 40% separation increase values were used. The difference was of 0.12% or 0.45 seconds.
- Separation increases of 40% and 60% increased the fuel consumption by 0.2% when a Reaper was used instead of the Global Hawk. This represents an additional 0.3 kg of fuel burnt by the flights while in the sector.
- There was no significant difference with respect to gained / lost altitude or altitude deviation between the two RPAS cases for any of the separation values that were considered.

10.7. Conclusions of ANOVA Tests

The results discussed in this chapter for each of the four cases are summarized in this section for each key performance indicator. Where available, a comparison is also made between the results obtained for this experiments and those found in literature from similar experiments. These results were discussed in Section 2.5 where the state-of-the-art was presented.

Number of potential conflicts (KPI_1)

- Enforcing the same separation as for manned aircraft (5 NM / 1,000 ft) did not impact this KPI. Using an RPAS with a performance similar with that of the Global Hawk does not increase the number of potential conflicts with respect to the baseline when separation is increased by up to 60%. An RPAS with a performance close to that of the Reaper resulted in a significant increase in the number of potential conflicts compared to the baseline: 8.3%, 9.2% and 12.0% (for separation increases of 20, 40 and 60%).
- For this metric the differences between the two performing RPAS were significant. The MQ-9 scenarios created 6.8% - 9.7% more conflicts than the RQ-4A scenarios when the same separation was used.
- Switching 10, 20 and 30% of the flights to RPAS and having one which encounters a C2 link loss (around which separation is doubled) increased this KPI by 39.7%, 56.8% and 72.9% with respect to the baseline. A linear relationship was found between the number of potential conflicts and the percentage of flights switched to RPAS. This was also the outcome of [42] which performed 9 real-time human-in-the-loop simulations of an ATC sector in which 1 - 4 flights were replaced by an RPAS. Furthermore, these values are in the same range of those obtained in a study of the US National Airspace which considered two future scenarios (10% and 40% increase in the number of flights) and replaced 20% of the flights by RPAS. In this case the number of blind encounters increased by 41% and 67% compared to the baseline case. [5]
- In an environment with 20% RPAS flights, the effect of varying the size of the separation bubble around the one RPAS with C2 link failure (increasing it by 60, 100 and 200%) was to increase the number of potential conflicts by 47.8%, 56.8% and 109.6% compared to the baseline. A linear relationship was found between the number of potential conflicts and the percentage increase in separation around the RPAS with C2 link failure.

Controller Task Load (KPI_2)

- Varying the size of the separation bubble (20 - 60% increase) did not result in a significant change of this KPI. The ERAINT project, which also used the MQ-9 for its simulations, revealed that using the same contingency for a C2 link loss as in this experiment has a limited impact on ATCo task load. [30]
- For this metric the differences between the two performing RPAS were significant. The MQ-9 scenarios increased task load by 0.7% - 0.8% compared to the RQ-4A scenarios when the same separation was used. The study of Vu et al. also concluded that RPAS with lower speeds increase controller task load. [42].
- Switching 10, 20 and 30% of the flights to RPAS and having one which encounters a C2 link loss (around which separation is doubled) increased this KPI by 2.0%, 2.7% and 3.5% with respect to the baseline. A linear relationship was found between controller task load and the percentage of flights switched to RPAS.
- In an environment with 20% RPAS flights, increasing the size of the separation bubble around the one RPAS with C2 link failure by 100 and 200% increased this KPI by 2.7% and 7.6% compared to the baseline. A separation of 60% increase resulted in the same controller task load as in the 100% increase case.

Sector Occupancy (KPI_3)

- Varying the size of the separation bubble (20 - 60% increase) did not result in a significant change of this KPI.
- For this metric the differences between the two performing RPAS were significant. The MQ-9 scenarios increased sector occupancy by 0.4% - 0.5% compared to the RQ-4A scenarios.

- Switching 10, 20 and 30% of the flights to RPAS and having one which encounters a C2 link loss (around which separation is doubled) increased this KPI by 3.6%, 7.3% and 11.2% with respect to the baseline. A linear relationship was found between sector occupancy and the percentage of flights switched to RPAS. A study of the US National Airspace determined that switching 20% of the flights to RPAS and using the same separation standards has a small effect on the agglomeration of the sector (increase was of 0.3%). [5] However, this study considered the same separation standard around RPAS.
- In an environment with 20% RPAS flights, increasing the size of the separation bubble around the one RPAS with C2 link failure by 100 and 200% increased sector occupancy by 7.3% and 7.7% compared to the baseline. However, an increase in separation of 60% resulted in the same value of this KPI compared to the 100% separation increase case.

Distance flown (KPI_4)

- Having an RPAS with a failed C2 link did not affect the distance flown by the other (non-RPAS) flights when the size of the separation bubble was increased by up to 60%. In an environment with 20% RPAS flights, distance flown increases by 0.5%, but varying the size of the separation bubble around the one RPAS with C2 link failure between 60 - 200% does not affect this metric.
- Switching 10 - 30% of the flights to RPAS and having one which encounters a C2 link loss (around which separation is doubled) increased this KPI by 0.5 - 0.6% with respect to the baseline. The differences between the scenarios themselves were not found to be significant. This was also the finding in [42] and [44] which concluded that there is no trend between the distance travelled and the number of RPAS present in the sector.

Flight Time (KPI_5)

- Varying the size of the separation bubble (20 - 60% increase) did not result in a significant change of this KPI. This is in accordance with the study of the US National Airspace which found that replacing 20% of the flights by RPAS and maintaining the same separation standards does not result in delays of manned flights. [5] This was also the outcome of the ERAINT project. [45]
- Compared to the RQ-4A, the MQ-9 scenarios increased flight times by 0.12% when the size of the separation bubble was increased by 20 and 40%.
- Switching 10, 20 and 30% of the flights to RPAS and having one which encounters a C2 link loss (around which separation is doubled) increased this KPI by 0.7%, 1.0% and 1.4% with respect to the baseline. A linear relationship was found between flight time and the percentage of flights switched to RPAS.
- In an environment with 20% RPAS flights, increasing the size of the separation bubble around the one RPAS with C2 link failure by 60% and 100% increased flight times by 0.4% and 0.6% compared to the baseline. However, further increasing separation by 200% did not results in an increase in flight times compared to the 100% case.

Fuel Consumption (KPI_6)

- Having an RQ-4A with a failed C2 link did not affect the fuel consumption of the other (non-RPAS) flights when the size of the separation bubble was increased by up to 60%. The MQ-9 increased fuel consumption only when a separation increase of 60% was enforced.
- Compared to the RQ-4A, the MQ-9 scenarios increased fuel consumption by 0.2% when the size of the separation bubble was increased by 20 and 40%.
- Switching 10, 20 and 30% of the flights to RPAS and having one which encounters a C2 link loss (around which separation is doubled) increased this KPI by 0.7%, 0.8% and 1.0% with respect to the baseline. Between the scenarios themselves, the differences were not significant.
- In an environment with 20% RPAS flights, increasing the size of the separation bubble around the one RPAS with C2 link failure by 100 and 200% increased fuel consumption by 0.8% and 1.5% compared to the baseline. However, an increase in separation of 60% resulted in the same value of this KPI compared to the 100% separation increase case.

Altitude Deviation (KPIs 7 - 9)

- Having an RPAS with a failed C2 link did not affect the gained/lost altitude of the non-RPAS flights when the size of the separation bubble was increased by up to 60% and the RQ-4A was used. The MQ-9 penalized the flights by reduced lost altitude with respect to the baseline only when separation increased by 60%.
- There were no differences observed for these metrics between the RQ-4A/ MQ-9 cases.
- Switching 10, 20 and 30% of the flights to RPAS and having one which encounters a C2 link loss (around which separation is doubled) reduced lost altitude by 0.6%, 1.2% and 1.6% with respect to the baseline. A linear relationship was found between the altitude dropped by the non-RPAS flights and the percentage of flights switched to RPAS. The gained altitude was not influenced by increasing the percentage of RPAS flights.
- In an environment with 20% RPAS flights, increasing the size of the separation bubble around the one RPAS with C2 link failure by 100 and 200% decreased this KPI by 1.1% and 1.7% compared to the baseline. A separation of 60% increase resulted in the same value of the lost altitude metric as in the 100% increase case. The gained altitude was not influenced by varying the separation around the RPAS.

11

Analyzing Simulation Results using MANOVA tests

In Section 10 the 14 scenarios were split in 5 cases and the results were analyzed using ANOVA tests, which looked at the difference between groups by considering one dependent variable. For instance, Case 3 revealed that by switching more than 10% of the flights with an MQ-9 Reaper, potential conflicts increased by 18%, average controller task load went up with 0.4% and the sector became 5.5% more agglomerated. The ANOVA test could not capture any potential relationship between conflicts and ATCo task load or sector occupancy. For this, the Multivariate Analysis of Variance (MANOVA) test is introduced in Section 11.1. The results obtained by applying MANOVA to 6 different cases using IBM SPSS are given in Section 11.2.

11.1. Theory on Multivariate Analysis of Variance (MANOVA)

MANOVA (multivariate analysis of variance) is useful to detect group differences when there are multiple dependent variables. While ANOVA only looks at differences between groups when there is one dependent variable, MANOVA considers the interactions between several dependent variables simultaneously, which makes it a multivariate test. The main advantage of using this technique, as opposed to performing multiple ANOVA tests on the data, is that the familywise error rate will be kept under control (the more dependent variables that were measured, the more ANOVA test are required and thus, the greater the chance of making a Type I error). [72][78]

MANOVA tests the hypothesis that one or more independent variables have an effect on a set of two or more dependent variables. The mathematical formulation of the null hypothesis is given in Equation 11.1, which looks at whether the vectors of the means on n decision variables are equal between k groups.

$$H_0: \begin{bmatrix} (\mu_{DV_1})_{G_1} \\ (\mu_{DV_2})_{G_1} \\ \vdots \\ (\mu_{DV_n})_{G_1} \end{bmatrix} = \begin{bmatrix} (\mu_{DV_1})_{G_2} \\ (\mu_{DV_2})_{G_2} \\ \vdots \\ (\mu_{DV_n})_{G_2} \end{bmatrix} = \quad \cdots \quad = \begin{bmatrix} (\mu_{DV_1})_{G_k} \\ (\mu_{DV_2})_{G_k} \\ \vdots \\ (\mu_{DV_n})_{G_k} \end{bmatrix} \tag{11.1}$$

H_1: at least one of the vectors of means is different

Before performing a MANOVA test on a set of data, it must be checked whether the data fulfills the four assumptions of MANOVA [72][78]:

- Observations should be statistically independent;
- Data should be randomly sampled from the population that was considered;
- Data should be normally distributed (collectively and within the groups);

- Homogeneity of covariance matrices (variances in each group and the correlations between any two dependent variables are equal).

The first two assumptions are met from the way the experiment was set up. For each run the flight that was switched to an RPAS is randomly selected from the available flights and the sector entry times are uniformly randomly varied between +/- 1 minute around the original sector entry time of the flight. According to the central limit theorem, the distribution of the sample mean is approximately normally distributed as the sample size n is large. Montgomery et al. in [55] state that n should be at least 30 for the normal approximation to be satisfactory. Furthermore, non-normality does not affect the statistical validity of the analysis when group sizes are equal and since the number of runs performed for all scenarios is equal, the third assumption can be ignored in this case. [72] [79] Checking for equality of covariance matrices is done with Levene's test. [72] This test should not be significant for any of the dependent variables. Breaking this assumption means that covariance matrices are heterogeneous which can lead to p-values that are either too small or too large. [79]

The results of a MANOVA test will be reported according to the APA format as follows: $F(df_M, df_R)$ = F-ratio, p = p-value. The degrees of freedom between groups are represented by df_M and those for the residuals of the model by df_R. [72]

The three sum of squares SS_T, SS_M and SS_R are calculated using Equations 10.2 - 10.4 exactly as was done for the ANOVA test. Since MANOVA deals with determining how the relationships between the dependent variables influence the results between groups, three different cross-products are calculated: CP_T, CP_M and CP_R.

The formula to calculate the total cross-product CP_T when two dependent variables DV_1 and DV_2 are considered is given in Equation 11.2, in which for each dependent variable the score is subtracted from the grand mean of that variable and these differences are multiplied with each other. [72]

$$(CP_T)_{DV_1,DV_2} = \sum_{i}^{N} (x_{i,DV_1} - \overline{X}_{grand,DV_1}) \cdot (x_{i,DV_2} - \overline{X}_{grand,DV_2}) \tag{11.2}$$

The model cross-product, CP_M is used to determine how the dependent variables are influenced by the experiment manipulation (increase in separation/ change of RPAS type/ etc.). First the differences between each group mean and the grand mean is calculated. These differences are multiplied by the number of observations in a group and finally, the results are summed up for all the groups. This is shown in Equation 11.3 for dependent variables DV_1 and DV_2. [72]

$$(CP_M)_{DV_1,DV_2} = \sum_{groups} n \cdot [(\overline{x}_{group,DV_1} - \overline{X}_{grand,DV_1}) \cdot (\overline{x}_{group,DV_2} - \overline{X}_{grand,DV_2})] \tag{11.3}$$

The error in the model, or the relationship between dependent variables and individual differences can be assessed through CP_R. The residual cross-product is calculated in a similar way to the total cross-product, except that the group means are used for comparing individual results. The formula for CP_R is given in Equation 11.4 for two decision variables DV_1 and DV_2. [72]

$$(CP_R)_{DV_1,DV_2} = \sum_{groups} (x_{i,DV_1} - \overline{X}_{group,DV_1}) \cdot (x_{i,DV_2} - \overline{X}_{group,DV_2}) = (CP_T)_{DV_1,DV_2} - (CP_M)_{DV_1,DV_2} \tag{11.4}$$

Once the sum of squares for each dependent variable and the cross-products between any two dependent variables have been computed, three sum of squares and cross-product (SSCP) matrices are constructed: T (total SSCP matrix), E (residual SSCP matrix) and H (model SSCP matrix). The general formula for the total SSCP matrix (for n decision variables) is given in Equation 11.5. This matrix is a representation of both the variation that exists within the data and the co-dependence that exists between dependent variables. [72]

$$T = \begin{pmatrix} (SS_T)_{DV_1} & (CP_T)_{DV_1,DV_2} & \cdots & (CP_T)_{DV_1,DV_n} \\ (CP_T)_{DV_2,DV_1} & (SS_T)_{DV_2} & \cdots & (CP_T)_{DV_2,DV_n} \\ \vdots & \vdots & \ddots & \vdots \\ (CP_T)_{DV_n,DV_1} & (CP_T)_{DV_n,DV_2} & \cdots & (SS_T)_{DV_n} \end{pmatrix} \tag{11.5}$$

The residual sum of squares and cross-products matrix E is obtained for n decision variables as shown in Equation 11.6. This matrix is a measure of unsystematic variation for each dependent variable and the co-dependence that exists between dependent variables due to random factors. [72]

$$E = \begin{pmatrix} (SS_R)_{DV_1} & (CP_R)_{DV_1,DV_2} & \cdots & (CP_R)_{DV_1,DV_n} \\ (CP_R)_{DV_2,DV_1} & (SS_R)_{DV_2} & \cdots & (CP_R)_{DV_2,DV_n} \\ \vdots & \vdots & \ddots & \vdots \\ (CP_R)_{DV_n,DV_1} & (CP_R)_{DV_n,DV_2} & \cdots & (SS_R)_{DV_n} \end{pmatrix} \tag{11.6}$$

Matrix H, the model sum of squares and cross-products matrix, represents systematic variation between dependent variables and co-dependence between dependent variables due to experimental conditions. [72] Equation 11.7 shows how this matrix is obtained when an experiment involved n decision variables.

$$H = \begin{pmatrix} (SS_M)_{DV_1} & (CP_M)_{DV_1,DV_2} & \cdots & (CP_M)_{DV_1,DV_n} \\ (CP_M)_{DV_2,DV_1} & (SS_M)_{DV_2} & \cdots & (CP_M)_{DV_2,DV_n} \\ \vdots & \vdots & \ddots & \vdots \\ (CP_M)_{DV_n,DV_1} & (CP_M)_{DV_n,DV_2} & \cdots & (SS_M)_{DV_n} \end{pmatrix} \tag{11.7}$$

Whereas in univariate tests (such as ANOVA) the ratio of systematic to unsystematic variance is calculated as shown in Equation 10.7, for multivariate test like MANOVA, there is a matrix equivalent of this ratio: HE^{-1}. However, as opposed to univariate tests there will no longer be only one value for this ratio, but n^2, where n represents the number of decision variables that were considered. In order to determine which value should be used to assess statistical significance, discriminant function variates will be used. The procedure is outlined in [72] and the main steps are summarized below.

The discriminant function variates convert the dependent variables into underlying factors (dimensions), each variate being a linear combination of the dependent variables. Equation 11.8 shows the general equation of a variate V_i for n dependent variables. [72]

$$V_i = b_{1_i} \cdot DV_1 + b_{2_i} \cdot DV_2 + \cdots + b_{n_i} \cdot DV_n \tag{11.8}$$

The number of variates is calculated by taking the minimum between the number of dependent variables (n) and k-1, where k is the number of groups that are considered (Equation 11.9). For instance if five scenarios are considered and the effect of 3 metrics is investigated, the number of variates would be min(3;5-1) = 3.

$$\text{number of variates} = min(n; k-1) \tag{11.9}$$

By calculating the eigenvectors of the matrix HE^{-1}, the values of the *b*-coefficients from Equation 11.8 are obtained. [72] Then, after computing the variate score for each of the measurements (by plugging in the experimental results into the variate equations 11.8) and calculating the SSCP H, E, T and HE^{-1} matrices by following the same procedure as previously explained, the following is obtained (Equation 11.10):

$$(HE^{-1})_{variates} = \begin{pmatrix} \lambda_1 & 0 & \cdots & 0 \\ 0 & \lambda_2 & \cdots & 0 \\ \vdots & \vdots & \ddots & \vdots \\ 0 & 0 & \cdots & \lambda_n \end{pmatrix} \tag{11.10}$$

The values obtained on the diagonal represent the eigenvalues of the original HE^{-1} matrix and the other values are zero because the variates that were extracted from the data are orthogonal (uncorrelated). [72] Thus, instead of having n^2 values to assess significance, the method of discriminant functions reduced the number to *n*. When sample sizes are equal (which is true for this experiment because the number of measurements that were performed for each scenario is the same), Pillai-Bartlett's trace is the most robust test to be performed ([72] [79]). The ratio used by this test is shown in Equation 11.11, where s represents the total number of variates, and is the equivalent of the SS_M/SS_R ratio (the F_{ratio}) used in univariate tests (Equation 10.7):

$$V = \sum_{i=1}^{s} \frac{\lambda_i}{1+\lambda_i} \tag{11.11}$$

11.2. MANOVA Results

Whereas an ANOVA test could still be performed if the assumption of homogeneity of variance is broken (by using Welch's ANOVA which was explained in Section 10.1), as discussed in the previous section the equality of covariance matrices is imperative for a MANOVA test. Table J.1 in Appendix J shows the results of Levene's test for 18 cases that were considered for the MANOVA analysis. As can be seen in this table, there is no situation in which Levene's test was non-significant for all KPIs. However, there are 6 situations in which there were more than two KPIs for which the MANOVA test can be applied.

The results of the MANOVA test can be seen in Table 11.1. The 6 situations and KPIs that were considered are given in columns two and three, and the fourth one shows the outcome of the MANOVA test. V represents Pillai's Trace which is calculated by Equation 11.11 and the p-value is used to determine whether the H_0 hypothesis of the test (equal vectors of means for all KPIs) is rejected.

Table 11.1: MANOVA Results

Case	Scenarios	KPIs	MANOVA Result	H_0 Rejected?
1	1_1 - 1_4	2 - 9	V= 0.01, F(24, 12639) = 0.97, p = 0.51	No
2	1_5 - 1_8	1, 2, 3, 6	V= 0.01, F(12, 12705) = 3.99, p = 0	Yes
3	1_1, 1_5	4 - 9	V= 0, F(6, 2113) = 0.95, p = 0.46	No
4	1_2, 1_6	1, 2, 4 - 9	V= 0.02, F(8, 2111) = 6.54, p = 0	Yes
5	1_3, 1_7	4, 5, 6, 9	V= 0.01, F(4, 2115) = 2.67, p = 0.03	Yes
6	1_4, 1_8	4 - 7	V= 0, F(4, 2115) = 1.87, p = 0.11	No

As can be seen in Table 11.1 the null hypothesis of the MANOVA test was rejected for 3 cases. Cases 3 and 6 looked at whether the performance of the RPAS (MQ-9/ RQ-4A) for separation values of 0% and 60% increase influenced KPIs 4 - 7 (case 6) and 4 - 9 (case 3). The non-significant MANOVA means that the vectors of means were equal between scenarios 1_1 and 1_5 and 1_4 and 1_8 and that having an RPAS with a slower performance did not influence the considered metrics. This validates the results presented in Section 10.6 which reached the same conclusion. Case 1 also rejected the MANOVA null hypothesis meaning that when separation was increased between 0 - 60% around a Global Hawk, KPIs 2 - 9 are not influenced. Section 10.3 reached the same result by performing multiple ANOVA tests, for which only the impact on KPI_1 (number of potential conflicts was found to be significant).

For the three cases in which the MANOVA test was found to be significant, the relationship between the dependent variables will be studies by analyzing the covariance matrix, which is a direct output of IBM SPSS. These matrices are useful in determining how the relationships between dependent variables change from one group to another. [72]

The covariance matrix for Case 2, which can be seen in Table 11.2, shows how the relationships between the four metrics change from one scenario to another. For instance, as the number of potential conflicts increases (KPI_1), both the controller task load (KPI_2) and the sector occupancy (KPI_3) increase. In the first scenario considered, the covariance between conflicts and task load is 1.97 and that with occupancy 0.04. Increasing separation does not affect the relationship between conflicts and occupancy (the covariance is between 0.04 – 0.05 for all four scenarios), or that between conflicts and task load (1.95 – 2.15). The positive relation was to be expected since an increase in the number of conflicts means that the ATCo would have to instruct one or more of the flight to perform resolution actions in order to prevent an actual conflict from occurring. The increase in occupancy can be explained by the fact that the resolution action penalizes at least one of the flights to deviate from its original flight plan, forcing it to spend more time or interact with more flights in the sector. Furthermore, occupancy and task load are also positively related for all scenarios, meaning that more flights being present in the sector at the same time, increase controller task load. Since in the procedure to measure controller task load the number of aircraft that a controller handles influences the monitoring-based task load, a positive covariance was expected.

In Table 11.2 the number of conflicts and the fuel burnt are negatively related in the first two scenarios, but

Table 11.2: Covariance Matrix (Case 2)

		KPI_1	KPI_2	KPI_3	KPI_6
Scn. 1_5 (1 MQ-9, 0% Sep. Incr.)	**KPI_1**	3.58	1.97	0.04	-0.24
	KPI_2	1.97	2.26	0.04	-0.12
	KPI_3	0.04	0.04	0.01	-0.03
	KPI_6	-0.24	-0.12	-0.03	7.65
Scn. 1_6 (1 MQ-9, 20% Sep. Incr.)	**KPI_1**	3.89	1.95	0.04	-0.07
	KPI_2	1.95	2.22	0.03	0.15
	KPI_3	0.04	0.03	0.01	-0.03
	KPI_6	-0.07	0.15	-0.03	8.22
Scn. 1_7 (1 MQ-9, 40% Sep. Incr.)	**KPI_1**	4.29	2.15	0.05	0.07
	KPI_2	2.15	2.38	0.04	0.13
	KPI_3	0.05	0.04	0.01	-0.01
	KPI_6	0.07	0.13	-0.01	8.36
Scn. 1_8 (1 MQ-9, 60% Sep. Incr.)	**KPI_1**	4.14	1.98	0.04	0.79
	KPI_2	1.98	2.13	0.03	0.36
	KPI_3	0.04	0.03	0.01	-0.01
	KPI_6	0.79	0.36	-0.01	9.12

positively related in the last two cases. This means that for separation values of 0% and 20% increase a greater number of potential conflicts reduces the fuel burnt by the flights, while for the 40% and 60% separation increase cases, more conflicts results in more fuel being burnt. This difference is likely to be due to different resolution strategies used to solve the conflicts.

The covariance matrices of scenarios 1_2 and 1_6 for KPIs 1, 2, 4 - 9 (Case 4) can be found in Table J.2 in Appendix J. As the lost altitude decreases (flights descent less), fuel consumption increases. The relationship is stronger in the case of the MQ-9, for which the covariance coefficient between fuel and lost altitude is larger than in the RQ-4A case (-20.5 vs. -0.4). This also has an impact on controller task load: the covariance coefficient between lost altitude and ATCo task load is negative, meaning that controller task load increases as they have to instruct flights on approach to stop their descent manoeuver. A lower RPAS performance further increased task load, as this covariace coefficient was lower for the MQ-9 (-21.3) as opposed to the RQ-4A (-10.6). Furthermore, instructing the flights to stop their descent manoeuvers was also responsible for the increase in number of potential conflicts as the covariance coefficient is negative.

The covariance matrices of scenarios 1_3 and 1_7 for KPIs 4, 5, 6 and 9 (Case 5) can be found in Table J.3 in Appendix J. As the flights are spending more time in the sector, the distance travelled increases (the covariance between distance and time is positive). Similarly, spending a longer time in the sector or travelling longer distances increases fuel consumption. Decreasing altitude deviation (stopping the climb and descent of the flights) results in additional fuel being burnt. The role played by the performance of the RPAS can be seen through the difference in magnitude of the covariance coefficient between fuel and altitude deviation of the two performance models: -5.9 (RQ4-A) vs. -44.7 (MQ-9). This means that the MQ-9 increases the fuel consumption of the manned flights more when climb/descend manoeuvers are stopped compared to the case when the Global Hawk is used (this is in accordance with the ANOVA results for KPI_6 for scenarios 1_3 vs. 1_7 in Section 10.6).

11.3. Conclusion

As opposed to the ANOVA test which is a univariate test, MANOVA can detect group differences when there are multiple dependent variables and establish whether the relationships between them change from one scenario to another.

The scenarios were grouped in 18 possible cases for the MANOVA test. However, only 6 met all four requirements of MANOVA, the most restrictive one being the assumption of homogeneity of covariance matrices. Out of the 6 cases, the MANOVA test was significant for only 3 which were analyzed in this chapter.

The MANOVA tests conducted revealed that KPIs 1, 2 and 3 are positively correlated: as the number of potential conflicts increases, both sector occupancy and air traffic controller task load increase. Also, an increase in sector occupancy results in an increase in ATCo task load. A positive correlation was also found between flight time, distance and fuel consumption.

On the other hand, lost altitude and fuel consumption are negatively correlated. As flights stop their descent manoeuvers, more fuel is being used. There is a negative correlation also between lost altitude and controller task load, the more the flights stop their descent, the more ATCo task load increases.

For the same separation, having an RPAS with a lower performance (MQ-9 Reaper) resulted in stronger correlations than an RPAS with a higher performance, such as the RQ-4A Global Hawk (lost altitude - fuel and lost altitude - ATCo task load).

However, the MANOVA approach does not provide a mathematical relationships between the dependent variables, but only a correlation between them.

PART V

CONCLUSIONS AND RECOMMENDATIONS

12

Conclusions and Recommendations

The conclusions that can be drawn from this project are given in Section 12.1. Recommendations on further work are addressed in Section 12.2.

12.1. Conclusions

The SESAR Joint Undertaking (SJU) estimates that by 2050 20% of the traffic will be remotely piloted, their popularity flourishing in sectors such as: precision agriculture, emergency delivery of medical aid, preventive maintenance, public safety and traffic monitoring. Handling RPAS operations on a case-by-case basis in segregated airspace as currently done will no longer be an option, making RPAS integration in non-segregated airspace a requirement of the future ATM system. In doing so, the current levels of safety and efficiency should not be compromised and remotely piloted aircraft should emulate themselves to the current operational requirements and procedures.

RPAS encompass three elements: the remotely piloted aircraft (RPA), the remote pilot station (RPS) and the command and control link (C2). The C2 link is defined as the data link responsible for managing the flight, connecting the remotely piloted aircraft and the remote pilot station. From a technical standpoint, the C2 link is used for exchanging information and safely integrating the RPAS into the global aviation, communication, navigation and surveillance operational environment. For assessing C2 link performance, the Required (C2) Link Performance concept (RLP) was proposed by JARUS which sets requirements on the performance required for communication capabilities without reference to any specific technology. The purpose of this project was to study how different values of the failure rate of the C2 link affect the capacity of the airspace by analyzing the number of separation losses (blind encounters) once an RPAS experiences a failure of the C2 link.

The flights in the Dutch airspace during a 24 hour period (2^{nd} of March, AIRAC 1703) were considered for this project. 4,049 fast time simulations were performed in AirTOp in which 10 - 50% of the flights were switched to RPAS and the failure rates were varied between 0.01 - 0.001. The performance of the remotely piloted aircraft was assumed to be the same with that of the aircraft that it replaced. Once a failure occurred the separation was doubled around the RPAS and the remotely piloted aircraft continued to fly to its destination along the initially submitted flight plan. The number of additional blind encounters that were generated was between 1.8 - 23.6, representing an increase of 0.09 - 1.18% compared to the baseline situation.

The methodology established in the project can be applied to other airspaces and even extended to the entire European Airspace such that lower values of the mean time between failures of the C2 link can be investigated. This would be necessary in order to establish a requirement on the failure rate of the C2 link which is an essential requirement for the safe integration of RPAS in non-segregated airspace.

The second part of the project zoomed in on a sector level to analyze what the effects of an RPAS with a failed C2 link are on key ATM performance indicators. This analysis considered the German airspace, which is is

Europe's busiest in terms of IFR movements and focused on Langen FIR, the busiest flight information region in the country. Sector EDGGPHHM was selected as it combined both cruising, climbing and descending flights, bringing together routes from four different German airports. The flights during the busiest 1-hour period were considered (6-7 a.m. on March 2^{nd}, AIRAC 1703) and 14,840 fast time simulations were performed (divided in 13 scenarios plus baseline) in which the sector entry times of the flights were uniformly randomly varied (+/- 60 seconds around actual sector entry time) and the flight that was switched to RPAS was randomly selected from the 53 flights. Two RPAS performance models were used: RQ-4A Global Hawk (which has a performance closer to that of commercial aircraft) and MQ-9 Reaper (with a lower overall performance). Once the RPAS with C2 link failure entered the sector, a separation bubble was created around it which was varied in size between 0 - 200% increase compared to the minimum separation standards of 5 NM / 1,000 ft imposed by ICAO. The analysis also considered replacing 10 -30% of the flights to RPAS, but only one experienced a failure of the C2 link.

The following Key Performance Indicators (KPIs) were considered: number of potential conflicts, air traffic controller task load, sector occupancy, distance flown, flight time, fuel consumption and altitude deviation. The results were analyzed by performing ANOVA (analysis of variance) tests on the mean values of the KPIs to determine whether the differences measured were significant or not from a statistical point of view. Having a separation bubble which is up to 60% larger than the one currently used around manned aircraft only influences the number of potential conflicts. There were 8.3%, 9.2% and 12.0% more potential conflicts than in the baseline when an MQ-9 RPAS was used and separation was increased by respectively 20%, 40% and 60%. The performance of the remotely piloted aircraft was found to be significant in how some of the KPIs are affected. Having an MQ-9 (which has a lower performance) as opposed to the RQ-4A increased the number of potential conflicts by 6.8 - 9.7%, controller task load by 0.7 - 0.8% and sector occupancy by 0.4 - 0.5% when the same separation standard was used. Flight times went up by 0.12% and fuel consumption by 0.2% when an MQ-9 Reaper was used compared to the RQ-4A for separation increases of 40 and 60%.

Switching 10, 20 and 30% of the flights to RPAS and having one which encounters a C2 link loss (around which separation is doubled) revealed that there is a linear relationship between the percentage of flights switched to RPAS and the following KPIs: number of potential conflicts, controller task load, sector occupancy, flight time and dropped altitude. While all these KPIs increase with increasing number of RPAS flights, the altitude dropped metric decreases meaning that non-RPAS flights had to stop their descent manoeuvers in order to avoid an actual conflict, penalizing their overall flight efficiency.

In an environment with 20% RPAS flights, the effect of varying the size of the separation bubble around the one RPAS with C2 link failure (increasing it by 60, 100 and 200%) was tested. All metrics were significantly affected by the multiple RPAS flights ($p < 0.05$ for all ANOVA tests). A linear relationship was found between the number of potential conflicts and the percentage increase in separation around the RPAS with C2 link failure (with respect to the minimum ICAO values of 5 NM / 1,000 ft). Distance travelled and gained altitude were not affected by increasing the separation around the RPAS with C2 link failure. Also, there was no difference found between the 60 and 100% increase case for ATCo task load, sector occupancy, fuel consumption and lost altitude. However, flight time increased by 0.2% when separation was increased from 60 to 100%. Therefore, the separation standards which will be enforced around remotely piloted aircraft will play an important role on how the efficiency of the ATM Network is affected. The methodology established in this project for analyzing the impact of different separation standards when dealing with a C2 link loss will help at integrating RPAS in non-segregated airspace and can be extended to other ATC sectors.

A multivariate analysis of variance (MANOVA) was applied on 6 cases in order to determine how the relationships between the KPIs changed from one scenario to another. It was determined that there is a positive correlation between the number of potential conflicts, sector occupancy and air traffic controller task load and between flight time, distance and fuel consumption. On the other hand, lost altitude and fuel consumption are negatively correlated because as the flights stop their descent manoeuvers to avoid conflicts with the RPAS with C2 link failure, more fuel is being used. There is also a negative correlation between lost altitude and controller task load, the more the flights stop their descent, the more ATCo task load increases. For the same separation, having an RPAS with a lower performance (MQ-9 Reaper) resulted in stronger correlations than for an RPAS with a higher performance.

12.2. Recommendations

The sector approach considered in this project should not be generalized as ATM is not a linear problem. Experiencing a delay in one sector will propagate in the sectors around and affects the efficiency of the network as a whole. This dimension cannot be captured when only one sector is simulated. Therefore, before commencing with real flight trials, network wide simulations of RPAS operations and C2 link losses should be performed. Currently the ability to perform such large scale simulations is limited by either the very large computational time or the unavailability of simulation platforms with a network-wide conflict detection and resolution module. Existing conflict detection and resolution modules in fast time simulators should be validated when the simulation area contains a larger number of sector. Furthermore, the EUROCONTROL NEST modelling tool should be updated such that different separation standards can be tested around specific aircraft or areas. This will be beneficial not only for RPAS studies but also in studies on the redefinition of current separation standards for manned aircraft. Also, the AirTOp conflict resolution and task load models for a given airspace should be fine-tuned by consulting real air traffic controllers.

This project analyzed the effect of imposing different separation values around the RPAS that experiences a loss of the C2 link. The idea behind it was that by increasing the separation around the RPAS, the other traffic would be kept further away from the remotely piloted aircraft until the link is recovered. This would also serve as a buffer for air traffic controllers to solve any potential conflicts if the RPAS starts to deviate from its course. As the size of this bubble has an impact on the metrics (the methodology to determine these effects was the purpose of this project), further studies should be carried out in order to determine how small this bubble can be without it affecting the safety of surrounding traffic.

For the scenarios that considered multiple RPAS flights out of which only one experienced a failure of the C2 link and the other flights were active participants in conflict detection and resolution, the assumption of no C2 link communication delay was present. Future work should also focus on the delay encountered by the C2 link and establish how the magnitude of the delay influences the same KPIs. In conjunction with this study, this would help in setting performance requirements on the C2 link, not only with respect to its failure rate, but also with respect to to the communication transaction time. Current simulation tools should be enhanced such that they are able to simulate delays in communication for specific flights only and additional controller task load tasks that might be necessary once RPAS operations are in place.

This project analyzed en-route traffic, between FL115 and FL245 which covers for instance the portion of an RPAS trip from its departure airport to the location of its mission or reverse. It did not focus on flights below 500 ft, which depending on the mission type, could be a big part of the flight time of the RPAS (for example in precision agriculture or preventive maintenance). Future studies could also focus on the impact of loosing a C2 link on final approach or immediately after take-off when the RPAS would return to base.

This study revealed that the performance of the RPAS used influences the considered key performance indicators. Future work should focus on setting limits on the performance of an RPAS that is allowed to operate in non-segregated airspace in order to ensure the same levels of safety and efficiency. For this, further RPAS BADA models would be required. This is a complicated process as limited performance data on remotely piloted aircraft is currently available and there is no proper data base with the most common RPAS types in Europe. [80]

Future studies could also consider an increase in current traffic in addition to certain percentage of flights being operated by an RPAS. This should be in line with SJU's forecast on RPAS operations and should include RPAS flights plans which are closer to those envisioned for future operations and not simple flights from A to B. This is required to understand how flights holding for longer times above a certain area or performing specific mission have an impact on non-RPAS traffic.

PART VI

APPENDICES

A

Creating the simulation environment in AirTOp for Experiment 1

The experimental set-up for Experiment 1 is shown in Figure A.1. The lower side of Figure A.1 shows that there will be two iteration loops when performing the experiments: one in which the selection of aircraft that will be converted to an RPAS type is randomized (Iteration Loop 1) and another in which the percentage of flights that are switched to an RPAS type is gradually increased (Iteration Loop 2).

A.1. Importing traffic files to AirTOp

This section describes how the simulation environment was created in AirTOp. By default, the fast-time simulator comes with the world map, but does not contain any further information on ATC sectors, waypoints, routes, airports, etc. It is basically a blank world, that can be customized based on the wishes of the user.

The first step is to import the BADA directory. This is required in order to avoid any errors from appearing later on, when flights are imported and their aircraft type is missing from the default ones that come with the simulator. The procedure to import the BADA files is the following: File > Import > Import BADA Directory. Click *Next* and select the location where the BADA files are stored on the computer. Then, Click *Next*, select which aircraft type should be imported and again the *Next* button. In the next window the user can select to leave out certain aircraft properties (by default all the BADA properties will be imported) and then the *Finish* button must be pressed. The BADA directory will now be imported. Following this, the aircraft type profiles have to be updated from: Tools > Aircraft > Profiles > Calculate/update Aircraft Type Profile. This final step makes sure that when the flights will be imported, the newly imported BADA models will be used.

After updating the aircraft database, the simulation environment can now be created. The GASEL and ALL_FT+ files which are downloaded from EUROCONTROL's Demand Data Repository contain flight and environment information for the entire world. Since this analysis only focuses on one country, a method was searched in order to only import the elements that would be necessary for the simulation. This was preferred because it would keep to a minimum the volume of data required by the simulator, which in turn would minimize the run-time of each simulation. Because pre-filtering was not possible from DDR itself before downloading the actual files, it was decided to use the option *Area of Interest* from AirTOp before importing the environment and traffic files. With this option, the user can specify a geographic area and the simulator will only import the environment elements or flights that are enclosed withing the mentioned boundaries. As the coordinates of the countries are not known to AirTOp, the user has to specify them as well.

Once the area of interest has been defined, the GASEL environment can be imported from File > Import > Import GASEL Directory. Then, the ALL_FT+ traffic file can be added from File > Import > Import File. It is important to specify the area of interest previously defined when importing both files. Once the flights have been added, the departure times for each flight plan need to be calculated. This can be done from Tools >

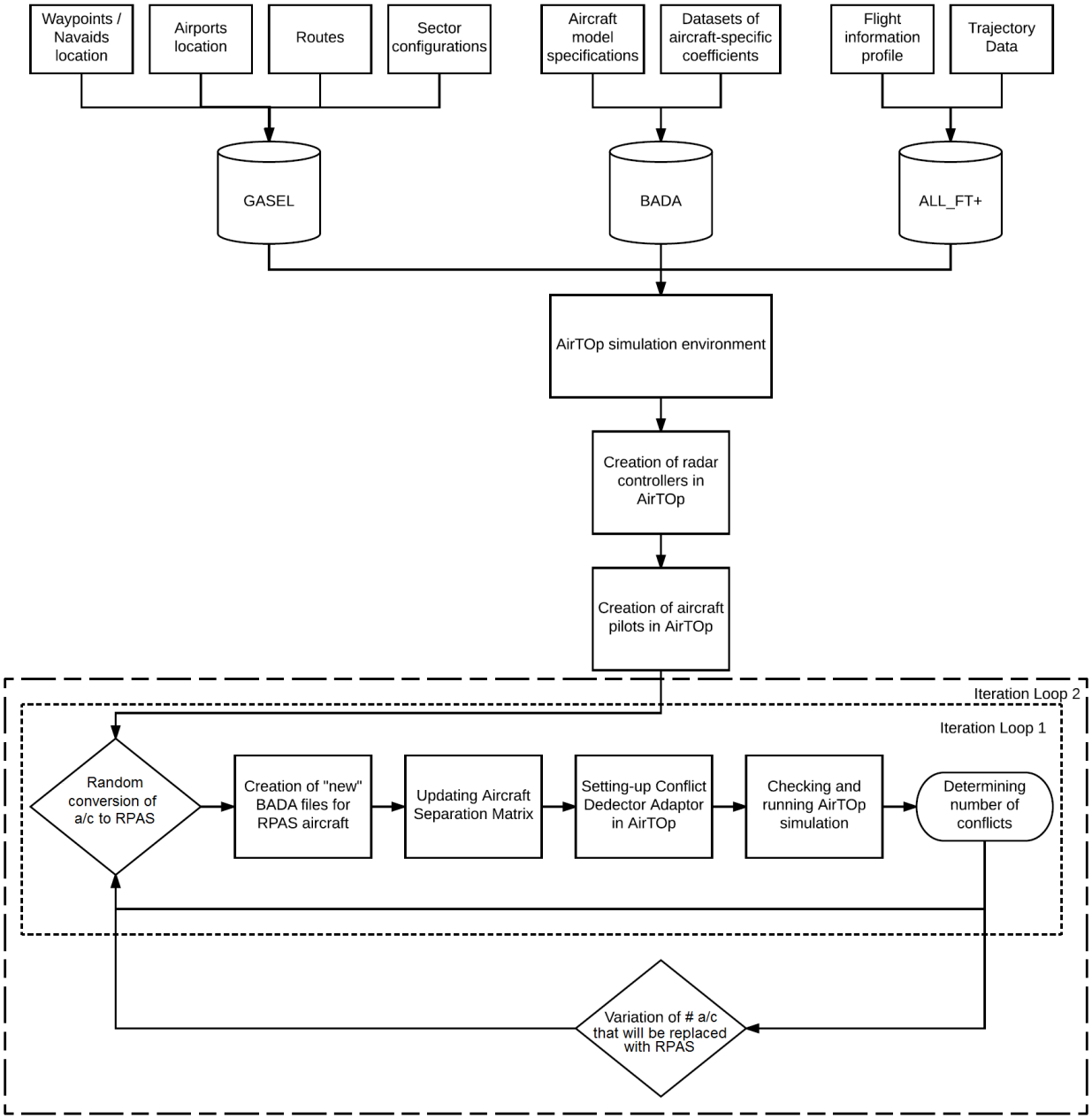

Figure A.1: Experimental Set-up

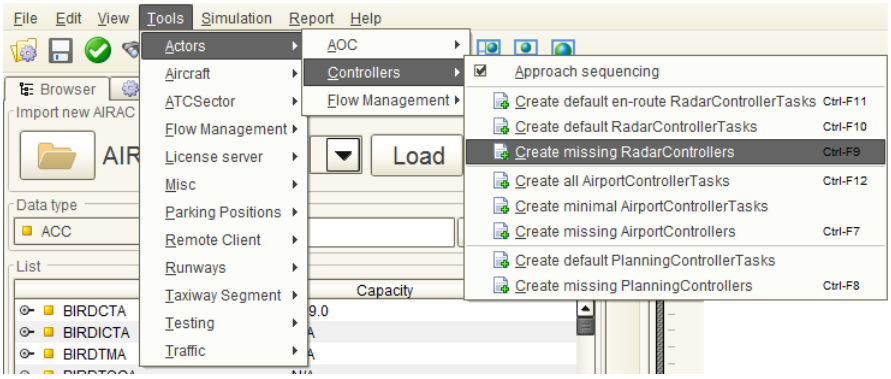

Figure A.2: Creating Pseudo-Radar Controllers in AirTOp

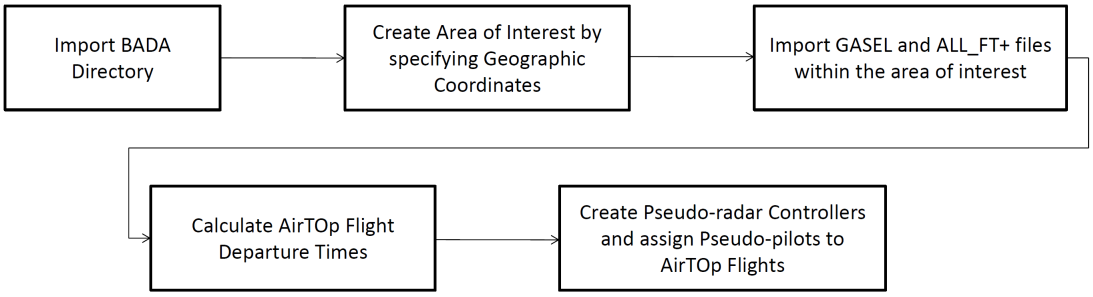

Figure A.3: Steps to be followed when creating the AirTOp Simulation Environment

Traffic > Calculate Flight Plan Estimated Times. Then the V3 estimation method has to be selected, which corresponds to the most recent version of AirTOp. This way the simulator takes the information from the ALL_FT+ file and determines for each flight at what time it should appear in the simulation.

In order to properly run an AirTOp simulation, pseudo-radar controllers and aircraft pilots need to be created. These represent the next two steps in the experimental set-up given in Figure A.1 and will enable the user to impose specific separation requirements between aircraft. In order to assign pseudo-radar controllers for each ATC sector in the AirTOp simulator, the user should go to: Tools > Actors > Controllers and select *Create Missing Radar Controllers*. This is also shown in Figure A.2. Pseudo-pilots are created in a similar manner from: Tools > Actors > Pilots > Create Default Aircraft Pilot Tasks.

The steps that were followed to create the simulation environment and import the flights that will be part of the analysis are summarized in Figure A.3. The next section will explain the process of creating an "RPAS" aircraft type in AirTOp.

A.2. Creating new *RPAS* aircraft types in AirTOp

Each AirTOp project generates two outputs: a file with the extension .prj and a project folder with the same name as the .prj file. This file contains information on the AirTOp version that was used and all the user settings that were applied during the creation of the project, such as windows and map views and table outlines. The folder that is generated has all the information required for the simulator to run. This data is grouped in 21 sub-folders, as can be seen in Figure A.4 which shows the outline of an AirTOp project. The files that deal with aircraft types are located in the *aircraft* folder. Four .csv files that will be explained in this section are shown in Figure A.4. The number of conflicts will be saved in a Conflict.csv file in the *report* folder.

The creation of RPAS aircraft types will be done by editing four files in the *aircraft* folder of the main project: Aircraft.csv, AircraftType.csv, AircraftSizeType.csv and AircraftTypeProfile.csv. The first step is to change the aircraft type for the chosen flight in the Aircraft.csv file. This file contains an entry for each flight. Each line

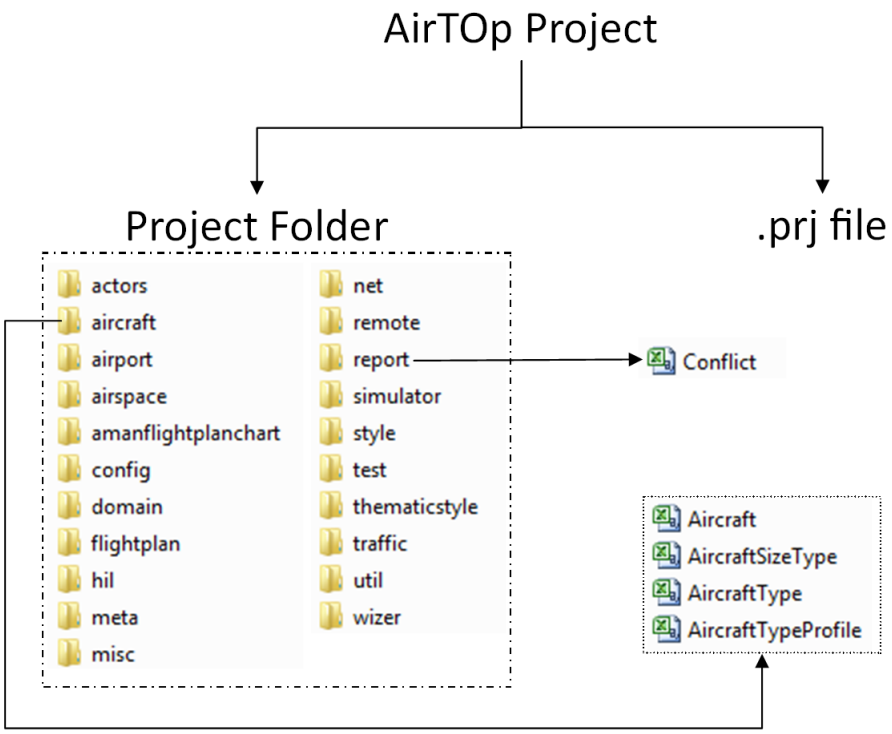

Figure A.4: Input / Output Files for an AirTOp Project

```
#Header:aircraft-version1.0
#Registration AircraftTypeAsString Na
 TrajectoryPredictor Airline Comment
IsRequestedCTAComplyingWithETAMinMax
#LineCount=2969
RYR12UM;B738;;;;RYR;;;;false;
SWR736;A320;;;;SWR;;;;false;
KAL908;B77W;;;;KAL;;;;false;
BAW237;A321;;;;BAW;;;;false;
BAW444;A320;;;;BAW;;;;false;
BCS6724;A306;;;;BCS;;;;false;
WZZ8FV;A320;;;;WZZ;;;;false;
```

(a) British Airways Flight 237 operated by A321

```
#Header:aircraft-version1.0
#Registration AircraftTypeAsString N
 TrajectoryPredictor Airline Comment
IsRequestedCTAComplyingWithETAMinMax
#LineCount=2969
RYR12UM;B738;;;;RYR;;;;false;
SWR736;A320;;;;SWR;;;;false;
KAL908;B77W;;;;KAL;;;;false;
BAW237;A321-RPAS;;;;BAW;;;;false;
BAW444;A320;;;;BAW;;;;false;
BCS6724;A306;;;;BCS;;;;false;
WZZ8FV;A320;;;;WZZ;;;;false;
```

(b) British Airways Flight 237 operated by A321-RPAS

Figure A.5: Extract from an Aircraft.csv file

consists of the flight number, the aircraft type and other parameters such as registration, navigation equipment, communication equipment, airline, etc. The field of interest in this case is the second one, which deals with the aircraft type. Figure A.5a shows a portion of the Aircraft.csv file that contains all the 2,969 flights that are part of the simulations. If one would like to make flight BAW237 (which corresponds to the 4^{th} entry in this list) an unmanned one, the text *"-RPAS"* shall be appended to the aircraft type code in the second column of the flight. The resulting file is shown in Figure A.5b, where the differences are highlighted with blue rectangles.

The second step is to define the new remotely piloted aircraft type in the AircraftType.csv file. This file contains one line for each aircraft type and each line 71 entries. These entries cover aircraft properties such as: aircraft type name, wake turbulence category, climb and descent performance parameters, number of engines, fuel consumption, CO_2 emissions, etc. Following the example of flight BAW237 from above, in this case the line containing the data for Airbus A321 shall be duplicated and fields 1, 3 and 24 shall be replaced by *A321-RPAS*. The first two fields refer to the names under which the aircraft type will be displayed in AirTOp, will the last one links the aircraft type with one from the AircraftSizeType.csv, which will be covered at step 4. No other values need to be changed because the performance of the RPAS will be identical with that of the original aircraft.

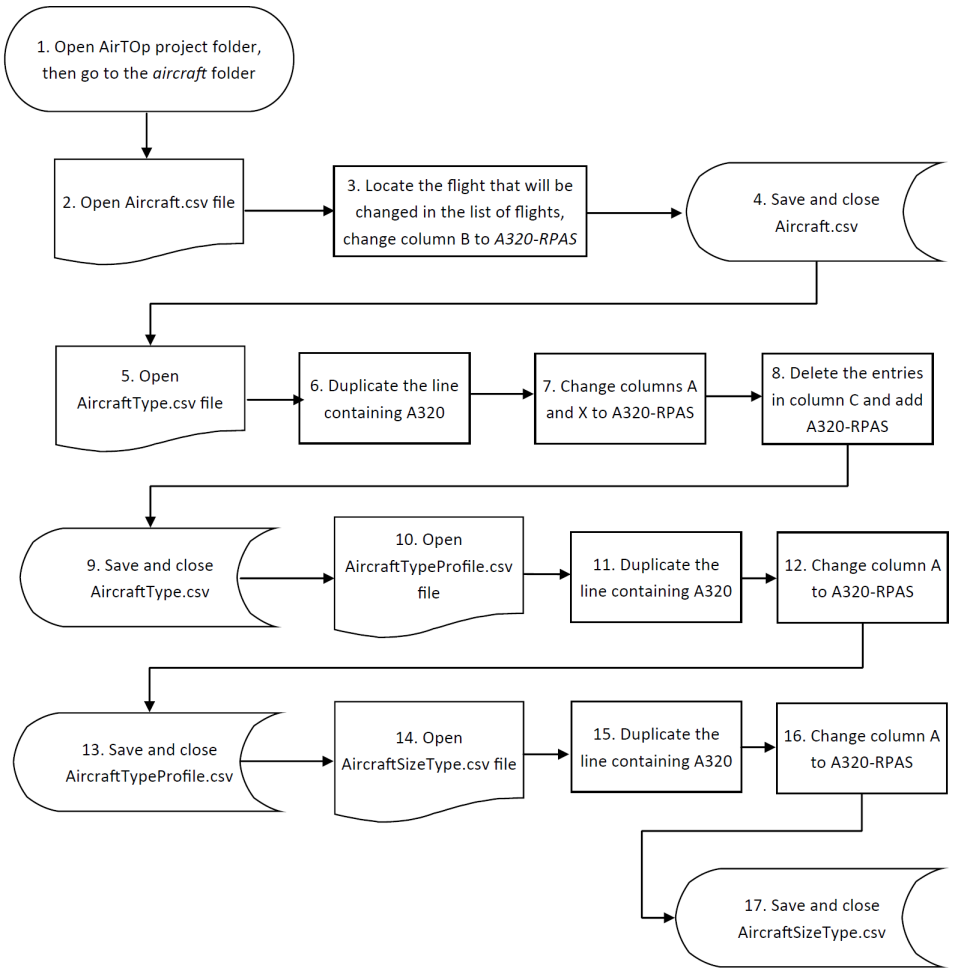

Figure A.6: Flowchart for creating a remotely piloted A320 in AirTOp

The third step defines the profile type of the RPAS. For this, the AircraftTypeProfile.csv file needs to be edited. As with the previous file, this one also contains an entry for each aircraft type. There are 11 entries for each aircraft type, such as: aircraft type name, climb/descent time, climb/descent distance, average climb/descent speed, etc. As with the AircraftType.csv file previously discussed, the line representing the original aircraft is duplicated and the suffix *"-RPAS"* is added to the aircraft type name which represents the first entry.

Similarly, for the fourth and final step, the AircraftSizeType.csv file is edited by adding an entry for the RPAS. This file contains 6 entries for each aircraft type (aircraft type name, size category, length, wing span, wing tip clearance and height). Again, only the first entry will be changed and all other values are kept the same. The four steps for creating an RPAS in AirTOp are summarized in Figure A.6 which illustrates how a remotely piloted A320 can be added to the simulation environment. These steps can be followed to create any new aircraft type in AirTOp. However, in order for the newly created aircraft to behave like and RPAS for the purpose of this experiment, one needs to specify additional separation requirements that should be enforced around it. This will be the topic of the next section.

A.3. Setting up lateral and vertical separation requirements

First, two conditions shall be created in AirTOp to distinguish between RPAS and non-RPAS aircraft. Figure A.7 shows one of them, which looks at whether the aircraft type name contains or not the text *"RPAS"* in it. The other is just the revers of the shown condition. This way AirTOp can distinguish between manned and unmanned flights. Then, the user shall now select the bottom field from the Conflict Detector Adapter (Figure

A.8). The vertical separation matrix can be edited after selecting the two previously created conditions. The outcome is shown in Figure A.9. The required separation values shall now be entered and the same procedure shall be followed for the definition of lateral separation requirements.

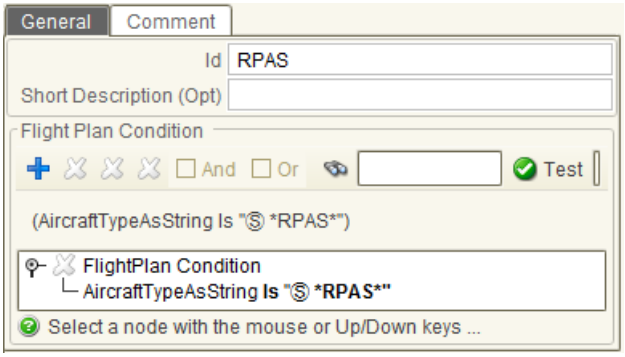

Figure A.7: AirTOp Flight Plan Condition for selecting remotely piloted Aircraft

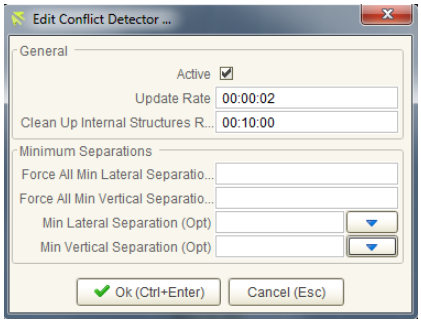

Figure A.8: AirTOp Conflict Detector Adapter Window

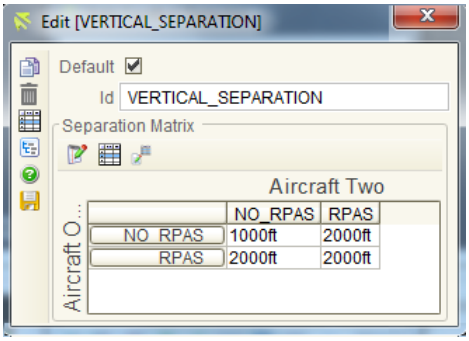

Figure A.9: AirTOp Vertical Separation Matrix Window

B

Outline of an ALL_FT+ file

Figure B.1 shows an extract of an ALL_FT+ file. The information enclosed in the blue boxes is explained below. For each flight there are 143 fields. The ones which are relevant to the AirTOp simulations deal with departure and arrival airports and times and the specific routing of each flight.

1. ICAO code of departure aerodrome (Stuttgart Airport)
2. ICAO code of arrival aerodrome (Milan Malpensa Airport)
3. Callsign or flight identifier
4. ICAO aircraft operator designator (Air Berlin)
5. ICAO Aircraft type designator (de Havilland Dash 8-400)
6. Initial estimated Off Block as of first flight plan (04:35 a.m. on the 30^{th} of September 2010)
7. Various flight plan information (route, source of flight plan, slot allocation, etc.)

EDDS[1] LIMC[2] BER8754[3] BER[4] DH8D[5] 20100930043400 AA79201658
20100930043500[6] FPL FPL FPL NEXE NEXE N N N
20100930043500 20100930043500 TE FI NS 699756 N
N N 0 0 FPL N N Y
N 900 900 N
0 0 LGW N 300 0 N DABQHS
DGRSY N N
K 0 0 339 12971 2
7 F230:N0347:0 F190:N0347:215 38 044600:EDDS:SUL2B:13:0:A:484124N0091319E::Y
044620::DCT:20:2:V:484103N0091128E:29:Y 044650::DCT:30:5:V:484030N0090842E:71:Y
044705:SY:SUL2B:35:7:N:484009N0090651E::Y 044720::DCT:40:9:V:483925N0090539E:4:Y
044910::DCT:80:23:V:483417N0085716E:34:Y 045225::D 37

Figure B.1: Extract from an ALL_FT+ traffic file [81]

C

Description of BADA Files

The BADA files are required in order to have accurate prediction of the aircraft trajectory. For each aircraft type, there are 4 BADA files associated to it.[82] The names and file extensions used is shown below in brackets:

1. Operations Performance File (<ICAO_code>__.OPF)
2. Airline Procedures File (<ICAO_code>__.APF)
3. Performance Table File (<ICAO_code>__.PTF)
4. Performance Table Data (<ICAO_code>__.PTD)

The Operations Performance File contains data on the mass, flight envelope, drag, engine thrust and fuel consumption of each aircraft type. The Airline Procedures File specifies the speeds at which different maneuvers are to be performed, while a summary of the speeds, climb/descend rates and fuel consumption at various flight levels is included in the Performance Table File. A detailed table of the computed performance values at various flight levels for each aircraft type can be found in the Performance Table Data file. In addition to the four files which are present for each aircraft type, the BADA directory also contains two other files: a Synonym File (named SYNONYM.NEW) and a Global Parameter File (BADA.GPF). The Synonym File contains a list of all aircraft types that are supported by BADA and indicates for each aircraft type whether the four files explained above are provided directly, or if files of another equivalent aircraft type should be used for that model. For instance, in the case of Airbus A350-800, the Synonym file shows that the performance model that should be used is that of the Boeing B787-900. The BADA.GPF file in an ASCII file that contains information on the global aircraft parameters such as maximum bank angle, minimum speed coefficients, descend speeds, lift coefficients, etc.

An example of an Operations Performance File of an Airbus 300B4-600 can be seen in Figure C.1. All other files are constructed in a similar manner. The first two characters at the beginning of a line establish whether that line is a comment line (CC), data line (CD) or end-of-file line (FI). As can be seen in Figure C.1, there are eight blocks in which the data is divided, each of them separated by a comment line which contains the block name and the equal signs. This is done in order to increase the readability of the file.

```
CCCCCCCCCCCCCCCCCCCCCCCCCCCCCCC A306__.OPF CCCCCCCCCCCCCCCCCCCCCCCCCCCCCC/
CC                                                                      /
CC               AIRCRAFT PERFORMANCE OPERATIONAL FILE                  /
CC                                                                      /
CC                                                                      /
CC      File_name: A306__.OPF                                           /
CC                                                                      /
CC      Creation_date: Apr 30 2002                                      /
CC                                                                      /
CC      Modification_date: Sep 05 2008                                  /
CC                                                                      /
CC                                                                      /
CC====== Actype ========================================================/
CD   A306__          2 engines    Jet                          H         /
CC  A300B4-622    with PW4158 engines                       wake        /
CC                                                                      /
CC====== Mass (t) ======================================================/
CC    reference      minimum      maximum     max payload  mass grad  /
CD     .14000E+03   .87000E+02   .17170E+03   .39000E+02   .15103E+00 /
CC====== Flight envelope ===============================================/
CC     VMO(KCAS)       MMO        Max.Alt       Hmax        temp grad  /
CD     .33500E+03   .82000E+00   .41000E+05   .32378E+05   -.2716E+02 /
CC====== Aerodynamics ==================================================/
CC Wing Area and Buffet coefficients (SIM)                              /
CCndrst Surf(m2)     Clbo(M=0)        k          CM16                   /
CD 5   .26000E+03   .13150E+01   .84080E+00   .00000E+00                /
CC   Configuration characteristics                                      /
CC n Phase  Name    Vstall(KCAS)    CD0          CD2         unused     /
CD 1 CR   Clean     .15100E+03   .20591E-01   .51977E-01   .00000E+00 /
CD 2 IC   S15F00    .11700E+03   .33057E-01   .45362E-01   .00000E+00 /
CD 3 TO   S15F00    .11700E+03   .33057E-01   .45362E-01   .00000E+00 /
CD 4 AP   S15F15    .10900E+03   .38031E-01   .44932E-01   .00000E+00 /
CD 5 LD   S30F40    .97000E+02   .78935E-01   .44822E-01   .00000E+00 /
CC   Spoiler                                                            /
CD 1      RET                                                           /
CD 2      EXT                               .00000E+00   .00000E+00    /
CC   Gear                                                               /
CD 1      UP                                                            /
CD 2      DOWN                   .22500E-01   .00000E+00   .00000E+00 /
CC   Brakes                                                             /
CD 1      OFF                                                           /
CD 2      ON                                .00000E+00   .00000E+00    /
CC====== Engine Thrust =================================================/
CC         Max climb thrust coefficients (SIM)                          /
CD     .29716E+06   .51306E+05   .56296E-10   .84814E+01   .44597E-02 /
CC     Desc(low)    Desc(high)   Desc level   Desc(app)     Desc(ld)   /
CD     .32012E-01   .40310E-01   .15161E+05   .13124E+00   .39136E+00 /
CC     Desc CAS     Desc Mach     unused       unused       unused     /
CD     .30000E+03   .78000E+00   .00000E+00   .00000E+00   .00000E+00 /
CC====== Fuel Consumption ==============================================/
CC   Thrust Specific Fuel Consumption Coefficients                      /
CD     .63936E+00   .10047E+04                                         /
CC   Descent Fuel Flow Coefficients                                     /
CD     .21196E+02   .67071E+05                                         /
CC   Cruise Corr.    unused       unused       unused       unused     /
CD     .98852E+00   .00000E+00   .00000E+00   .00000E+00   .00000E+00 /
CC====== Ground ========================================================/
CC        TOL          LDL         span         length       unused     /
CD     .23620E+04   .15550E+04   .44840E+02   .54080E+02   .00000E+00 /
CC=====================================================================/
FI                                                                      /
```

Figure C.1: Example of Operations Performance File of Airbus 300B4-600 [82]

D

Influence of different Confidence Intervals on Results and Number of Iterations

This Appendix investigates whether there are any benefits of using a higher confidence interval (98% or 99%) compared to the one typically used in Monte Carlo analyses (95%).

In Section 4.5, the criteria for ending the simulations for a particular scenario was that the standard error would drop below 0.5 when the 95% confidence interval is used. This is similar to saying that as soon as the width of the 95% confidence interval drops below 1.0, the analysis can move to the next scenario. While the full results of Experiment 1 were discussed in Section 6.1, this section considers only the first three scenarios of this experiment and looks at how the number of iterations required to reach convergence are influenced by selecting a higher confidence interval (98 and 99%). The confidence interval is calculated by Equation 5.7. In the case of the 95% confidence interval, the value of $z_{\delta/2}$ is 1.96, while for the 98 and 99% confidence interval the $z_{\delta/2}$ is 2.33 and 2.58, respectively.

Figures D.1 - D.3 show how the widths of the 95%, 98% and 99% confidence intervals ($2 \cdot z_{\delta/2} \cdot RMSE$) vary as the number of iterations is increased for the first three scenarios of experiment 1. These results are also summarized in Table D.1.

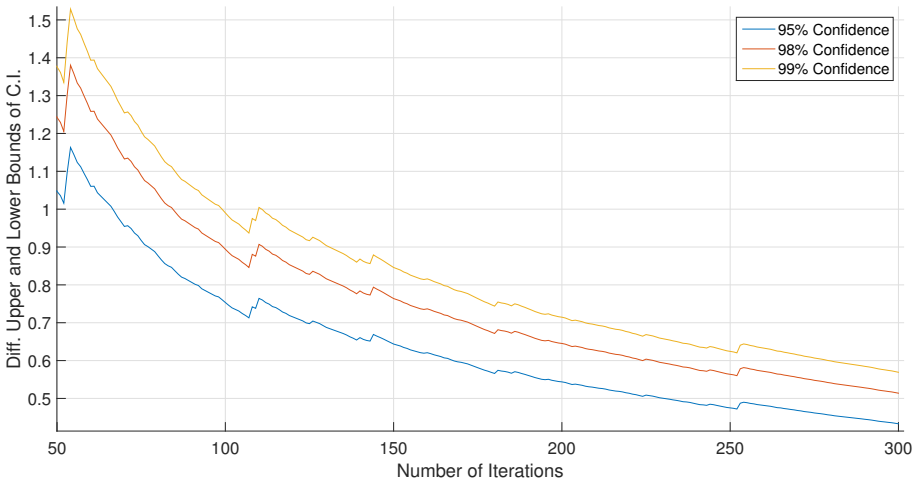

Figure D.1: Effect of choosing a different Accuracy on the Number of Iterations for Scenario 1 of Experiment 1

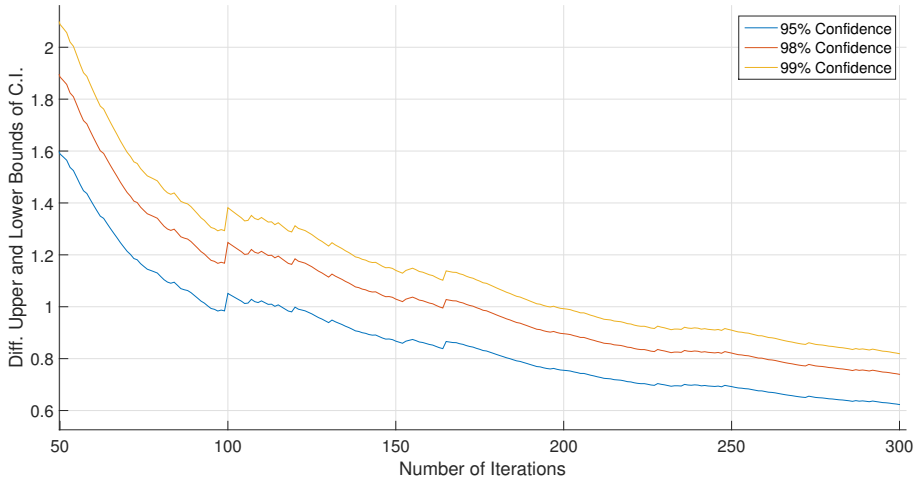

Figure D.2: Effect of choosing a different Accuracy on the Number of Iterations for Scenario 2 of Experiment 1

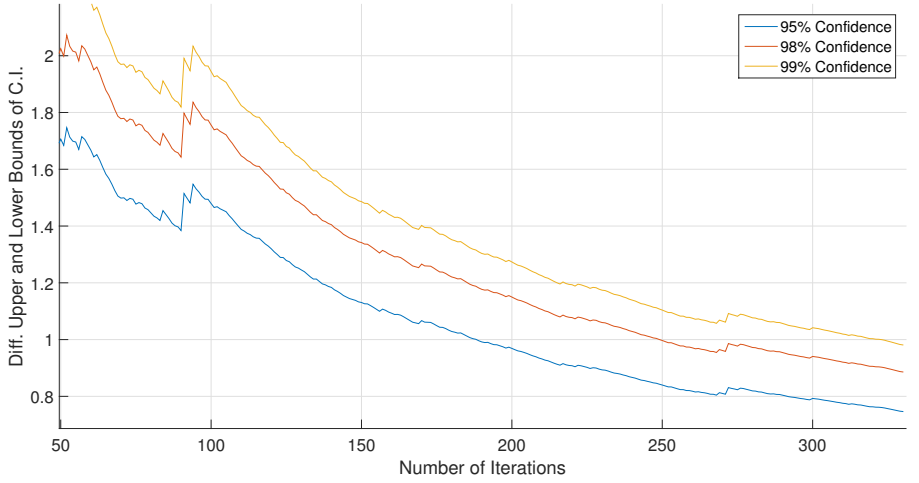

Figure D.3: Effect of choosing a different Accuracy on the Number of Iterations for Scenario 3 of Experiment 1

Table D.1: Impact of different Confidence Intervals on Results and Number of Iterations (Experiment 1)

Scenario No.	**95% Confidence**				**98% Confidence**				**99% Confidence**			
	No. of Runs	**Mean** (Z_N^{MC})	**Std. dev.** (σ)	**RMSE**	**No. of Runs**	**Mean** (Z_N^{MC})	**Std. dev.** (σ)	**RMSE**	**No. of Runs**	**Mean** (Z_N^{MC})	**Std. dev.** (σ)	**RMSE**
1	87	1.84	1.95	0.21	104	1.73	1.9	0.19	119	1.81	2	0.18
2	140	3.04	2.72	0.23	193	3.19	2.72	0.2	214	3.16	2.69	0.18
3	207	4.67	3.46	0.24	268	4.59	3.36	0.21	318	4.71	3.48	0.19

As can be seen here, in the case of the first scenario, 17 and 32 additional iterations are required for the results to converge when 98% and 99% confidence intervals are considered. The mean number of conflicts decreases from 1.84 to 1.81, which shows that there is no real benefit from the additional increase in accuracy. Similarly, for the second scenario 53 and 74 additional iterations are required for the 98% and 99% confidence intervals (an increase of 38% and 53%). At the same time, the mean number of conflicts increases from 3.04 to 3.16. A similar trend is observed for the third scenario, where 29% more iterations are required for the 98% confidence case, and 53% more runs for the 99% confidence one. The mean number of conflicts increases from 4.67 to 4.71. As can be seen from this analysis, opting for a different confidence level would have resulted in an increase of computation time, while the results would not have been affected.

E

Histograms of Simulation Results for Experiment 1

This Appendix shows the histograms of the number of conflicts that were obtained for the 9 scenarios of the first experiment (Figure E.1 - E.9).

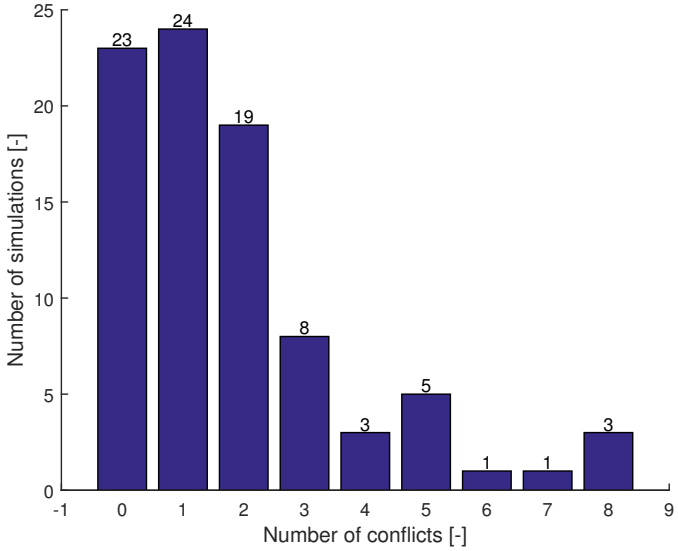

Figure E.1: Histogram of Simulation Results for Scenario 1

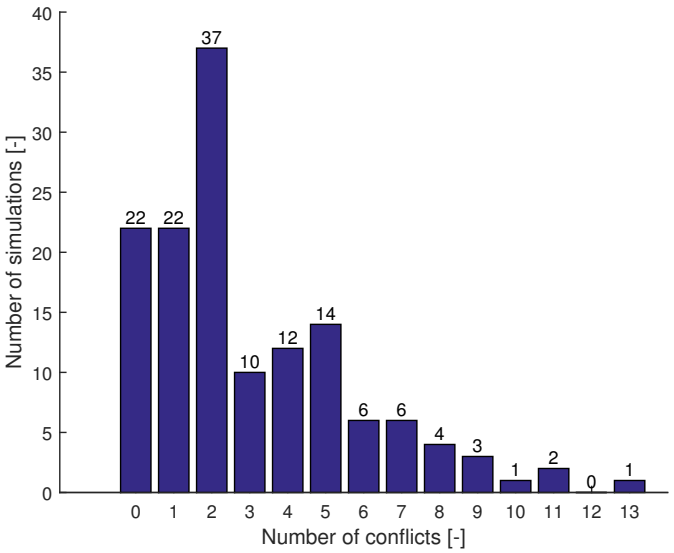

Figure E.2: Histogram of Simulation Results for Scenario 2

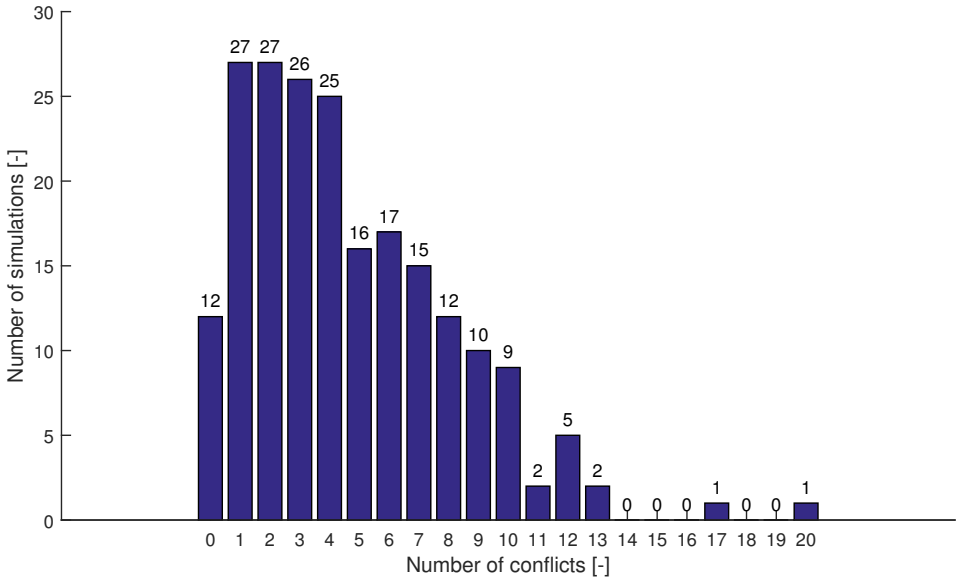

Figure E.3: Histogram of Simulation Results for Scenario 3

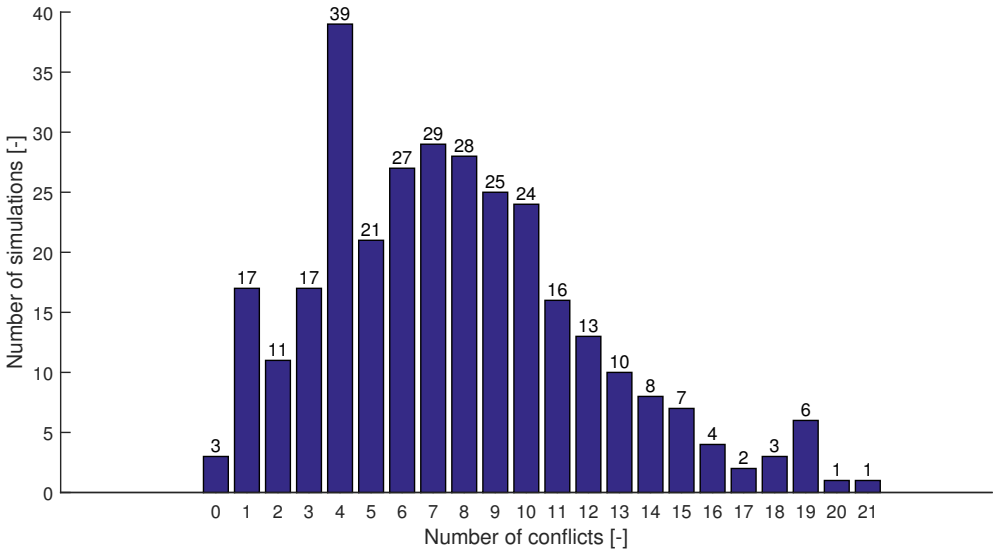

Figure E.4: Histogram of Simulation Results for Scenario 4

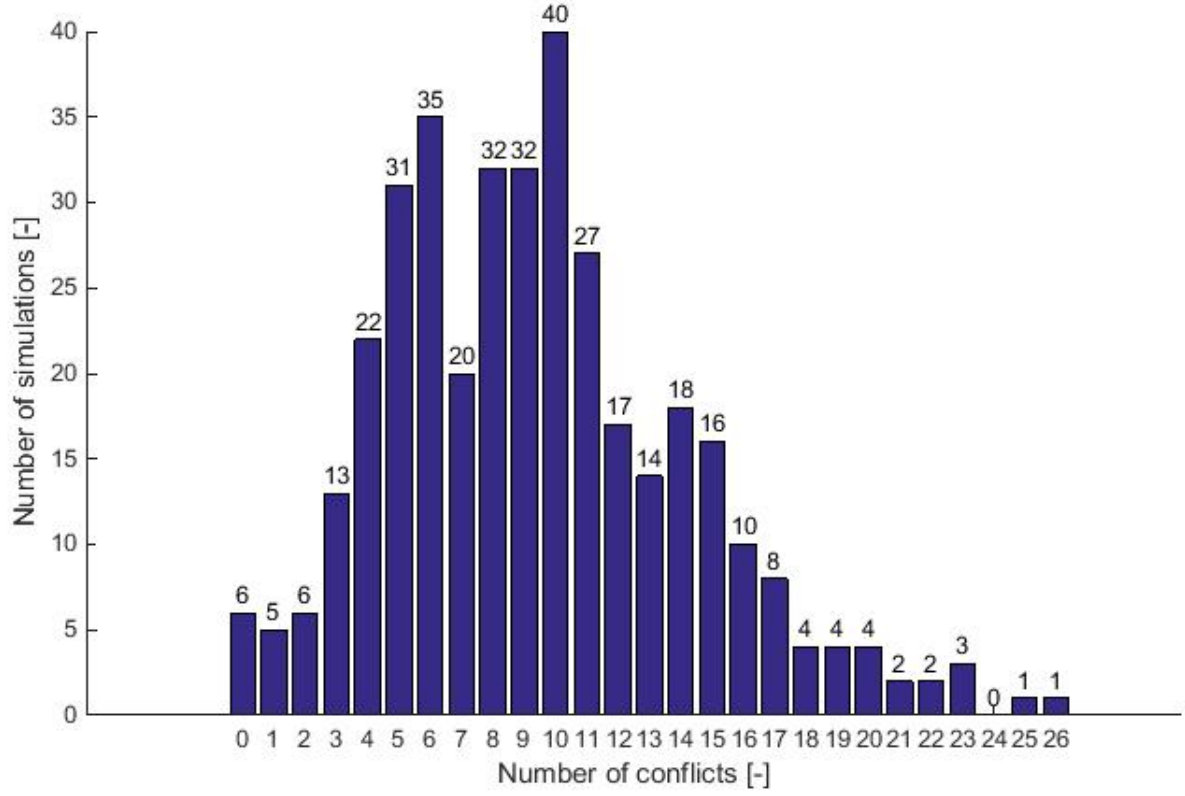

Figure E.5: Histogram of Simulation Results for Scenario 5

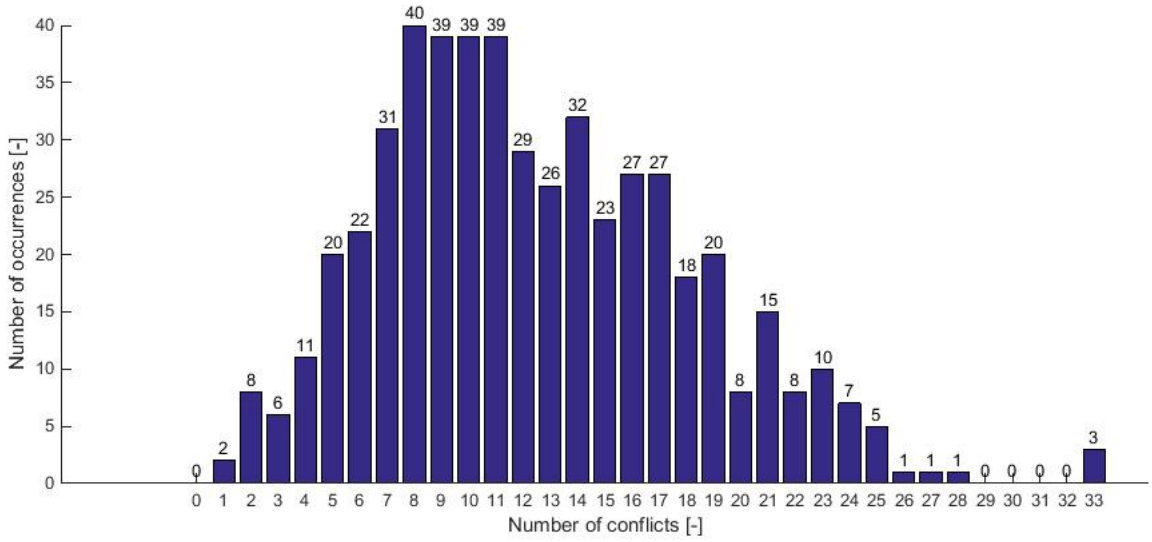

Figure E.6: Histogram of Simulation Results for Scenario 6

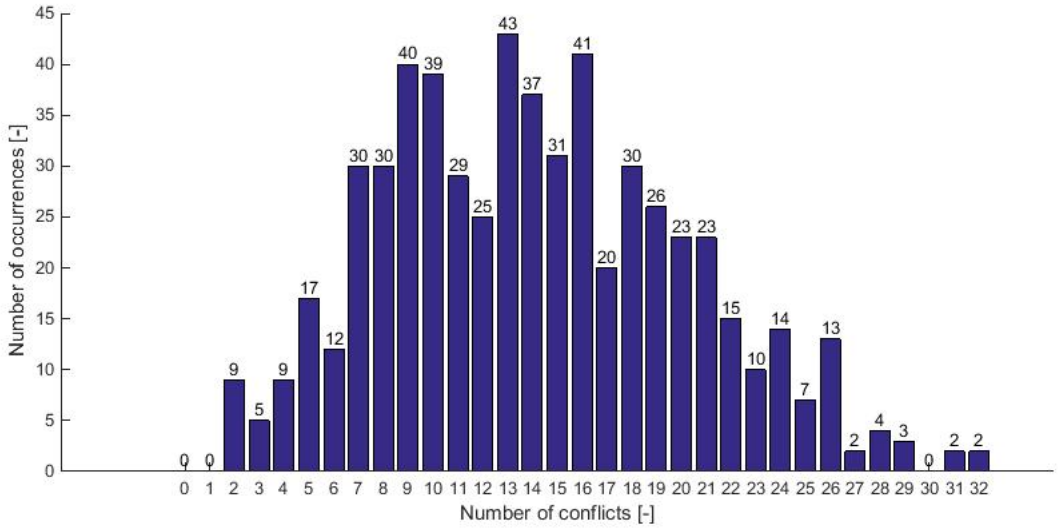

Figure E.7: Histogram of Simulation Results for Scenario 7

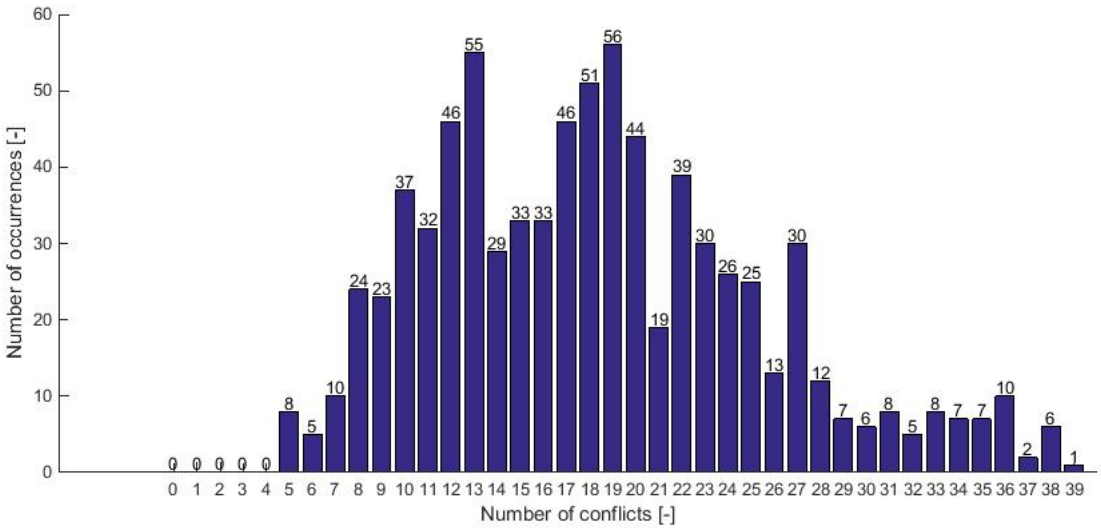

Figure E.8: Histogram of Simulation Results for Scenario 8

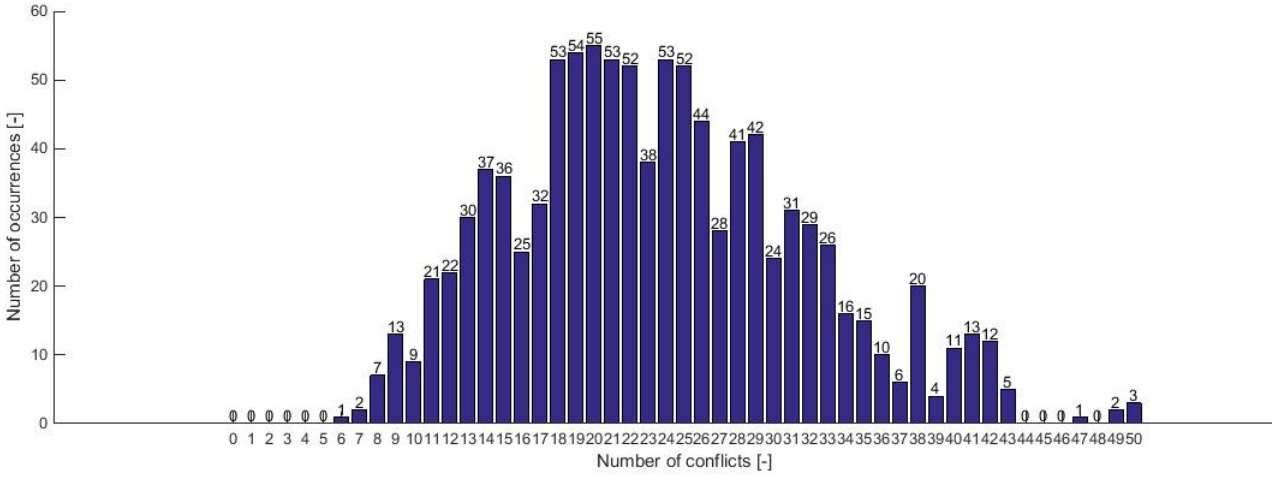

Figure E.9: Histogram of Simulation Results for Scenario 9

F

AirTOp Conflict Resolution Actions

In order to solve potential conflicts in AirTOp, the Conflict Resolution module of the simulator shall be activated. This requires the air traffic controllers to follow a Conflict Resolution Rule Base Tree (Figure 8.1) to solve conflicts. The way in which the ATCo deals with a potential conflict was explained in Section 8.1. This section explains the 10 conflict resolution actions that can be taken in AirTOp. These are given in the list below: [47]

- **Stop climb/descent:** the selected aircraft stops its climb/descent and cruises at a lower/higher flight level until lateral separation is reached. Then, it will resume its original climb/descent procedure.
- **Accelerate climb/descent:** increases the climb/descent rate of an aircraft that is ascending/descending.
- **Change cruise level up/down** instructs the selected aircraft climb/descend and maintain a new cruise altitude.
- **Change speed:** one or both aircraft increase/decrease their speed.
- **Direct shortcut:** instructs the selected aircraft to fly a shorter path through the sector by directing it to the sector exit waypoint.
- **Following at the same speed:** makes the aircraft behind reduce its speed to match that of the aircraft in the front. The two aircraft follow each other until the first waypoint at which their routes diverge and then the speed of the aircraft that was behind is restored.
- **Follow separated:** applied when one or both aircraft are descending by matching their descend rates such that vertical separation is maintained.
- **Vectoring behind:** makes the selected aircraft perform two heading changes and fly behind the other aircraft. It will direct the selected aircraft away from the closest point of approach (CPA) and once lateral separation has been achieved, back to its original trajectory.
- **Vectoring parallel (opposite):** the selected aircraft performs three heading changes. The first one directs the aircraft to a point located behind the other aircraft at the CPA. Then the second turn will bring it parallel to the original trajectory and will continue flying for 2 NM. The last heading change brings it back to the original trajectory. If required, this resolution action can modify the trajectory of both flights.
- **Vectoring parallel (same track):** instructs the selected aircraft to perform three heading changes. During the first one the aircraft flies towards a point that is located at a distance equal to the minimum separation plus a buffer perpendicular from the conflict location. The second heading change makes it fly parallel to its original trajectory and then once it reaches the required lateral separation with the second aircraft, a third heading change returns it to its original trajectory.

G

Calculating Fuel Consumption

This appendix outlines the procedure followed to calculate the fuel consumption of a flight according to the data in the BADA performance files [82]. The values of the C_f coefficients in the formulas below shall be extracted from the BADA files of each aircraft.

The nominal fuel flow is calculated from Equation G.1 (jet) and G.2 (turboprop). The trues airspeed, V_{TAS}, is measured in kts and the Thrust, Thr, in kN.

$$f_{nom} = C_{f1} \cdot (1 + \frac{V_{TAS}}{C_{f2}}) \cdot Thr \quad \text{[kg/min]} \tag{G.1}$$

$$f_{nom} = C_{f1} \cdot (1 - \frac{V_{TAS}}{C_{f2}}) \cdot (\frac{V_{TAS}}{1000}) \cdot Thr \quad \text{[kg/min]} \tag{G.2}$$

The nominal fuel flow expressions given in Equations G.1 and G.2 can be used in all flight phases except for cruise and idle descent. For both jet and turboprop engines during idle descent the minimum fuel flow is given by Equation G.3, where H_p represents the geopotential pressure altitude and is measured in feet.

$$f_{min} = C_{f3} \cdot (1 - \frac{H_p}{C_{f4}}) \quad \text{[kg/min]} \tag{G.3}$$

Once the aircraft switches to approach and landing configuration, thrust is increased and Equation G.3 can no longer be used. Instead the maximum between the nominal and minimum fuel flow shall be considered, as shown in Equation G.4.

$$f_{ap/ld} = \text{MAX}(f_{nom}, f_{min}) \tag{G.4}$$

During cruise, the fuel flow is calculated for both het and turboprop engines using Equation G.5.

$$f_{cr} = f_{nom} \cdot C_{fcr} \quad \text{[kg/min]} \tag{G.5}$$

Using AirTOp, the fuel used by a flight during the time it spent in the sector is calculated automatically.

H

Creating the simulation environment in AirTOp for Experiment 2

The following 23 steps shall be followed to create the simulation environment for the second experiment (one time only):

SE-1: Take sector EDGGPHHM (from now on referred to as SECT) coordinates from NEST.

SE-2: Create in AirTOp a polygon with the coordinates of SECT.

SE-3: Create a sector block from the previously created polygon.

SE-4: Divide the sector block in three sectors: SECT-DN (FL0-FL115), SECT (FL115-FL245) and SECT-UP (FL245+). This is required in order to be consistent with the real-life definition of sector EDGGPHHM.

SE-5: Create an ATC sector for each of the three previously created sector blocks.

SE-6: Repeat steps SE-1 – SE-5 and create two additional sectors around SECT: SECT-EAST and SECT-WEST. SE-4 can be omitted in this case, since no vertical division is required for these two sectors. Their purpose is to accommodate the flights prior to their entry in SECT. They will be part of the simulation environment, but the behaviour of the flights in these two boundary sectors (or SECT-UP/DN) will not be analyzed.

SE-7: Import the BADA-4 performance models (including the RPAS performance package) to AirTOp. Then, update all aircraft type profiles in AirTOp to make sure the newly added performance files will be used.

SE-8: Import the GASEL directory to AirTOp (location of airports, waypoints, navaids, ATS routes, etc.)

SE-9: Import all the flights for the selected date from the ALL_FT+ traffic file for the created polygons only.

SE-10: Run AirTOp once to determine the entry times of the flights in SECT.

SE-11: Update the flight plan for each of the flights, such that the start and end points are within the simulated area (SECT-EAST / SECT-WEST). This means that the flight plans of the flights have to be manually checked and updated.

SE-12: Create a new waypoint at the intersection at the location where each flight enters SECT. Add this waypoint to the respective ATS route that the flight is using.

SE-13: Edit each of the flight plans such that the newly defined waypoint is included in the flights' route.

SE-14: Create a constraint on the time when each of the flights arrives at the previously defined waypoint.

SE-15: Create pseudo-radar controllers for the 5 ATC sectors. This is required to enforce the separation of the flights, solve conflicts and measure ATCo task load.

SE-16: Define the lateral and vertical separation requirements. (in accordance with ICAO Doc. 4444)

SE-17: Enable the conflict detector and resolution adapter. (this means that the radar controllers are assigned the task to detect and solve conflicts)

SE-18: Create an Aircraft condition that checks whether a flight is an RPAS/non-RPAS flight, by looking at the aircraft type. This condition will be used when enforcing the separation bubble and solving the conflicts.

SE-19: Edit the conflict resolution adapter such that no resolution commands will be given to the RPAS (this way the simulator takes into account the C2 link failure). AirTOp's default conflict resolution tree contains 338 nodes. Each of these nodes must be manually updated. This means that a condition has to be added such that the aircraft that performs the manoeuvre cannot be of RPAS type.

SE-20: Edit all flight plans and add a condition on the flight departure time: add a MinMax distribution for the flight departure time. This means that the flight departure time will be uniformly randomly varied between -1 minute and +1 minute around the calculated departure time. If the generated time duration is negative this means that the flight will leave early and in case of a positive value, the flight will be delayed. Because of the waypoint constraint at SECT entry (SE-14) this condition will actually vary the flight entry time in the sector at each run.

SE-21: Change all flights to RPAS and calculate the new departure times of the flights. This step is required to determine the new departure time of an RPAS flight in order to make sure that the waypoint constraint added at SE-14 is met. Save the results for future use when generating new project folders in Matlab.

SE-22: Repeat SE-21 for every type of RPAS that will be part of the analysis.

SE-23: Save and close the project.

The following 10 steps shall be followed for conducting the experiments (see Figure 7.12 for a graphical representation of these steps):

1. Use Matlab script to generate new project folders based on the current scenario that is analyzed.

2. For each individual run, the project folder obtained at SE-23 above shall be copied. Through Matlab a new .prj file is created that makes this a new "valid" AirTOp project.

3. Paste the Aircraft.csv file generated by Matlab in Project Folder>aircraft. This makes sure that the desired aircraft is switched to the RPAS of choice (depending on the Scenario).

4. Paste the AdapetrSetting.cvs file in Project Folder > simulator. This file specifies the ATCo what separation matrix should be used (depending on the scenario: 0-20-40% increase w.r.t. minimum ICAO values).

5. Paste FlightPlan.csv file in Project Folder > flightplan. This updates the departure time of the flight that is now operated by an RPAS.

6. When running the simulations for one scenario, there are 53 possibilities to select the aircraft that will be changed to an RPAS. At each run, because of the condition at SE-20, the time when the flights enter SECT is randomly varied.

7. Each time an AirTOp project is run, 64 output files are generated in the «report» folder. Out of these files, 4 of them are of importance to the study and should be saved. Each of the runs is in a different folder and by default each «report» folder has subfolders where the files are located. Thus, a Windows PowerShell ISE script was written to copy all the necessary output files in a separate «Results» folder, rename them in an ascending sequence for simplicity by adding "_runX" at the end of each file, and then deleting the «report» folder altogether to free up the disk space for the next runs. The four files which are saved after each run are described below:

(a) *Conflict.csv* – contains the total number of potential conflicts that were solved in all the 5 ATC sectors which are part of the simulation environment and then one line for each conflict. On each line of the Conflict.csv file there are multiple entries (detection time, resolution time, conflict type, lateral separation, vertical separation, etc.) The fourth column contains the sector where that potential conflict occurred. By going through the file line by line and summing the number of lines where SECT is the entry of the 4th column, the number of potential conflicts for that particular run has been determined.

(b) *Flight_ATC_Sector_Entered.csv* – contains one line for each time when a flight enters in one of the 5 ATC sectors. Each line contains 15 entries, such as: flight number, old ATC sector, new ATC sector, time, altitude, distance flown in previous sector, fuel burn in previous sector, etc. By going through the file line by line the following values are saved in a separate Results_RunX.csv. This way the *Results_RunX.csv* generated for each run contains only 53 lines with the final values of the above metrics per flight:

i. For each flight, when old ATC sect value is *SECT*, the distance, duration, fuel burn and altitude (exit altitude) are saved.

ii. For each flight, when new ATC sect value is *SECT*, the time (sector entry time) and altitude (entry altitude) are saved.

(c) *ATC_Sector_Radar_Controller_Workload_Calculated.csv* – contains the ATCo task load, one line for each 10 minute time block. Using Matlab, the file is read line by line and only the values for SECT are stored in a separate file *Workload.csv* for the 6 blocks between 06:00-07:00.

(d) SeedNumber.csv - contains a 19 digit number which represents the value used to initialize the pseudorandom number generator. All the values are saved such that the simulations can be traced back.

8. Run the *Read_Results* MATLAB script which will process the results from the 4 files above which are generated for each run in 3 summary files as described at Step 7.

9. Run the *Process_Results* MATLAB script which compiles the average values of each of the metrics (total flight distance, total flight duration, total fuel burn, etc.) in one file for all the runs of a scenario.

10. Run *Create_Plots* Matlab script which generates the variation of the mean of each metric as a function of increasing number of runs for all the metrics considered. Then calculate confidence intervals, and check for convergence.

ANOVA Results Case 5

This appendix contains the ANOVA results for Case 5, which compares the differences between the two RPAS performance models (MQ-9 and RQ-4A) when the same separation standard is enforced around the RPAS with a failure of the C2 link. The results are given in Tables I.1 - I.4.

Table I.1: ANOVA Results RQ-4A Vs. MQ-9 (0% Separation Increase)

KPI	**Levene's Significance**	**ANOVA Type**	**ANOVA Result**	H_0 **Rejected?**
KPI_1	0.00	Welch's ANOVA	[F(1,2087.5) = 21.77, p = 0]	Yes
KPI_2	0.00	Welch's ANOVA	[F(1,2090.69) = 21.06, p = 0]	Yes
KPI_3	0.00	Welch's ANOVA	[F(1,2017.44) = 38.4, p = 0]	Yes
KPI_4	0.91	One-way ANOVA	[F(1,2118) = 1.97, p = 0.16]	No
KPI_5	0.61	One-way ANOVA	[F(1,2118) = 3.32, p = 0.07]	No
KPI_6	0.93	One-way ANOVA	[F(1,2118) = 0.86, p = 0.35]	No
KPI_7	0.49	One-way ANOVA	[F(1,2118) = 0.2, p = 0.66]	No
KPI_8	0.95	One-way ANOVA	[F(1,2118) = 0.26, p = 0.61]	No
KPI_9	0.91	One-way ANOVA	[F(1,2118) = 0, p = 0.96]	No

Table I.2: ANOVA Results RQ-4A Vs. MQ-9 (20% Separation Increase)

KPI	**Levene's Significance**	**ANOVA Type**	**ANOVA Result**	H_0 **Rejected?**
KPI_1	0.14	One-way ANOVA	[F(1,2118) = 40.05, p = 0]	Yes
KPI_2	0.19	One-way ANOVA	[F(1,2118) = 26.21, p = 0]	Yes
KPI_3	0.00	Welch's ANOVA	[F(1,2042.07) = 30.55, p = 0]	Yes
KPI_4	0.22	One-way ANOVA	[F(1,2118) = 3.51, p = 0.06]	No
KPI_5	0.60	One-way ANOVA	[F(1,2118) = 4.88, p = 0.03]	Yes
KPI_6	0.57	One-way ANOVA	[F(1,2118) = 2.7, p = 0.1]	No
KPI_7	0.07	One-way ANOVA	[F(1,2118) = 1.06, p = 0.3]	No
KPI_8	0.79	One-way ANOVA	[F(1,2118) = 0.01, p = 0.91]	No
KPI_9	0.52	One-way ANOVA	[F(1,2118) = 0.07, p = 0.79]	No

Table I.3: ANOVA Results RQ-4A Vs. MQ-9 (40% Separation Increase)

KPI	Levene's Significance	ANOVA Type	ANOVA Result	H_0 Rejected?
KPI_1	0.00	Welch's ANOVA	[F(1,2075.02) = 24.24, p = 0]	Yes
KPI_2	0.01	Welch's ANOVA	[F(1,2103.36) = 12.89, p = 0]	Yes
KPI_3	0.00	Welch's ANOVA	[F(1,2050.41) = 53.92, p = 0]	Yes
KPI_4	0.22	One-way ANOVA	[F(1,2118) = 7.81, p = 0.01]	Yes
KPI_5	0.17	One-way ANOVA	[F(1,2118) = 6.1, p = 0.01]	Yes
KPI_6	0.76	One-way ANOVA	[F(1,2118) = 5.9, p = 0.02]	Yes
KPI_7	0.01	Welch's ANOVA	[F(1,2096.04) = 0.92, p = 0.34]	No
KPI_8	0.01	Welch's ANOVA	[F(1,2104.91) = 0.19, p = 0.66]	No
KPI_9	0.08	One-way ANOVA	[F(1,2118) = 0.1, p = 0.75]	No

Table I.4: ANOVA Results RQ-4A Vs. MQ-9 (60% Separation Increase)

KPI	Levene's Significance	ANOVA Type	ANOVA Result	H_0 Rejected?
KPI_1	0.00	Welch's ANOVA	[F(1,2082.45) = 32.49, p = 0]	Yes
KPI_2	0.00	Welch's ANOVA	[F(1,2104.4) = 18.54, p = 0]	Yes
KPI_3	0.00	Welch's ANOVA	[F(1,2054.76) = 30.74, p = 0]	Yes
KPI_4	0.16	One-way ANOVA	[F(1,2118) = 2.85, p = 0.09]	No
KPI_5	0.07	One-way ANOVA	[F(1,2118) = 1.8, p = 0.18]	No
KPI_6	0.92	One-way ANOVA	[F(1,2118) = 5.32, p = 0.02]	Yes
KPI_7	0.14	One-way ANOVA	[F(1,2118) = 1.25, p = 0.26]	No
KPI_8	0.04	Welch's ANOVA	[F(1,2091.13) = 0.02, p = 0.89]	No
KPI_9	0.01	Welch's ANOVA	[F(1,2097.78) = 0.09, p = 0.77]	No

J

MANOVA Tables

This appendix contains the MANOVA tables that are referred to in Section 11.2.

Table J.1: Results of Levene's Test for the 18 Combinations considered for the MANOVA test

Scenarios Considered	**Levene's Test**								
	KPI_1	**KPI_2**	**KPI_3**	**KPI_4**	**KPI_5**	**KPI_6**	**KPI_7**	**KPI_8**	**KPI_9**
0 , 1_1 - 1_4	0.04	0.29	0.00	0.00	0.00	0.00	0.00	0.00	0.00
1_1 - 1_4	0.02	0.17	0.44	0.21	0.25	0.51	0.35	0.67	0.94
0, 1_5 - 1_8	0.00	0.01	0.00	0.00	0.00	0.00	0.00	0.00	0.00
1_5 - 1_8	0.19	0.37	0.69	0.03	0.02	0.41	0.05	0.03	0.03
0, 1_1, 1_5	0.00	0.00	0.00	0.00	0.00	0.00	0.00	0.00	0.00
1_1, 1_5	0.00	0.00	0.00	0.91	0.61	0.93	0.49	0.95	0.91
0, 1_2, 1_6	0.03	0.20	0.00	0.00	0.00	0.00	0.00	0.00	0.00
1_2, 1_6	0.14	0.19	0.00	0.22	0.60	0.57	0.07	0.79	0.52
0, 1_3, 1_7	0.00	0.00	0.00	0.00	0.00	0.00	0.00	0.00	0.00
1_3, 1_7	0.00	0.01	0.00	0.22	0.17	0.77	0.01	0.01	0.08
0, 1_4, 1_8	0.00	0.00	0.00	0.00	0.00	0.00	0.00	0.00	0.00
1_4, 1_8	0.00	0.00	0.00	0.16	0.07	0.91	0.14	0.04	0.01
0, 2_2, 2_4, 2_5	0.00	0.00	0.00	0.00	0.00	0.00	0.00	0.00	0.00
2_2, 2_4, 2_5	0.00	0.00	0.00	0.00	0.00	0.00	0.00	0.00	0.00
0, 2_1, 2_2, 2_3	0.00	0.00	0.00	0.00	0.00	0.00	0.00	0.00	0.00
2_1, 2_2, 2_3	0.00	0.00	0.10	0.00	0.00	0.00	0.00	0.01	0.00
0, 1_8, 2_1	0.00	0.00	0.00	0.00	0.00	0.00	0.00	0.00	0.00
1_8, 2_1	0.00	0.00	0.00	0.00	0.00	0.00	0.00	0.00	0.00

Table J.2: Covariance Marix (Case 4)

		KPI_1	KPI_2	KPI_4	KPI_5	KPI_6	KPI_7	KPI_8	KPI_9
Scn. 1_2 (1 RQ-4A, 20% Sep. Incr.)	**KPI_1**	3.32	1.72	-0.01	0.18	-0.72	-37.27	-16.82	-27.07
	KPI_2	1.72	1.98	0.04	0.61	-0.12	-10.56	-8.06	-8.89
	KPI_4	-0.01	0.04	0.13	1.30	0.56	12.54	-0.02	12.90
	KPI_5	0.18	0.61	1.30	14.54	4.40	100.68	11.71	111.75
	KPI_6	-0.72	-0.12	0.56	4.40	8.15	-0.41	77.51	-11.47
	KPI_7	-37.27	-10.56	12.54	100.68	-0.41	13997.70	864.15	9042.60
	KPI_8	-16.82	-8.06	-0.02	11.71	77.51	864.15	17850.41	6203.41
	KPI_9	-27.07	-8.89	12.90	111.75	-11.47	9042.60	6203.41	10842.35
Scn. 1_6 (1 MQ-9, 20% Sep. Incr.)	**KPI_1**	3.89	1.95	-0.01	0.14	-0.07	-52.42	-8.99	-30.52
	KPI_2	1.95	2.22	0.05	0.63	0.15	-21.26	-4.70	-14.12
	KPI_4	-0.01	0.05	0.13	1.32	0.52	12.50	1.20	13.30
	KPI_5	0.14	0.63	1.32	14.81	3.84	90.85	15.06	108.04
	KPI_6	-0.07	0.15	0.52	3.84	8.22	-20.47	97.13	-23.63
	KPI_7	-52.42	-21.26	12.50	90.85	-20.47	15881.64	447.40	9904.87
	KPI_8	-8.99	-4.70	1.20	15.06	97.13	447.40	17645.48	5846.23
	KPI_9	-30.52	-14.12	13.30	108.04	-23.63	9904.87	5846.23	11118.45

Table J.3: Covariance Matrix (Case 5)

		KPI_4	KPI_5	KPI_6	KPI_9
Scn. 1_3 (1 RQ-4A, 40% Sep. Incr.)	**KPI_4**	0.13	1.29	0.53	15.10
	KPI_5	1.29	14.29	3.72	135.24
	KPI_6	0.53	3.72	8.48	-5.92
	KPI_9	15.10	135.24	-5.92	10778.93
Scn. 1_7 (1 MQ-9, 40% Sep. Incr.)	**KPI_4**	0.13	1.30	0.51	14.33
	KPI_5	1.30	14.75	3.80	133.39
	KPI_6	0.51	3.80	8.36	-44.71
	KPI_9	14.33	133.39	-44.71	12242.82

Bibliography

[1] J. A. D. Ackroyd. Sir George Cayley: The Invention of the Aeroplane near Scarborough at the Time of Trafalgar. Journal of Aeronautical History. Paper No. 6, 2011.

[2] R. Holmes. Falling Upwards - How we took to the air. Pantheon, first edition, 2013, ISBN: 978-0307379665.

[3] J. Bueno et al. Human and Technical Performance Aspects in RPAS Integration Trials in Controlled Airspace. Sixth SESAR Innovation Days, December 2016.

[4] P. Kopardekar et al. Unmanned Aircraft System Traffic Management (UTM) Concept of Operations. 16th AIAA Aviation Technology, Integration and Operations Conference, Washington, DC, 2016.

[5] S. Ayyalasomayajula et al. Unamnned Aircraft System Demand Generation and Airspace Performance Impact Prediction. 32nd Digital Avionics System Conference, October, 2013.

[6] EUROCONTROL. RPAS ATM CONOPS. Internal Document Code: ATM.STR.CONOPS-RPAS.V(E), 2016.

[7] R. Cuadrado et al. Architecture Issues and Challenges for the Integration of RPAS in Non-segregated Airspace. IEEE/AIAA 32nd Digital Avionics Systems Conference (DASC), 2013.

[8] SESAR Joint Undertaking. Fact Sheet. Available Online: `http://www.sesarju.eu/sites/default/files/documents/events/showcase2016/Factsheet_SESAR_A4.pdf`, 2016, [accessed on 05/04/2017].

[9] European RPAS Steering Group. Roadmap for the integration of civil Remotely-Piloted Aircraft Systems into the European Aviation System. SESAR, Tech. Report, 2013.

[10] SESAR Joint Undertaking (SJU). European Drones Outlook Study - Unlocking the value for Europe, 2016.

[11] International Civil Aviation Organization. Doc.10019, Manual on Remotely Piloted Aircraft System (RPAS), 2015.

[12] International Civil Aviation Organization. Annex 7 to the Convention on International Civil Aviation: Aircraft Nationality and Registration Marks, 2012.

[13] International Civil Aviation Organization. Amendment 43 to the International Standards Rules of the Air of Annex 2 to the Convention on International Civil Aviation, 2012.

[14] International Civil Aviation Organization. ICAO Cir 328, Unmanned Aircraft Systems (UAS), 2011.

[15] H. Oh et al. Human-in-the-Loop Simulation Analysis of Conflict Resolution Maneuvers Using an Air Traffic Control. AIAA Modeling and Simulation Technologies Conference, 2016.

[16] S. Tsach et al. Development Trends for Next Generation UAV Systems. AIAA Aerospace Conference and Exhibit, 2007.

[17] P. Fahlstrom and T. Gleason. Introduction to UAV Systems. Wiley, 4th edition, 2012.

[18] V.G. Ambrosia A.C. Watts and E.A. Hinkley. Unmanned Aircraft Systems in Remote Sensing and Scientific Research: Classification and Considerations of Use. Remote Sens., 1671-1692, 2012.

[19] P. W. Merlin. Ikhana unmanned aircraft system Western states fire mission. National Aeronautics and Space Administration, Washington, DC, 2009.

[20] US Electric Power Research Institute. Utilizing Unmanned Aircraft Systems as a Solar Photovoltaics OM Tool. Source: `https://www.epri.com/#/pages/product/3002006216/`, 2015.

[21] C. Zhang and J. M. Kovacs. The application of small unmanned aerial systems for precision agriculture: a review, 2012.

[22] US Customs and Border Protection. Unmanned Aircraft System MQ-9 Predator B. Source: https://www.cbp.gov/sites/default/files/documents/FS_2015_UAS_FINAL_0.pdf.

[23] European Aviation Safety Agency (EASA). Concept of Operations for Drones. A risk based approach to regulation of unmanned aircraft, 2015.

[24] International Civil Aviation Organization. Annex 2 to the Convention on International Civil Aviation, 10th edition, 2005.

[25] JARUS CONOPS. Annex D - C2 Link, 2016.

[26] The European Organisation for Civil Aviation Equipment (EUROCAE). WG-73 Unmanned Aircraft Systems (UAS). Concept of RPAS Required Communication Performance Methodology for the Command, Control and Communication Link, 2015.

[27] R. Jay Shively et al. Human performance considerations for Remotely Piloted Aircraft Systems (RPAS). Remotely Piloted Aircraft Systems Panel (RPASP) - Second Meeting, Montreal, 2015.

[28] R. R. Cordon et al. RPAS Integration in Non-segregated Airspace: the SESAR Approach. Fourth SESAR Innovation Days, November 2014.

[29] H. Jung et al. RPAS Integration in Non-segregated Airspace within Comparison between Radar Vectoring and Trajectory Based Operation Using a Real-Time ATC Simulation. Air Transport Research Society World Conference, 2016.

[30] M. Perez-Batlle et al. Real-time Simulations to Evaluate RPAS Contingencies in Shared Airspace. Fifth SESAR Innovation Days, December 2015.

[31] E. Pastor et al. Preparing for an Unmanned Future in SESAR Real-time Simulation of RPAS Missions. Third SESAR Innovation Days, 2013.

[32] International Civil Aviation Organization (ICAO). Manual on Required Communication Performance, 2006.

[33] Joint Authorities for Rulemaking of Unmanned Systems. RPAS C2 link Required Communication Performance (C2 link RCP) concept. Available online: http://jarus-rpas.org/sites/jarus-rpas.org/files/jar_02_doc_-_jarus_rpas_c2_link_rcp_-_10_oct_2014_1.pdf, [accessed on 21/03/2017].

[34] International Civil Aviation Organization. Manual on Required Communication Performance (RCP). Doc. 9869, First Edition, 2006.

[35] K. Bilimoria et al. FACET: Future ATM Concepts Evaluation Tool. 3rd USA/Europe Air Traffic Management RD Seminar, June 2000.

[36] E. Theunissen et al. UAV Mission Management Functions to Support Integration in a Strategic and Tactical ATC and C2 Environment. AIAA Modeling and Simulation Technologies Conference and Exhibit, August 2005.

[37] R. Garcia and L. Barnes. Multi-UAV Simulator Utilizing X-Plane. Journal of Intelligent and Robotic Systems, Vol. 57, pp. 393–406, 2010.

[38] E. Pastor et al. Evaluating technologies and mechanisms for the automated/autonomous operation of UAS in non-segregated airspace. Proceedings of the 1st SESAR Innovation Days, 2011.

[39] P. Royo et al. ISIS+: A Software-in-the-Loop Unmanned Aircraft System Simulator for Nonsegregated Airspace. Journal of Aerospace Information Systems, Vol. 10, No. 11, November 2013.

[40] B. Korn et al. "File and Fly" - Procedures and Techniques for Integration of UAVs in Controlled Airspace. 25th International Congress of the Aeronautical Sciences, 2006.

[41] D. Schmitt et al. Real Time Simulation of Integration of UAV's into Airspace. 26th International Congress of the Aeronautical Sciences, September 2008.

[42] K-P. L. Vu et al. Air Traffic Controller Performance and Acceptability of Multiple UAS in a Simulated NAS Environment. Proceedings of the HCI-AERO conference, Silicon Valley, 2014.

[43] E. Pastor et al. Real-time Simulations to Evaluate the RPAS Integration in Shared Airspace. Fourth SESAR Innovation Days, November 2014.

[44] M. Perez-Batlle et al. A Methodology for Measuring the Impact o Flight Inefficiency of Future RPAS Operations. 34th Digital Avionics Systems Conference, September 2015.

[45] C. Barrado et al. Paired T-test Analysis to measure the Efficiency Impact of a flying RPAS in the non-segregated Airspace. 35th Digital Avionics Systems Conference, September 2016.

[46] L. Fresno et al. Human Factor Impact Assessment of RPAS Integration into Non-segregated Airspace. 6th SESAR Innovation Days, November 2016.

[47] Airtopsoft. AirTOp User Guide. Internal document, 2011.

[48] International Civil Aviation Organization. Procedures for Air Navigation Services. Available online: http://www.navcanada.ca/EN/media/Publications/ICAO-Doc-4444-EN.pdf, [accessed on 21/03/2017].

[49] International Civil Aviation Organization. Annex 11 to the Convention on International Civil Aviation, 13th edition, 2001.

[50] EUROCONTROL. Base of Aircraft Data (BADA) Product Management Document. EUROCONTROL Experimental Center Technical Scientific Report No. 2009-008 . Available online: http://www.eurocontrol.int/sites/default/files/field_tabs/content/documents/sesar/bada-product-management.pdf, 2009.

[51] P. Glasserman. Monte Carlo Methods in Financial Engineering. Springer, 2003.

[52] M. H. Kalos and P. A. Whitlock. Monte Carlo Methods. Wiley-VCH Verlag GmbH Co. KGaA, second edition, 2008, ISBN: 978-3-527-40760-6.

[53] J. Voss. An Introduction to Statistical Computing: A Simulation-based Approach. Wiley, 2013, ISBN: 978-1-118-35772-9.

[54] W. Verhagen. AE4465 Maintenance Modelling and Analysis Lecture Notes. Repairables: data analysis. Delft University of Technology, 2016.

[55] G. C. Runger D. C. Montgomery and N. F. Hubele. Engineering Statistics. John Wiley Sons, Inc. Publication, fifth edition, 2011, ISBN: 978-0-470-64607-6.

[56] EUROCONTROL. 7-year IFR Flight Movements and Service Units Forecast: 2015-2021, 2015.

[57] DFS Deutsche Flugsicherung and EUROCONTROL. Local Single Sky ImPlementation (LSSIP) Germany, 2013.

[58] DFS Deutsche Flugsicherung. Air traffic in Germany. Mobility Report, 2016.

[59] Airbus. Performance Characteristics of A320 Family. Source: http://www.aircraft.airbus.com/aircraftfamilies/passengeraircraft/a320family/, [accessed on: 23/08/2017].

[60] ATR. ATR Family Aircraft Specifications. available online: http://www.atraircraft.com/products_app/media/pdf/FAMILY_septembre2014.pdf, 2014.

[61] Boeing. Airplane Characteristics for Airport Planning. available online: http://www.boeing.com/assets/pdf/commercial/airports/acaps/737.pdf, 2013.

[62] Bombardier. CRJ Series Specifications Brochure. available online: http://commercialaircraft.bombardier.com/content/dam/Websites/bca/literature/crj/Bombardier-Commercial-Aircraft-CRJ-Series-Brochure-en.pdf, 2015.

[63] Bombardier. Q Series Specifications Brochure. available online: http://commercialaircraft.bombardier.com/content/dam/Websites/bombardiercom/supporting-documents/BA/Bombardier_Q%20Series_Final.pdf, 2017.

[64] Embraer. Performance Characteristics of E-Jets Family. Source: https://www.embraercommercialaviation.com/commercial-jets/, [accessed on: 23/08/2017].

[65] J. W. Taylor. Jane's All World Aircraft, 1988-1989. Jane's Information Group, 1988.

[66] EUROCONTROL. Release Note RPAS BADA Performance Files. EEC Technical Note No. 15/11/06-50, 2015.

[67] United States Government Accountability Office. Assessments of Selected Weapon Programs. 2013.

[68] M. Voskuijl. AE2230 Flight and Orbital Mechanics Lecture Notes. Unsteady Climb. Delft University of Technology, 2012.

[69] J.K. Kuchar. Aeronautical Surveillance Panel. Update on the Analysis of ACAS Performance on Global Hawk, 2006.

[70] J. Ittel. Static Flight Plan Validator, 2012.

[71] J. Hoekstra and J. Ellerbroek. AE4321 Air Traffic Management Lecture Notes. Free Flight. Delft University of Technology, 2016.

[72] A. Field. Discovering Statistics Using SPSS. SAGE Publications Ltd., third edition, 2009, ISBN: 978-1-84787-906-6.

[73] T.S. Donaldson. Robustness of the F-Test to Errors of Both Kinds and the Correlation Between the Numerator and Denominator of the F-Ratio. Journal of the American Statistical Association Vol. 63, No. 322 (Jun., 1968), pp. 660-676.

[74] G.H. Lunney. Using Analysis of Variance with a Dichotomous Dependent Variable: An Empirical Study. Journal of Educational Measurement Vol. 7, No. 4 (1970), pp. 263-269.

[75] A. Field. Welch's F. Additional Material to Discovering Statistics Using SPSS. available online: https://www.discoveringstatistics.com/docs/welchf.pdf, 2009.

[76] J.T. Newsom. USP 634 Data Analysis I. Portland State University. available online: http://web.pdx.edu/~newsomj/da1/ho_planned%20contrasts.pdf, 2013.

[77] L.E. Toothaker. Multiple comparison procedures. Sage university paper series on quantitative applications in the social sciences. SAGE Publications, 1993.

[78] R. Ho. Handbook of Univariate and Multivariate Data Analysis and Interpretation with IBM SPSS. CRC Press, second edition, 2014, ISBN: 978-1439890219.

[79] C. J. Huberty and S. Olejnik. Applied MANOVA and Discriminant Analysis. John Wiley Sons, Inc. Publication, second edition, 2006, ISBN: 978-0-471-46815-8.

[80] EUROCONTROL. Approach to the Introduction of RPAS in BADA 3 Aircraft Performance Model. EEC Technical Note No. 15/11/06-50, 2015.

[81] EUROCONTROL. NEST User Guide. Internal document, 2017.

[82] EUROCONTROL. User Manual for the Base of Aircraft Data (BADA). EUROCONTROL Experimental Center Technical Scientific Report No. 15/04/02-43 , 2015.